

NASA CR-1891

NASA CONTRACTOR
REPORT



NASA CR-1

C. I.

0060998



TECH LIBRARY KAFB, NM

LOAN COPY: RETURN TO
AFWL (DOUL)
KIRTLAND AFB, N. M.

THE EXPERIMENTAL DETERMINATION
OF ATMOSPHERIC ABSORPTION FROM
AIRCRAFT ACOUSTIC FLIGHT TESTS

by R. L. Miller and P. B. Oncley

Prepared by

THE BOEING COMPANY

Seattle, Wash. 98124

for Langley Research Center

NATIONAL AERONAUTICS AND SPACE ADMINISTRATION • WASHINGTON, D. C. • NOVEMBER 1971



0060998

1. Report No. NASA CR-1891	2. Government Accession No.	3. Recip.
4. Title and Subtitle THE EXPERIMENTAL DETERMINATION OF ATMOSPHERIC ABSORPTION FROM AIRCRAFT ACOUSTIC FLIGHT TESTS		5. Report Date November 1971
7. Author(s) R. L. Miller and P. B. Oncley		6. Performing Organization Code
9. Performing Organization Name and Address The Boeing Company Commercial Airplane Group P.O. Box 3707 Seattle, Washington 98124		8. Performing Organization Report No. D6-25492
12. Sponsoring Agency Name and Address National Aeronautics and Space Administration Washington, D.C. 20546		10. Work Unit No.
15. Supplementary Notes		11. Contract or Grant No. NAS1-10272
		13. Type of Report and Period Covered Contractor Report
		14. Sponsoring Agency Code
16. Abstract This report describes a method for determining atmospheric absorption coefficients from acoustic flight test data. Measurements from five series of acoustic flight tests conducted at Grant County Airport, Moses Lake, Washington, were included in the study. The number of individual flights totaled 24: six Boeing 707 flights performed in May 1969 in connection with the turbofan nacelle modification program, NASA contract NAS 1-7129, eight flights from Boeing tests conducted during the same period, and 10 flights of the Boeing 747 airplane conducted on August 4, 1969, April 18, 1970, and October 22, 1970. The effects of errors in acoustic, meteorological, and aircraft performance and position measurements are discussed. Tabular data of the estimated sample variance of the data for each test are given for source directivity angles from 75° to 120° and each 1/3-octave frequency band. Graphic comparisons are made of absorption coefficients derived from ARP 866, using atmospheric profile data, with absorption coefficients determined by the experimental method described in the report.		
17. Key Words (Suggested by Author(s)) Atmospheric Absorption Acoustic Flight Test Ground Reflection Reflection Interference Measured Attenuation		18. Distribution Statement Distribution of this report is provided in the interest of information exchange. Responsibility for the contents resides in the author or organization that prepared it.
19. Security Classif. (of this report) Unclassified	20. Security Classif. (of this page) Unclassified	21. No. of Pages 107
		22. Price* \$3.00



CONTENTS

	Page
SUMMARY	1
INTRODUCTION	1
SYMBOLS	3
BASIC CONCEPTS AND ALGORITHM	5
Time-Position Relations	5
Loss Calculations	7
Composite Plots	9
TEST PROCEDURES AND INSTRUMENTATION	10
Test Site Description	10
Test Weather Conditions	10
Flight Test Procedures and Instrumentation	12
Aircraft Performance Instrumentation	12
Aircraft Space-Position Instrumentation	12
Acoustic Instrumentation	13
Meteorological Measurements and Instrumentation	14
Meteorological Measurements	14
Meteorological Instrumentation	14
ERROR ANALYSIS	15
Acoustic Instrumentation Errors	16
Aircraft Position Errors	17
Doppler Shift	18
Ground Reflection Interference	19
Meteorological Error Sources	20
Errors in Meteorological Measurements	20
Atmospheric Variability	20
Atmospheric Gradients	21
Atmospheric Turbulence	22
SUMMARY OF TEST RESULTS	22
CONCLUSIONS	24
APPENDIX A Estimated Sample Variances and Summary Plots of Differences Between Experimental and ARP 866 Absorption Coefficients	27
APPENDIX B Atmospheric Absorption Computation Using ARP 866 for a Stratified Atmosphere	29
REFERENCES	31

THE EXPERIMENTAL DETERMINATION OF ATMOSPHERIC ABSORPTION FROM AIRCRAFT ACOUSTIC FLIGHT TESTS

By R. L. Miller and P. B. Oncley

The Boeing Company

SUMMARY

This report was prepared under contract NAS 1-10272 with the National Aeronautics and Space Administration, Langley Research Center, Hampton, Virginia. It describes a method for determining atmospheric absorption coefficients from acoustic flight test data and discusses the assumptions and limitations of this method. Errors associated with (a) aircraft position and performance, (b) acoustic measurements, and (c) meteorological measurements are discussed. Graphic comparisons of atmospheric absorption coefficients derived from Aerospace Recommended Practice (ARP) 866 are made with experimentally derived coefficients. Tabular data of the estimated sample variances for each test flight are given for 1/3-octave frequency band and for 10 source directivity angles from 75° to 120°.

The results of the analysis of data from 24 flights over a grid of eight or more microphones support the validity of ARP 866 for the ranges of atmospheric conditions sampled. This significant conclusion could only be reached after extensive statistical analysis of a large volume of data to remove the effects of random errors in the acoustic, meteorological, aircraft position, and flight performance measurements. It now appears that many of the complaints that have been attributed to inaccuracies in the ARP 866 standard absorption rates were probably generated by noise floor limitations in acoustic data recording and analysis. The systematic difference or bias between experimental and ARP 866 absorption coefficients was approximately 1 dB for the frequency range from 50 to 10 000 Hz when data from 10 directivity angles for all 24 flights are combined.

INTRODUCTION

With the growing concern about the problem of community noise, the rate of attenuation of airborne sound is no longer only of academic interest. Since reduction of aircraft jet engine noise is obtainable only at appreciable financial and performance cost, and since noise certification of new aircraft is required by the Federal Government, both the airplane industry and the Federal and state governments have an important stake in the establishment of standard measurement procedures. Such procedures will ensure that measurements made at one time and place can be normalized to standard conditions or compared with measurements made at other times and places. This requirement applies to the evaluation of other transportation system noises (trucks, trains, etc.) as well as aircraft.

It is well known that the rate of attenuation of noise in air is highly dependent on meteorological factors—in particular, the temperature and humidity of the air. Since this rate, at frequencies from 8000 to 10 000 Hz, can vary from 35 dB to more than 60 dB per 1000 ft (305 mtr) depending on the atmosphere, it is necessary to measure the atmospheric parameters involved and to normalize the noise measurements to reference day conditions. The procedure now used for this purpose was developed by the A-21 committee of the Society of Automotive Engineers and is known as Aerospace Recommended Practice 866 (ARP 866, ref. 1).

This standard is based on theoretical studies (ref. 2) and laboratory experiments by Harris and others (refs. 3 and 4), with some adjustments derived from measurements of airplane noise by several airplane manufacturers and government agencies. Limited confidence in ARP 866 when the absorption rates are appreciably different from reference day conditions has led to the adoption of a rather restricted window of temperature and humidity conditions deemed acceptable for certification testing to FAA standards (ref. 5). This restriction increases the cost of testing and may cause delays when near-reference conditions cannot be obtained. Furthermore, depending upon the extent to which atmospheric conditions are determined in space and time, restricted window testing does not necessarily ensure improved data accuracy.

During the various product-improvement, certification, and precertification noise tests conducted by The Boeing Company, a great deal of significant information related to sound attenuation in the atmosphere is gathered. Recordings of aircraft sounds are made at outdoor test ranges such as that at the Grant County Airport, Moses Lake, Washington, with microphone arrays totaling as many as 27. Each microphone is time-synchronized with aircraft-tracking devices and radiosonde sampling of the atmospheric parameters. Both The Boeing Company and NASA have been interested for some time in the use of available information to provide an independent check on the reliability of the ARP 866 procedure. The NASA involvement dates particularly from the tests performed in May 1969 for the Boeing 707 turbofan nacelle modification program (ref. 6). During these tests, NASA-specified test conditions were run (referred to in this document as "series 15"). Certain additional flights were conducted by Boeing in weather outside the NASA-suggested meteorological qualification window. These flights are here referred to as "series 17." A preliminary report on these test series plus data from Boeing tests of the 747 airplane on August 4, 1969, was submitted to NASA in the spring of 1970, and led to the award of contract NAS 1-10272 under which this report has been prepared.

Partially as an outgrowth of these absorption studies, the techniques involved in outdoor airplane sound measurements and in the analysis of the data have been subjected to extensive scrutiny. This procedural review led to modifications that provide a marked improvement in the accuracy and reliability of the data. The Boeing Acoustics Laboratory has developed electronic pre-emphasis equipment that has improved the amplitude range of the recording systems in the high-frequency bands (6300-10 000 Hz), and in the last 9 months, improvements in the spectrum analysis equipment have extended its useful signal range from about 40 dB to 75 dB. As a result, data from recent test series indicate better reliability at high frequencies than data from the earlier measurements.

However, there are still serious sources of error. When absorption may be as high as 60 dB/1000 ft and propagation distances range from a few hundred to over 3000 ft, it is apparent that signal-to-noise ranges of even 80 dB are far from adequate. Multichannel, limited bandwidth recording systems are being studied for these extreme but not uncommon cases. A computational procedure developed under this contract removed much of the data affected by the noise floor and produced better high-frequency absorption results. Several statistical tests have been used to evaluate and compare the flight test results with ARP 866. These tests cannot be applied with great authority, however, unless it is known that the errors in the data are largely random in distribution. Such assurance is possible only for certain parts of the data included in this report.

SYMBOLS

A	Y intercept of the plot of Y' versus R
A_(i)	altitude of aircraft at position P _{vo(i)}
C_A	speed of sound
f_d	Doppler-shifted frequency as heard at a point on the ground
f_m	frequency of the moving source
f_o	lowest frequency at which a minimum in SPL occurs as a result of interference between direct and reflected sound
h_m	microphone height
h_s	height of sound source
Loss_(SD)	attenuation of sound from a point source due to energy spreading by spherical divergence: loss _(SD) = 20 log ₁₀ R/R ₀
M_(i)	"i"th microphone in test array
P_{a(i,φ)}	position of aircraft when sound was emitted
P_{v(i,φ)}	position of aircraft at time sound reaches microphone
P_{vo(i)}	point directly over microphone on the aircraft flightpath
R_(i,φ)	sound path length from microphone to aircraft position P _{a(i,φ)}
R₀	reference distance (1000 ft)
S	distance from overhead point to point of sound emission
S²_{dy}	sample estimate of variance
Slope B	measured atmospheric attenuation coefficient, including an error distribution term ϵ
t_(i,φ)	time sound was emitted from aircraft
t_{vo(i)}	visual overhead time of aircraft
V_{ac}	velocity of aircraft
W_(φ,f)	sound output of aircraft as a function of directivity angle and frequency
Y'	spectrum pressure level with spherical divergence removed, measured at microphones in the grid at various distances from the noise source

Y''	parameter combining the term Y' , the loss term resulting from atmospheric absorption, and error ϵ
$\alpha(f)$	atmospheric absorption coefficient
Δ	difference between calculated (ARP 866) absorption coefficient and experimentally determined coefficient
ϵ	error term
θ	angle of flightpath with respect to the ground
ϕ	sound source directivity angle measured from the aft end of the aircraft

BASIC CONCEPTS AND ALGORITHM

When sound originating at a distant point is measured at several positions, intuition leads us to expect the measured sound level to be lower at points more remote from the source. Under practical conditions, however, where the microphones are usually near the ground or some other reflecting surface, the atmospheric medium of propagation is neither uniform nor stationary, and, where temperature and wind gradients cause refraction or scattering, the relationship between sound pressure level and distance may not easily be defined. If the source, moreover, is a jet aircraft that is strongly directive in its acoustic output, and is moving at an appreciable fraction of the speed of sound, the precise description of the relationship becomes impossible without certain simplifying assumptions. To the extent that these assumptions are inaccurate, errors will be introduced in the results.

Several approaches are possible for determining atmospheric absorption from aircraft overflights. Three that have been used are:

- (1) Level flybys repeated at different altitudes with ground microphone(s) directly under the flightpath.
- (2) A single level flyby with an array of ground microphones perpendicular to the flightpath.
- (3) A single flight at constant climb angle with an array of microphones along the ground track.

Combinations of these approaches are also possible. The assumptions required in the various approaches are somewhat different, as seen in table 1.

The assumptions involved in the third approach appear to be the most reasonable. Therefore, the measurements on which this report are based were made during constant-climb-angle flights. For some tests it was necessary to use sideline microphones. When sideline microphones were used, the method is a combination of the second and third approaches. Because flight test patterns were not prescribed for the express purpose of atmospheric absorption studies, only a limited number of test conditions were appropriate for use in this study.

Time-Position Relations

The basic geometry employed in the third approach, using a single flight at constant climb angle, is given in figure 1.

The aircraft is assumed to proceed along a flightpath forming a constant angle θ with respect to the ground and to pass directly over a line of microphones $M_{(i)}$. During each test flight, identified by a condition number, sound is recorded from each microphone on an FM magnetic tape recorder along with time pulses for synchronization. The sound reaching the microphone $M_{(i)}$ at some particular time $t_{(i, \phi)}$, was emitted when the plane was at position

Table 1. Assumptions in Determining Atmospheric Absorption

Assumptions	Approach		
	(1)	(2)	(3)
Aircraft is a <i>constant noise source</i> with uniform pattern during each single flight	X	X	X
Aircraft generates fixed, repeatable noise level and pattern during several flights	X		
Aircraft noise pattern is circularly symmetrical around flight axis		X	
Aircraft maintains constant angle of attack and climb angle during flight	X	X	X
Atmosphere is adequately described by radiosonde profile near time of test	X	X	X
Atmosphere is not significantly changed between successive flights	X		
Spectrum modifications from ground reflection at different incidence angles are insignificant at frequencies of interest		X	

$P_{a(i, \phi)}$, and traveled along a path of length $R_{(i, \phi)}$, forming a directivity angle ϕ , with the aircraft flightpath. From radar tracking data, or stadiometric camera photographs, the visual overhead time $t_{vo(i)}$ when the aircraft passed through point $P_{vo(i)}$ directly over the microphone, is known. The altitude $A_{(i)}$ directly over each microphone and the aircraft velocity V_{ac} , are also known from tracking data.

During the time sound was traveling from $P_{a(i, \phi)}$ to the microphone at a speed of sound C_A , the aircraft was traveling from $P_{a(i, \phi)}$ to $P_{v(i, \phi)}$ at the aircraft velocity V_{ac} . Since the aircraft was at $P_{vo(i)}$ at the known overhead time $t_{vo(i)}$ and is at $P_{v(i, \phi)}$ at time $t_{(i, \phi)}$, we can calculate $t_{(i, \phi)}$ from

$$t_{(i, \phi)} = t_{vo(i)} + (S/V_{ac}) + (R_{(i, \phi)}/C_A) \quad (1)$$

where S , the distance from $P_{vo(i)}$ to $P_{a(i, \phi)}$ and $R_{(i, \phi)}$ can be computed from the law of sines,

$$R/\sin \gamma = S/\sin \beta = A/\sin \phi \quad (2)$$

and where

$$\gamma = 90^\circ + \theta, \text{ and } \beta = 180^\circ - \gamma - \phi.$$

In this way a time $t_{(i, \phi)}$ is computed for each microphone $M_{(i)}$ and each directivity angle ϕ chosen. From the times $t_{(i, \phi)}$, interpolated SPL values for each directivity angle and each microphone are computed. The directivity angles in this study are the 5° increments between 75° and 120° , ten in all. (Note that the directivity angle is measured from the aft end of the aircraft.) The analog recordings from the flight test are processed through 1/3-octave-band spectrum analyzers, giving the 24 spectrum pressure level (SPL) values for each 0.5-sec sample of the original record.

Loss Calculations

It has been assumed that for a particular directivity angle ϕ the acoustic output of the aircraft $W(\theta, f)$, is constant during the test condition. The attenuation of the sound with distance is composed of two main parts: (a) a distributive loss including the energy spreading over an ever-increasing sphere with increasing distance from the source, and (b) a dissipative loss due to conversion of sound into thermal energy in passing through the atmosphere. The distributive loss from energy spreading is independent of frequency and amounts to 6 dB each time the distance is doubled. It is often called "spherical divergence loss" and is expressed by

$$\text{Loss}_{(SD)} = 20 \log_{10} \frac{R}{R_0} \quad (3)$$

with R_0 representing some standard distance. One thousand feet has been used for R_0 in this report.

There are other important distributive parameters resulting from reflections and from ray-bending as a result of temperature or wind gradients. These may introduce important distortions in the frequency spectrum as measured at any one point, causing data taken at various microphone positions to be quite different. Problems arising from these sources will be discussed later, but it has not been possible to explore them extensively in this study.

Dissipative losses vary linearly with distance and depend very strongly on frequency as well as on the temperature and humidity of the atmosphere. Their main component is atmospheric absorption, which has been studied extensively in theoretical and laboratory investigations, and in various field tests. There are presumably other losses from such phenomena as turbulence but they have not yet been adequately isolated and are believed to be small under the relatively quiet air conditions usually chosen for aircraft acoustic tests. The ARP 866 standard is based on the premise that atmospheric absorption is the only important linear loss factor.

For the present, consider that the SPL at some microphone $M(i)$, for sound arriving from an aircraft with output $W(\phi, f)$ at a directivity angle ϕ , over a path length $R(i, \phi)$ is given by

$$SPL(i, \phi, f) = Y(i, \phi, f) = W(\phi, f) \cdot 20 \log_{10} \frac{R(i, \phi)}{R_o} - \alpha(f) R(i, \phi) + \epsilon \quad (4)$$

where $\alpha(f)$ is the absorption coefficient and ϵ is an error term.

Since the spherical divergence term is independent of frequency and atmospheric conditions, the first step in the computation is the substitution of a new variable Y' with the divergence factor eliminated;

$$Y'(i, \phi, f) = Y(i, \phi, f) + 20 \log_{10} \frac{R(i, \phi)}{R_o} \quad (5)$$

$$= W(\phi, f) - \alpha(f) R(i, \phi) + \epsilon \quad (5a)$$

This implies that a plot of the values of Y' versus R should fall along a straight line with Y' -intercept, equal to $W(\phi, f)$ and a slope equal to $-\alpha(f)$ with some error distribution resulting from the values of ϵ . The calculation of this regression line is described in standard texts on statistics (for example, ref. 7). The intercept and slope of the regression line are given by

$$\text{Intercept } A, = \frac{\sum Y' \cdot \sum R^2 - \sum R \cdot \sum RY'}{N \sum R^2 - (\sum R)^2} \quad (6)$$

$$\text{Slope } B = \frac{\sum RY' - (\sum R \sum Y')/N}{\sum R^2 - (\sum R)^2/N} \quad (7)$$

where N is the number of measurement points or microphones. The slope B , equivalent to $-\alpha$ in equation (5a) is the experimental value of the absorption coefficient. These

computations are performed by a digital computer, which also plots the points (Y' , R) for each microphone and the derived regression line. Such a plot is generated for each directivity angle and each frequency band. Examples of plots of this type are given in figure 2.

Certain other statistical parameters are used to indicate the "goodness of fit," such as the sample estimate of variance S^2_{dy} :

$$S^2_{dy} = \frac{\sum(Y'_i - A - BR_i)^2}{N - 1} \quad (8)$$

Values of S^2_{dy} are given in the tables of appendix A.

Since the comparison of the experimental results and the values from ARP 866 is the primary concern, these latter values are calculated for each data point, using the assumption of a stratified atmosphere and following the procedure described in appendix B. The resulting loss term is added to the value of Y' previously obtained to yield another parameter Y'' :

$$Y''(i, \phi, f) = Y'(i, \phi, f) + \text{loss}(i, \phi, f) \quad (9)$$

$$= W(\phi, f) + \epsilon + \Delta R(\phi, f) \quad (9a)$$

where Δ represents the difference between the measured and predicted absorption rates. Again the regression line analysis is used and the slope Δ of the new line is calculated to give minimum error terms ϵ . Plots of these data points are obtained after first subtracting from the points their mean value, which is approximately equivalent to $W(\phi, f)$, so the curve is centered around the zero axis. Figure 3 gives examples of these plots.

Composite Plots

For convenience and visibility the attenuation values for each frequency are plotted against frequency band number to give another series of curves, one for each directivity angle, of which an example is given in figure 4. The discrete points are the experimentally obtained values, while the solid curve is the absorption rate calculated from ARP 866, using average values of temperature and humidity. Note that this ARP 866 curve cannot be calculated for a stratified atmosphere since this can be computed only for some specific source height, temperature, and humidity. For this reason, the curves should be considered only approximate, but they are useful because they present the information in a familiar form.

A more accurate presentation of the data is shown in figure 5. Here the values of Δ (eq. 9a) corresponding to the slope of the unploted regression lines of graphs of the type shown in figure 3 are plotted against frequency band number. Since Δ is calculated from differences between experimental values and those obtained by applying ARP 866 point by point for a stratified atmosphere, these curves are a true comparison of experimental results and the ARP 866 standard. A curve of this type is obtained for each directivity angle. The values for the ten angles are then summarized in a single plot, such as that in figure 6. For the sake of clarity, discrete points are plotted for only five angles, but the solid curve is the mean of all ten. Curves of this type, for all of the 24 test flights included in this study, are given in appendix A.

TEST PROCEDURES AND INSTRUMENTATION

Test Site Description

The acoustic flight test data analyzed in this report were obtained by The Boeing Company during tests conducted at the Grant County Airport, previously Larson AFB, located about 5 miles north of the town of Moses Lake, Washington. The airport was formerly a Strategic Air Command B-52 base, and the facilities are designed to accommodate large aircraft.

Runway 14L-32R, which was used for the tests, is 13 500 ft long and 300 ft wide with virtually zero slope and has a 1000-ft asphalt overrun on each end. The airport has a listed altitude of 1186 ft above mean sea level (msl). Terrain in the airport vicinity is characterized by gentle slopes and, near the runway, relief is limited to coulees and dirt ridges of 5 to 10 ft in height. Figure 7 is a map of the microphone grid area to the north of the runway showing contours at 10-ft intervals referenced to msl. The elevation along the microphone grid varies from about 1160 ft msl at each end to a maximum of 1194 ft at the midpoint. The terrain slopes upward to the west of the extension of the runway centerline and downward to the east.

The vegetation is grass and scattered patches of sagebrush. Most of the area has a continuous ground cover, although there are exposed patches of sand and dirt. Both terrain and vegetation are characteristic of the arid climate and appear to exhibit no excessive sound absorption characteristics.

Figure 8 shows typical terrain and ground cover in the test area. This is a view near the north end of the runway looking toward the east at one of the 1500-ft sideline microphone stations. Figure 9 is an aerial photograph showing the airport facilities, runways, and adjacent terrain.

Test Weather Conditions

All of the test flights included in this report with the exception of 17.08 were carried out under the surface weather conditions listed below. (During test 17.08, the relative humidity was less than 30%).

- No rain or other precipitation
- Relative humidity between 30% and 90%
- Temperature between 32° and 68°F
- Surface wind speed 10 kn or less

Table 2 lists the surface weather conditions for each test flight included in this report. The tabulated values are averages over a period of about 1 min during the time the test aircraft passed over the microphone grid. Most of the tests were scheduled during the early morning hours to take advantage of the higher relative humidity. The higher humidities result primarily from the decrease of temperature due to radiational cooling of the ground surface at nighttime. Further, the resulting thermal atmospheric stability reduces mixing by convection and confines the moisture to the surface layers.

Table 2.—Surface Meteorological Measurements, Grant County Airport, Moses Lake, Washington

Date	Time	Condition number	Temp, °F	Ht, mtr	Rel Hum, %	Ht, mtr	Wind		Ht, mtr
							Dir, deg *	Speed, kn	
5/17/69	0642	15.01	50	1.5	52	1.5	300	1	10
5/17/69	0651	15.02	53	↑	52	↑	320	1	
5/18/69	0553	15.03	48		61		350	5	
5/17/69	0951	15.04	63		34		280	4	
5/20/69	0721	15.05	50		86		320	4	
5/20/69	0653	15.06	49		86		300	5	
5/16/69	0640	17.01	51		55		040	4	
5/16/69	0648	17.02	52		50		020	4	
5/18/69	0601	17.03	48		61		350	5	
5/18/69	0749	17.07	59		41		330	8	
5/17/69	1054	17.08	67		27		090	1	
5/18/69	0714	17.09	54		47		320	6	
5/18/69	0722	17.10	57		45		330	7	
5/18/69	0733	17.11	57		44		340	8	10
8/4/69	0811	14.01	63		49		130	3	3
8/4/69	0637	14.02	56		70		130	2	↑
8/4/69	0645	14.03	57	↓	67	↓	110	4	↓
8/4/69	0654	14.04	57	1.5	66	1.5	130	5	3
4/18/70	0608	10	33	10	68	1.2	070	2	10
4/18/70	0621	11	34	↑	66	↑	100	2	
4/18/70	0631	12	35		64		060	3	
4/18/70	0645	13	37		60		120	3	
10/22/70	0750	004.1	34	↓	82	↓	160	7	
10/22/70	0905	006	34	10	83	1.2	150	5	10

*Wind direction from which the wind is blowing referenced to magnetic north.

Flight Test Procedures and Instrumentation

Data selected for this study were taken from noise tests of the Boeing 707 airplane conducted on May 16, 17, 18, and 20, 1969 (series 15 and 17), and of the 747 on August 4, 1969, April 18, 1970, and October 22, 1970. Only takeoffs, or simulated takeoffs, without power cutback are included in this report. Takeoffs were from a full stop, while simulated takeoffs were performed by making a low-level pass over the runway until the normal climb path was intercepted, and then proceeding with the climbout over the microphone grid. The climb angles varied from 5° to 10° for the 707 tests and from 3° to 6° for the 747 tests. The flight procedure required the pilot to maintain, as closely as possible, a constant first-stage rotor speed and indicated airspeed during the climbout, since these are the primary factors controlling the noise generated by the test airplanes. Airspeeds varied from about 285 to 325 fps during the flights. The height of the aircraft above the microphone grid varied from 425 to 3500 ft during the 707 flight tests and from 300 to 1400 ft for the 747. Table 3 lists the height range of the test aircraft for each flight from the first microphone in the grid, along the extension of the runway centerline, to the last microphone used in the data analysis. The average climb angle and air speed for each flight are also included in the table. It should be noted that the range of heights of the airplane over the microphone grid is not a true representation of the range of distances used in calculating atmospheric attenuation. Measurements from directivity angles of 75° to 120° for each microphone along the centerline were included in the analyses, and for some flights data from 1500- and 2000-ft sideline microphones were used to increase the propagation path length.

Aircraft performance instrumentation.—Calibrated instruments installed in the aircraft included those necessary to indicate and record aircraft speed, altitude, gross weight, ambient pressure and temperature, first-stage rotor speed, and engine parameters required to compute net thrust. All performance parameters were time-correlated with acoustic and position measurements made by ground-based equipment. Manual recordings were made of aircraft gross weight and relevant aerodynamic systems.

Aircraft space-position instrumentation.—An M-33, X-band radar was used for tracking the aircraft and for providing time-correlated position data synchronized with the noise recordings. A continuous plot of aircraft position (altitude and ground track) was available for on-line assessment of satisfactory compliance with planned flight patterns. On-line vectoring guidance was provided to the pilot by means of voice communications from the radar instrumentation van.

During the May 1969 tests, the M-33 radar van was located southwest of the intersection of runway 14L-32R and runway 3-21, as shown in figure 9. During later tests the radar was moved to the compass rose, about 2000 ft east of the main runway, to improve tracking ability and data accuracy.

Though the accuracy of the radar has been improved since May 1969, it is still deficient at extreme ranges. In addition to the M-33 radar, the aircraft radio altimeter provided height information along the flightpath. For the April 1970 tests, a stadiometric camera system was installed on the ground to provide more accurate height and overhead time at the 3.5-nmi point. Before the October 1970 tests, the stadiometric camera was relocated in the airplane, looking downward at ground targets. This arrangement gives high accuracy at a

Table 3.—Test Aircraft Flight Data

Date	Time	Number	Climb angle, deg	Height range, ft	Average air speed, fps
5/17/69	0642	15.01	5.2	560-1810	315
5/17/69	0651	15.02	7.3	730-2280	322
5/18/69	0553	15.03	4.9	690-1990	315
5/17/69	0951	15.04	8.3	1400-3530	288
5/20/69	0721	15.05	8.0	1200-3100	290
5/20/69	0653	15.06	7.8	1100-2880	288
5/16/69	0640	17.01	4.9	424-1184	290
5/16/69	0648	17.02	6.1	684-1582	322
5/18/69	0601	17.03	5.6	554-1404	312
5/18/69	0749	17.07	9.7	600-2200	290
5/17/69	1054	17.08	10.3	704-2304	295
5/18/69	0714	17.09	7.9	544-1804	295
5/18/69	0722	17.10	7.5	604-1784	295
5/18/69	0733	17.11	7.5	604-1674	290
8/4/69	0811	14.01	6.1	402-1380	325
8/4/69	0637	14.02	4.4	383-1072	285
8/4/69	0645	14.03	4.8	322-1038	315
8/4/69	0654	14.04	4.5	326-997	320
4/18/70	0608	10	5.2	375-1125	316
4/18/70	0621	11	5.5	375-1125	316
4/18/70	0631	12	5.3	330-1275	316
4/18/70	0645	13	5.0	500-1375	316
10/22/70	0750	004.1	2.9	354-552	300
10/22/70	0905	006	4.1	294-548	305

number of points over the microphone grid. The reduced scatter of the attenuation measurements for tests 004.1 and 006 on October 22, 1970 (see tables A-23 and A-24 in appendix A) is indicative of the improved time resolution. It will be shown later that the accuracy of the absorption data depends significantly on the accurate correlation of time and position information.

Acoustic Instrumentation

Acoustic instrumentation for data acquisition was contained in two vans, which were linked for communication by VHF radios, CB radios, or landline intercom systems. The functional checkout and precalibrations were performed at each van simultaneously. Figure 10 shows the microphone grid for each test series. The microphone height was 1.5 mtr for

the May and August 1969 tests and 1.2 mtr for all later tests. A microphone station consisted of a capacitor microphone, preamplifier, wind screen, power supply, microphone stand, and a twisted pair of shielded cable that ran from the test point to the instrumentation van. Each van contained the following equipment: a 14-channel transformer bank, 14-channel tape recorder preamplifier, 14-channel monitor oscilloscope, time code generator, 14-channel tape recorder/reproducer, RMS voltmeter, frequency counter, and dc voltage source.

All components of the test instrumentation systems were calibrated according to the manufacturer's specifications prior to use. An insert voltage calibration was performed on the entire microphone system after installation at Moses Lake. Before and after each test day a pistonphone was used to perform an end-to-end acoustical calibration of the system. The pistonphone signal was recorded on tape. The data reduction system was comprised of an analog magnetic tape playback unit, 24 parallel 1/3-octave-bandwidth filters, a multiplexer and analog-to-digital converter, a computer, and a digital magnetic tape recorder. Analyzers developed by Hewlett-Packard, Hydrospace, and General Radio have been used in reducing data from the various test series. The output data used in this report consist of 1/3-octave-band spectrum pressure levels analyzed at 0.5-sec intervals from each microphone in the grid.

Meteorological Measurements and Instrumentation

Meteorological measurements.—Measurements of wind, temperature, and humidity were recorded continuously during each of the test periods at a location representative of weather conditions in the test area. Wind and temperature were monitored at two locations in the microphone grid area to detect horizontal differences that might exist over the test range. In addition to the surface meteorological measurements, soundings of temperature and relative humidity were made to the height of the test aircraft at intervals of approximately 1 hr or less during each series of flights. The procedures used for interpolation of the soundings to obtain data at the required time and altitudes for each test flight are described in appendix B.

Meteorological instrumentation.—Standard wind systems with cup and vane sensors mounted on a mast or tower were used to measure the wind at the specified height above the ground. Analog recordings of wind speed and direction were made on strip charts during each test flight.

The ambient temperature was sensed by thermocouples housed in motor-aspirated radiation shields mounted on a tower or mast. The thermocouple was electrically referenced to 32° F, and its output of a 1-sec average temperature printed every 4 sec. Relative humidity was recorded as continuous analog data on a single-pen strip chart recorder. The signal was the output of a bridge circuit driven by a lithium chloride transducer protected from the sun by a radiation shield. A hand-held, wet-and-dry-bulb psychrometer aspirated by a battery-powered fan was used as a check on both temperature and humidity. Both thermometers were shielded from the sun by a white plastic cover.

A dial-type aneroid barometer was used to measure atmospheric pressure. Readings were recorded manually during the test period.

Temperature and humidity profile data were measured using a standard radiosonde system. The system uses a balloon to lift a small radio transmitter at an ascent rate of about 400 fpm. Temperature, humidity, and pressure are sensed sequentially, by means of a clock or pressure switch mechanism, at height intervals of 300 to 400 ft. The transmitted data are recorded on a single pen strip chart recorder. The radiosonde transmitters are modified to terminate transmission at 5000 ft to eliminate interference with subsequent releases.

The estimated accuracy of each meteorological sensor is given in table 4. The estimates are based on manufacturer's data on the accuracies of similar equipment specified in IRIG document 110-64. It should be noted that the accuracies listed in the table are sensor accuracies and not total system accuracies. Such errors are larger than those listed in the table but cannot be evaluated quantitatively.

Table 4.—Accuracy of Meteorological Instrumentation

Parameter	Type of equipment	Errors, rms
Surface		
Temperature	Hand-held thermometer	0.2° F
	Thermocouple (cu/con)	0.5° F
Relative humidity	Hand-held psychrometer	5%
	Lithium chloride sensor	5%
Pressure	Aneroid barometer	0.3 mb
Wind: Direction	Sensitive vane	3°
Speed	Three-cup anemometer	1 kn
Upper air		
Temperature	Rod thermistor	1° F
Relative humidity	Lithium chloride sensor	5%
Wind direction and speed		5 kn (vector)

ERROR ANALYSIS

In deriving the algorithm for absorption calculation it was assumed that errors, ϵ in equation (4), are present in the measurements, and the regression analysis was based on the minimization of that error term. Various statistical tests have been applied to the data, but all such statistical methods tacitly imply that the errors are randomly distributed. Tables of the estimated sample variance are given in appendix A for each of the 5760 regression line computations incorporated in this study. Each regression line represents an average of six to seven microphones, making a total of approximately 35 000 data samples used. These data points are not completely independent, however, and it is necessary to consider certain systematic error sources in evaluating the results.

The variance tables contain many values of four or less, corresponding to an rms deviation of less than 2 dB in the individual data points. There are cases where variances well

below one dB are associated with completely unreasonable absorption values. For example, a high confidence level, based on accepted statistical tests, may be attached to calculated positive slopes (negative attenuation), which would lead to the absurd conclusion that the atmosphere amplifies rather than attenuates sound. Systematic errors of various sorts are present in all experimental absorption studies. Much of the effort in the present study has been directed toward isolating and reducing these errors, although the problem can by no means be considered solved. Various error sources will be discussed in subsequent sections.

Acoustic Instrumentation Errors

This group of errors is easy to understand and somewhat within our capacity to control. During the 2-year period represented by the tests in this study, the Boeing Acoustic Laboratory has made major advances in its measurement technology—advances which are evident in the improved quality of the data. Recording equipment with preemphasis networks gives improved dynamic range at high frequencies, and new acoustic data reduction equipment has considerably improved the dynamic range for spectrum analysis that restricted earlier data.

Nevertheless, system noise is still a limitation. Since the atmospheric absorption at 10 kHz may run as high as 60 dB/1000 ft, and since the overall maximum dynamic range of the system is probably of the order of 75 dB, it is apparent that measurements taken over distances of 1000 ft or more are likely to encounter noise floor distortion. This distortion is easily detected with the plotting techniques employed in this study.

It should be noted that the requirements for dynamic range in acoustic measurements are defined here on the basis of the range in SPL of 1/3-octave frequency bands. The dynamic range must be adequate to cover the range in SPL over the twenty-four 1/3-octave bands of any individual spectra. In addition, the requirements for dynamic range are established by the variation in each individual 1/3-octave band time history obtained from acoustic data measured at each microphone as the test airplane passes overhead. The recorded data normally cover a range in perceived noise level from the maximum to a point 10 dB below the maximum before and after overhead time. Because of the frequency dependence of atmospheric absorption, the dynamic range required to obtain valid data increases as the propagation distance increases until the lower limit is reached at the ambient noise floor. For some acoustic data analysis purposes, the effect of spectral distortions at high frequencies may be insignificant, especially when the SPLs at the upper end of the spectrum are significantly below the dominant mid- and low-frequency bands.

Until recently it was necessary to rely on manual methods for excluding data that encounter a noise floor limitation. This has meant losing the data from the more distant microphones, even at low frequencies where absorption is small and longer baselines are desirable. Sometimes it has meant improving the results at high frequencies only at the cost of degrading the results at lower frequencies. Recently the automated procedures were modified to exclude data whenever the product of the distance and the ARP 866 standard absorption loss for the frequency band in question exceeds a predetermined limit—usually 45 to 50 dB. This limit reflects the dynamic range of the system in use at that time. This procedure has resulted in extending the frequency range within which the experimental

values agree with ARP 866, and in the case of some more recent test results, good agreement has been found up to the 10-kHz band.

In earlier test data, particularly where the climb angle is steep, it has been found that so many microphones are excluded at high frequencies by this method that a meaningful regression line cannot be plotted. When the number of microphones remaining is two or less the plots have been terminated short of 10 kHz. In any case, when the curves identifying differences between ARP 866 and experimentally determined absorption (appendix A, figs. A-1 through A-24) fall off sharply to negative values in the highest frequency bands it is an indication that the procedure was not fully effective in eliminating noise floor limitations.

The effect of instrumentation errors is strongly dependent on the position of the microphone in the array. A microphone near the center of the array, for example, will have little effect on the slope of the regression line, although it will change the intercept. Microphones at either extreme of distance will strongly influence the slope. Since the noise floor is generally encountered first at the large distances, noise floor limitations heavily affect the calculated absorption coefficients.

In general, the present acoustic instrumentation system meets the required accuracy except for limitations in the dynamic range discussed above. With low wind speeds a dynamic range of 100 dB is desired. As the wind speed increases, the requirements for dynamic range are reduced accordingly. With wind speeds of 3 kn or less a noise floor near -5 dB has been measured at Moses Lake. The effect of wind speed on the ambient noise floor increases nearly exponentially with increasing speed. The noise floor is increased by 30 to 40 dB at wind speeds of 8 to 10 kn, even though wind screens are used. Since much of the noise testing is conducted at low wind speeds, the increased dynamic range would result in a significant improvement in noise measurement, especially at high frequencies.

Aircraft Position Errors

A basic premise of this investigation is the interrelation of time and position. The first step in the analysis is the determination of sound spectra corresponding to specific directivity angles from the aircraft. The sound is recorded on tape along with a time synchronization code. Aircraft position from radar or other tracking methods is also recorded separately along with a time synchronization code. Some time after the test, the acoustic data are processed and rerecorded on a digital magnetic tape giving spectrum levels for 0.5-sec intervals. These intervals must be time related to the original time synchronization code. The primary aircraft time-position measurement system used by Boeing for the first series of acoustic tests in May 1969 was a modified, World War II, M-33, X-band radar. This equipment was better adapted to tracking at large distances than at the short distances and high angular rates encountered in low-altitude flyovers. For large jet aircraft flying only a few hundred feet from the radar, the angular size of the target makes skin tracking impractical, and problems have been encountered in the optimum location of the transponder.

Even small time errors are significant. For example, at an altitude of 500 ft the airplane passes through the range of directivity angles 120° to 75° in 1.4 sec. An error of 1 sec in overhead time can cause a difference of as much as 8 dB in calculated SPL values. Since data

samples are 0.5 sec in duration they do not accurately portray the rapid pressure level changes at the overhead point. Shorter data time samples present a dilemma, however, since they will not adequately integrate the time variations in the noise output of the airplane.

Time-position synchronization provided by the M-33, X-band radar during the 707 acoustic tests of May 1969 did not satisfy the precision required for absorption studies. Therefore, time traces for several of the 1/3-octave-band spectrum pressure levels were plotted and the aircraft overhead time selected by engineering judgment. An example of plots of spectrum level versus time is given in figure 11, showing the time history of the 250-, 1000-, and 2500-Hz spectrum bands for a particular test condition. The peaks do not exactly coincide, since the directivity patterns vary with frequency. The peak was determined, not by the actual maximum value, but from a visually smoothed curve resulting from overlaying the curves from several microphones. The overhead times represented by these peaks were converted to visual overhead times by subtracting the time of propagation over the appropriate altitudes. All the data from series 15 and 17 tests (May 1969) have been reprocessed using overhead times so determined.

Problems with the radar have now largely been resolved; however, even more accurate position data are obtained from the stadiometric cameras now in use. The improved position data, in combination with improved acoustic data, yield higher confidence in recent test results. Planning is now in progress to increase the accuracy of the stadiometric camera system without use of the radar by recording detailed attitude and roll information from the test aircraft's inertial navigation system. This information will be used to obtain greater accuracy with the stadiometric cameras than is now possible.

Doppler Shift

Since the test aircraft is moving at speeds of near one-third of the speed of sound, consideration must be given to possible doppler shift phenomena on the attenuation measurements. Following the convention in which the directivity angle ϕ is measured from the aft of the aircraft, the relation of the doppler-shifted frequency f_d as heard on the ground, with relation to the frequency f_m moving with the source, is given by

$$f_d/f_m = C_A/(C_A - V_{ac} \cos \phi), \quad (10)$$

where C_A is the sound speed and V_{ac} is the velocity of the aircraft. Since only measurements made at the same angle ϕ are compared, the doppler effect should not contribute any inaccuracy; however, if there is an overhead time error, the true angle ϕ may be quite different from the one assumed, and a substantial error may result. This is particularly evident in strong discrete tones such as a fan tone in the 2500-Hz band. It could result in a comparison between a tone on the approach side of vertical with one on the departure side, where at low altitude the tone may shift by a full 1/3-octave band or more. This is possibly the source of the erratic results in the 2500-Hz band that have been reported in earlier studies.

Ground Reflection Interference

It has frequently been observed that the periodicity of absorption coefficients (or differences between ARP 866 and experimental coefficients versus frequency) at the low frequencies bears a strong resemblance to the periodicity of the spectral response of a single microphone as recorded over a reflecting surface. This type of interference curve has been studied in some detail at Boeing, both for acoustically hard surfaces and for porous surfaces (ref. 8), and will only be summarized here. Since there is a time difference between the sound path reaching the microphone directly from the source and that reflected from the ground, certain wavelengths will arrive in phase over both paths, leading to pressure doubling at some frequencies, while other wavelengths will be in phase opposition, leading to pressure minima. When the surface is acoustically hard (i.e., has a very large and real acoustic impedance), like concrete or water, it can be shown that the lowest frequency f_0 at which a minimum occurs is given by

$$f_0 = r C_A / 4 h_m h_s, \quad (11)$$

where r is the direct distance from source to microphone, h_m is the height of the microphone above the surface, h_s is the height of the source, and C_A is the sound speed. When the source is approximately overhead, r is nearly the same as h_s and the expression reduces to

$$f_0 = C_A / 4 h_m \quad (11a)$$

Thus, the first minimum f_0 occurs at approximately 70 Hz for a 4-ft microphone height. For microphones on the centerline below the flightpath this frequency changes only slightly for the directivity angles used in this study. For example, with a typical 5° climb angle the frequency would be 77 Hz for the maximum 120° directivity angle. Minima will appear in the spectrum response curve at all odd multiples of this frequency, and maxima will occur at $2f_0$, $4f_0$, etc. When the surface is porous, like natural soil, sand, or vegetation, the computation is considerably more complex. Calculations have shown, however, that for these near-normal incidence angles the frequencies of maxima and minima are very little different over soil from those over concrete. This is definitely not the case for the angles encountered in measurements at the 1500-ft sideline. Not only is the slant distance very much greater than the height, but the basic equation (11) cannot be used without making allowance for the phase shift due to reflection from the porous surface. The position of the lowest minimum is thus shifted to a lower frequency and the harmonic relationship of the various maxima and minima is destroyed. This is shown graphically in figure 12, which is a plot of the actual spectra at a 90° propagation angle for two microphones on the centerline and one microphone on the sideline. Note that the curves of the centerline microphones are very similar at the lower frequencies, even of distances differing by nearly 1000 ft, while the microphone at a distance of 1700 ft (1500-ft sideline microphone) gives a completely different curve. The difference in the curve shape is clearly reflected in figures 13 and 14, which were calculated from the same flight test data with and without the sideline microphones.

These results indicate that sideline microphones should not normally be used for absorption measurements if the lower frequencies are of any concern, unless the effect of incidence angle and surface impedance can be calculated and taken into account. This is a matter of particular concern in absorption measurements obtained from a level flight using

microphones perpendicular to the flightpath. Conceivably a compensation procedure could be developed for measurements over a uniform surface like water or concrete.

Meteorological Error Sources

It should be emphasized that the experimental attenuation coefficients derived by methods described previously include other atmospheric effects in addition to losses from the absorption of sound by molecular processes. These other effects include distributive losses from refraction and dissipative losses from turbulent scatter and air motion. These losses cannot be evaluated separately and appear as a portion of the error term ϵ . A further error results from the failure of meteorological instrumentation to measure accurately the temperature and humidity over the actual sound path.

Since all of the known atmospheric effects are expected to increase attenuation, the overall results of this study indicate that systematic meteorological errors are not present. It is possible that various errors in meteorological measurements are compensating or that they are compensated by errors from other sources. It is more likely, however, that within the time period of a single flight, meteorological errors may be systematic but are small because of the limitations of weather conditions allowable for acoustic testing.

Errors in upper air measurement result primarily from (a) lag in the sensors when large vertical gradients are present, (b) the assumption of horizontal atmospheric homogeneity, and (c) the assumption that atmospheric parameters vary linearly with time. There is a need for measurements of turbulence at greater heights above the ground than are now possible. Further research is needed to evaluate the effects of turbulence on noise propagation. Primary sources of error in meteorological measurements are discussed below.

Errors in meteorological measurements.—The accuracy of meteorological measurements from sensors mounted on towers or masts near the ground is generally considered to be adequate when compared to accuracies inherent in acoustic measurements. Small horizontal variations in wind, temperature, and humidity have been observed over the microphone grid area, but their effect on noise propagation from an airplane several hundred feet above the ground is considered to be insignificant.

The method of obtaining profile measurements of temperature and humidity by use of a free-rising balloon has inherent inaccuracies whose magnitude depends on such factors as sensor accuracy and response, balloon ascent rate, and sample rate of the various parameters measured. Errors caused by lag in sensor response as the balloon rises depend largely on the magnitude of vertical temperature and humidity gradients. Figure 15 shows the effect of 5% and 10% errors in relative humidity versus frequency at a temperature of 50° F and an average relative humidity of 40%. An error of 10% in a humidity profile is not unusual, especially at humidities below 30% and above 90%, or when the humidity decreases rapidly with increasing height.

Atmospheric variability.—Surface atmospheric measurements are not normally representative of the atmospheric layer from the ground to altitudes of several hundred feet. In the surface boundary layer, which usually varies in thickness from 150 to 300 ft, the

temperature and humidity depend largely on radiation effects and turbulent mixing. In the absence of strong wind flow, (i.e., with low levels of turbulence), nighttime cooling results in profiles of temperature, relative humidity, and atmospheric absorption coefficients such as those shown in figure 16, measured during test 10 on April 18, 1970.

All seasons of the year, except winter, are covered in the series of tests used in this study. Figure 17 is a plot of temperature versus relative humidity for all of the test flights included in this report. Surface values of temperature and humidity are indicated by a different symbol for each test series. Plots of upper-air data are indicated by a different type of cross hatching or shading for each test. The NASA tests (15 series) and Boeing tests (17 series) conducted in May 1969 are grouped together in this figure since the soundings overlap. These test series covered a 4-day period and varied in time of day from 0553 to 1054. Values of temperature and humidity are plotted to the maximum height for which acoustic data were recorded. Isolines of computed absorption coefficients (ARP 866) for 6300 Hz are shown as solid lines in the figure. Patterns of lower frequency coefficients are similar, except that they have lower absorption rates. Some of the flights which occurred within a short time interval, such as the four tests on April 18, 1970, are shown as a single shaded band.

Another source of error results from differences in the atmosphere between the measurement points and the sound path from airplane to microphone. Use of the method (described in appendix B) for calculating atmospheric absorption for a stratified atmosphere assumes a uniform horizontal stratification of the atmosphere, and further, that the changes between consecutive soundings are linear with time of day. Neither of these assumptions is strictly valid for all times, but the first is not unrealistic for the stable, fair-weather conditions that prevailed during the tests used in this report. With soundings at time intervals of 1 hr or less the second assumption should not produce serious errors in the calculated absorption coefficients.

It has been suggested that the interaction of the atmosphere and the test airplane may affect sideline noise measurements. Wing-tip vortices may produce atmospheric disturbances over the microphone grid area but should not influence the noise at the directivity angles used in this study. Consecutive passes of the 747 airplane within a time period of a few minutes have produced remarkably similar noise spectra and time histories. Since most of the flights used in this study have been under conditions of strong thermal stability, it appears that the restorative forces of a stable atmosphere were sufficient to damp the oscillation in a short period of time.

Atmospheric gradients.—Since sound velocity in air depends on temperature, humidity, and wind, vertical gradients of these factors determine vertical speed-of-sound gradients. The speed of sound is approximately proportional to the square root of the absolute temperature plus the component of the wind vector along the propagation path. The effect of wind is usually much greater than that of temperature. For example, a change of 10° F in temperature causes a change of only 1.4 mph or 2 fps in the speed of sound. On the other hand, a wind component of 10 mph, or 15 fps, changes the speed of sound by the same amount. For a broadband noise source at distances and directivity angles used in this study the effects of refraction by wind and temperature gradients should be small, except at far sideline distances where angles with respect to the horizontal ground surface are much smaller

than the directivity angle at the source. Wind profile measurements were not available for most of the test; however, visual tracking of the radiosonde balloon indicated that vertical wind gradients were small. No clear evidence of refraction effects was found in the noise measurements analyzed in this study, with the possible exception of test 004.1 on October 22, 1970. There is not sufficient detailed information available to explain such effects, which were absent in test 006 conducted 1 hr and 15 min later.

Atmospheric turbulence.—The effects of turbulence on noise propagation, and on measurements observed in laboratory experiments and from theoretical treatment of effects of atmospheric turbulence, remain to be verified by field experiments with a large, moving noise source that generates a large amount of turbulence itself.

It is generally agreed that the spectrum of atmospheric turbulence is continuous over a range from low frequencies, corresponding to eddy sizes so large they can hardly be classified as turbulence, to high frequencies where eddy sizes approach the scale of molecular motion. Though the precise effects of atmospheric turbulence on noise propagation are not known, there appears to be a strong dependence on the frequency and directional characteristic of the noise source. For a highly directional point source, atmospheric turbulence scatters and spreads the sound energy over a broader sector, causing an apparent attenuation in excess of that from spherical divergence and atmospheric absorption.

For sound traveling over short distances near the ground surface, turbulence may cause a phase shift which produces distortions in the interference patterns between direct and reflected sound waves. Variation over a period less than the sample length of acoustic data may effectively obliterate the characteristic dips and peaks expected in still air. Atmospheric turbulence may also cause a similar fluctuation in frequency and amplitude of a tone with higher SPLs than at adjacent frequencies. The effect on the measured spectrum will depend on the period of fluctuation caused by turbulence and the acoustic data sample length used in the analysis. The shorter the sample length, the greater the effects of fluctuations in SPL caused by turbulent eddies.

Although turbulence was not measured during the tests included in this study, it can be concluded that its effect on the calculated attenuation coefficients is negligible for two reasons. First, the stable atmospheric conditions and low surface wind speeds during all tests strongly inhibited turbulence caused by mechanical or frictional effects. Second, the slopes of the regression lines from which attenuation coefficients are calculated would be unaffected by losses caused by turbulence in the lower layer of the atmosphere, since the effects of turbulence in the lower boundary layer would have the same effect on SPLs measured at all microphones.

SUMMARY OF TEST RESULTS

This investigation is one of several field studies that have sought either to verify the validity of ARP 866 as applied to aircraft flyover measurements or to demonstrate a need for its revision. Among these studies are those by Hale (ref. 9) and by Bishop and Simpson (ref. 10), who have shown that, over a limited frequency range at least, and for the meteorological conditions covered in their studies, the validity of ARP 866 cannot be challenged

within the confidence limits of their data. The present study leads to the same conclusions, but it is now possible to extend the frequency range over the entire test spectrum from 50 to 10 000 Hz, provided adequate precautions are taken in measuring and processing data. The tests included in this study represent a much larger range of weather conditions than previous studies, and all ARP 866 values have been computed using a stratified atmosphere based on radiosonde measurements near the test time and location.

The results of the 24 test runs are reproduced in appendix A. Each solid curve is the mean of the difference between ARP 866 and experimental attenuation coefficients at 10 source directivity angles from 75° to 120°. Distinguishable points are plotted for five of the 10 angles, providing an indication of the data spread and also showing any evidence of an obvious systematic variation with angle. On the facing pages are tables of the sample estimate of variance for each frequency and each angle, including the number of microphone data points used in the regression line analysis. The number of microphones decreases at the high frequencies because automatic limiting excludes those microphones below the expected noise floor. When the number of microphones falls below three, the results are meaningless. Zeros are used to identify those conditions with less than three microphones. Tests of the Boeing 707 airplane in May 1969 were divided into two series interspersed in time. Series 15 tests were performed under NASA-approved conditions within the prescribed meteorological test window. Test series 17 included flights when meteorological conditions were marginal and, in one case, outside the test window. Figure 18 is a composite plot of the six tests of series 15, and figure 19 is a similar composite of the eight runs included from series 17. The most significant difference in the averages of the two series is in the three highest frequency bands. This was produced by the difference in data processing. The series 15 data were processed using a double pass through the analyzer, with substantial improvement in dynamic range.

Data from ten test runs of the 747 airplane are included in this report. Four tests were run on August 4, 1969, and are identified as series 14. Four were run on April 18, 1970 and two on October 22, 1970. The 1970 test series are identified by date and condition number only. These latter test series represented a further improvement in acoustic equipment dynamic range, since preemphasis networks were used giving an 18-dB/octave boost above 5 kHz, and improved spectrum analysis instrumentation was employed. Since aircraft altitude changes were small over the centerline microphone grid for the October 22 tests, sideline microphone data have been used to increase the propagation distances. The sideline measurements tend to increase the low-frequency periodic distortion attributed to ground reflection. The large positive values of attenuation difference at high frequencies in condition 004.1 on October 22 have been traced to the sideline microphone, number 13. It is believed that a cross-wind gradient caused the excessive high-frequency loss at this microphone. Sideline data were included only in these two test runs. Composite plots of differences between ARP 866 and experimental attenuation coefficients for each of the 747 test series are shown in figures 20, 21, and 22. Figure 23 is a composite plot of all three 747 test series.

The combined means of the six series 15 test conditions, of the eight series 17 tests, and of the ten tests of the 747 are plotted together in figure 24, and the final mean of all 24 conditions is given in figure 25. Ignoring the high-frequency dropoff caused by the noise floor in the earlier tests, and a slight residual ground reflection interference generated by the

sideline microphones in the October 22, 1970 data, the overall curves of the three sets of data are remarkably close together and are very close to the zero line. The experimental values do lie slightly below zero—about 1 dB/1000 ft on the average. If this value had been positive, it would have been tempting to explain the excess loss, almost independent of frequency, as arising from turbulence or some other meteorological process, but this is not the case. It cannot be justified by saying that ARP 866 produces too large attenuation values, because the negative value persists below 1000 Hz (band 14), where the ARP 866 coefficient becomes negligible. It may be that an explanation can be found in second-order effects related to ground interference, but for the present the slight negative attenuation difference is not believed to be significant.

CONCLUSIONS

There is a strong case, in the results of this study, for the validity of ARP 866 at all frequencies from 50 to 10 000 Hz, and over a large portion of the meteorological test window. There does not appear to be an increase in deviation from ARP 866 calculations when measurements are taken during weather conditions slightly outside the currently recommended test window—note the similarity in series 15 and 17 tests—although further study of the curves may identify certain conditions concealed in the averaging where ARP 866 might not be accurate. Additional data under more extreme conditions are needed before assurance can be given that the current test window can be widened. The effect of both parallel and crosswind components should be studied, as well as the effect of wind components and vertical gradients. More accurate and detailed wind measurements will be required to describe the atmosphere for such an investigation.

This study has shown the need for processing a very large number of data samples and the importance of accurate, reliable measurements of acoustic test parameters. Only by using data from a number of microphones and a relatively large number of directivity angles can statistically significant data samples be obtained. The method of analysis and data presentation used in this study is capable of treating a very large number of data points at reasonable cost and, at the same time, providing a means of tracing data back to individual microphones. This characteristic has been useful in identifying, and in many cases eliminating, systematic error sources.

There is little doubt that some of the apparent inconsistencies in acoustic test results previously attributed to ARP 866 can now be traced to deficiencies in acoustic test measurements. Because of their wider dynamic range and better position information, much higher confidence is attached to the results of recent tests than to those performed before April 1970. Only a few of these tests have been used, however, because the flight conditions required for atmospheric absorption studies with the present procedure were not generally those required for certification testing. With minor changes to the data processing routine, it should be possible to utilize more of the recent test results, but time did not permit extending further the data range in this study. It is highly desirable that absorption studies be extended to include meteorological conditions not covered at present.

Increased data accuracy in recent Boeing tests should also make it possible to identify and evaluate effects of changes in test variables which were previously overshadowed by the effects of measurement errors.

Improved atmospheric measurements could make it possible to increase the range of weather conditions suitable for acoustic testing. The present restricted window tends to reduce the effects of errors in present meteorological measurements to a level comparable to those from other measurement errors.

The Boeing Company
Commercial Airplane Group
Seattle, Washington, March 1971

APPENDIX A

ESTIMATED SAMPLE VARIANCES AND SUMMARY PLOTS OF DIFFERENCES BETWEEN EXPERIMENTAL AND ARP 866 ABSORPTION COEFFICIENTS

Tables A-1 through A-24 give the estimate of sample variance S^2_{dy} of the 24 flight tests included in the analysis. The number of microphones used in the data analysis is given within each table.

Figures A-1 through A-24 are summary plots of the differences between measured and calculated absorption coefficients. The curves were obtained by averaging 10 directivity angles from 75° to 120° for each one-third-octave frequency band.

The dates and number of flight in each series of acoustic tests included in the report are listed below:

Series 15, May 1969	six flights
Series 17, May 1969	eight flights
August 4, 1969	four flights
April 18, 1970	four flights
October 22, 1970	two flights



APPENDIX B

ATMOSPHERIC ABSORPTION COMPUTATION USING ARP 866 FOR A STRATIFIED ATMOSPHERE

In passing through the atmosphere, sound is absorbed by molecular processes that are strongly dependent on the temperature and humidity. The standard procedure recommended for calculating this absorption is given in SAE ARP 866. A Boeing computer program implements this procedure, giving the absorption in dB/1000 ft for each 1/3-octave frequency band for a given temperature and relative humidity.

The real atmosphere is not homogeneous in temperature and humidity, however, and this procedure cannot represent the total sound path. If the humidity and temperature at every point on the path could be known, the total absorption could be defined as

$$\text{Loss} = \int \alpha(H, T) \cdot dR \quad (\text{B1})$$

where R is the length of the propagation and α is the local attenuation along the path.

Under normal test conditions, humidity and temperature are generally quite uniform along a particular horizontal plane, but they may change materially as a function of height. As a good approximation to equation (B1) we may consider the atmosphere to be made up of a finite number of horizontal strata, each with a uniform temperature and humidity, and with a known thickness. The total absorption is then given by

$$\text{Loss} = \sum_{i=1}^K (\alpha_i \cdot d_i)$$

where K is the number of layers, α_i is the absorption coefficient in each layer, and d_i is the distance traversed by the sound within each layer.

Temperature and humidity are normally obtained from radiosonde equipment mounted on a free-rising balloon and transmitted by radio at discrete heights, which may vary with the rise rate of the balloon. Measurements are taken at regular intervals before and during the flight test period. The measurement times will not in general coincide exactly with the time of a particular test condition. Thus, the first step in utilizing the meteorological data is an interpolation between the measurements, both in time and in altitude, to give an approximation of the temperature and humidity at the time of each test condition for each of a number of standard heights: usually ground level, 125 ft, 250 ft, and each successive 250-ft increment up to the maximum altitude from which acoustic data are to be used.

The absorption coefficient is computed using the conditions at each standard height, and the value α_i is taken as the mean value between two adjacent heights. In the case of the layer containing the aircraft, the actual height of the aircraft is used instead of the standard stratum boundary for computing the upper absorption coefficient. The total loss is then calculated by equation (B2), summing the products of loss rate and distance traversed for each stratum up to the aircraft.

The accuracy of this procedure obviously depends on the accuracy of the radiosonde measurements, and also on the amount of interpolation required. Since the thermal and humidity gradients may be steep near the surface, frequent radiosonde readings are desired at the beginning of the ascent. Some judgment is required to determine how quickly the atmosphere is changing, so measurements will reflect accurately the situation for each flight test condition, without increasing test expense by taking soundings more frequently than needed. Particular care must be taken with tests shortly after sunrise, when the atmosphere may be changing rapidly.

REFERENCES

1. *Standard Values of Atmospheric Absorption as a Function of Temperature and Humidity for Use in Evaluating Aircraft Flyover Noise*, Society of Automotive Engineers, Inc., Aerospace Recommended Practice (SAE ARP) 866, August 31, 1964.
2. Nyborg, W. L., and D. Mintzer, WADC Technical Report 54-602, Wright Air Development Center, Wright Patterson AFB, Ohio, May 1955.
3. Harris, C. M., "Absorption of Sound in Air in the Audio-Frequency Range," *J. Acoust. Soc. Am.*, 35, 1963, pp 11-17.
4. Harris, C. M., *Absorption of Sound in Air Versus Humidity and Temperature*, NASA Contractor Report NASA CR-647, NASA, Washington, D.C., January 1967.
5. Federal Aviation Regulation, Part 36, Noise Standards: Aircraft Type Certification
6. *Study and Development of Turbofan Nacelle Modifications to Minimize Fan-Compressor Noise Radiation*, NASA Contract Report CR 1711 through 1717, NASA Langley Research Center, Hampton, Virginia.
7. Dixon, W. J., and Frank J. Massey, Jr., *Introduction to Statistical Analysis*, McGraw-Hill Book Company, 1969.
8. Oncley, P.B ., *J. Sound Vib.*, 13 (1), 1970, pp 27-35.
9. Hale, R. T., *An Investigation into Atmospheric Absorption Using B.A.C. Air to Ground Measurements*, Acoustics Report No. 156, Issue 2, British Aircraft Corporation, October 1968.
10. Bishop, D. E., M. A. Simpson, and D. Chang, *Experimental Atmospheric Absorption Values from Aircraft Flyover Noise Signals*, NASA CR-1751, 1971.

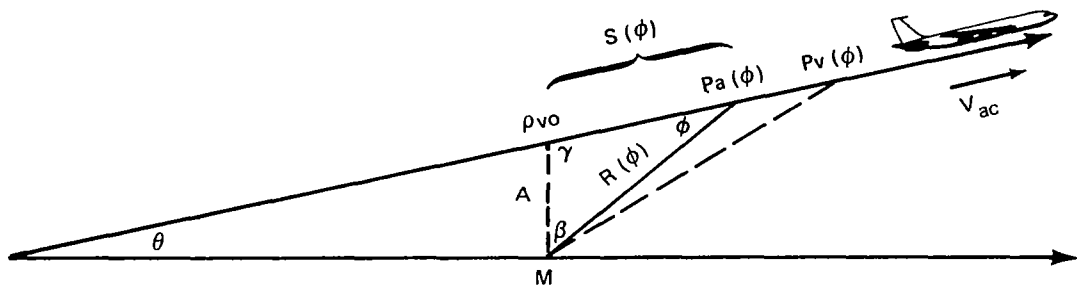


Figure 1. Geometric Representation of Test Approach

TEMP = 56 °F REL. HUMIDITY = 30%

BOEING 707 - MAY 1969

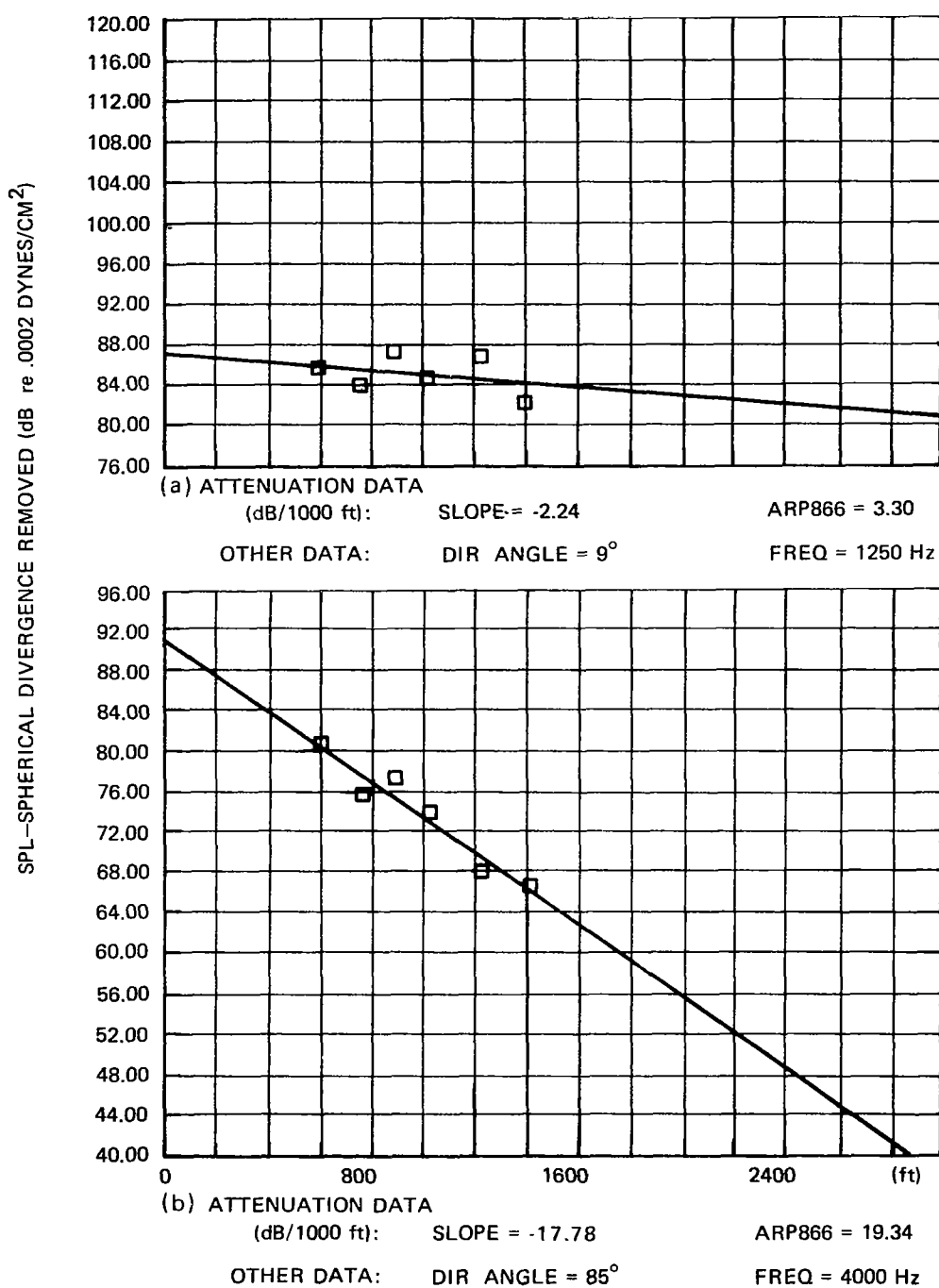


Figure 2. Typical Plots of Y' vs Distance for Condition 17.11

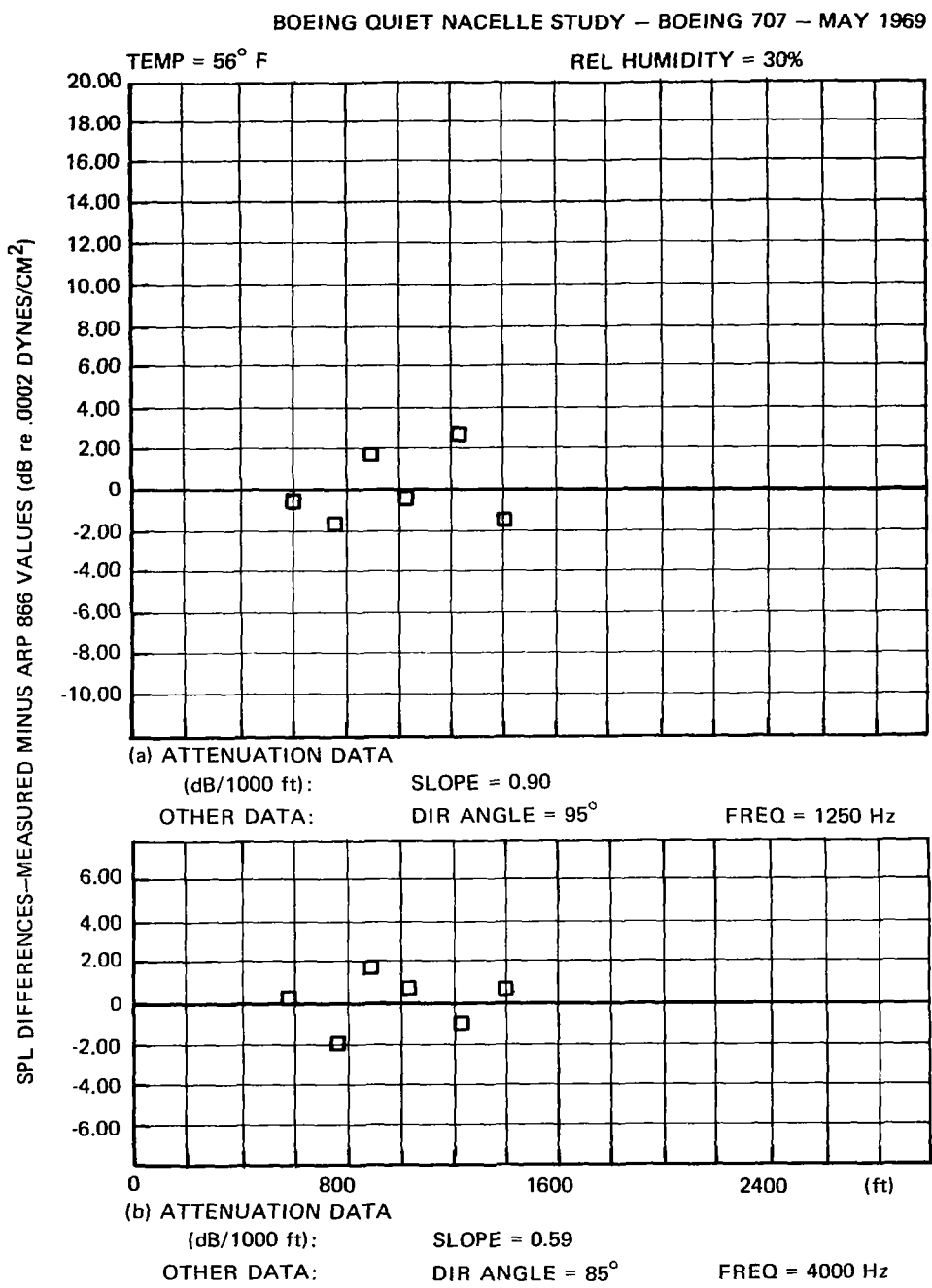


Figure 3. Typical Plots of Y'' vs Distance for Condition 17.11

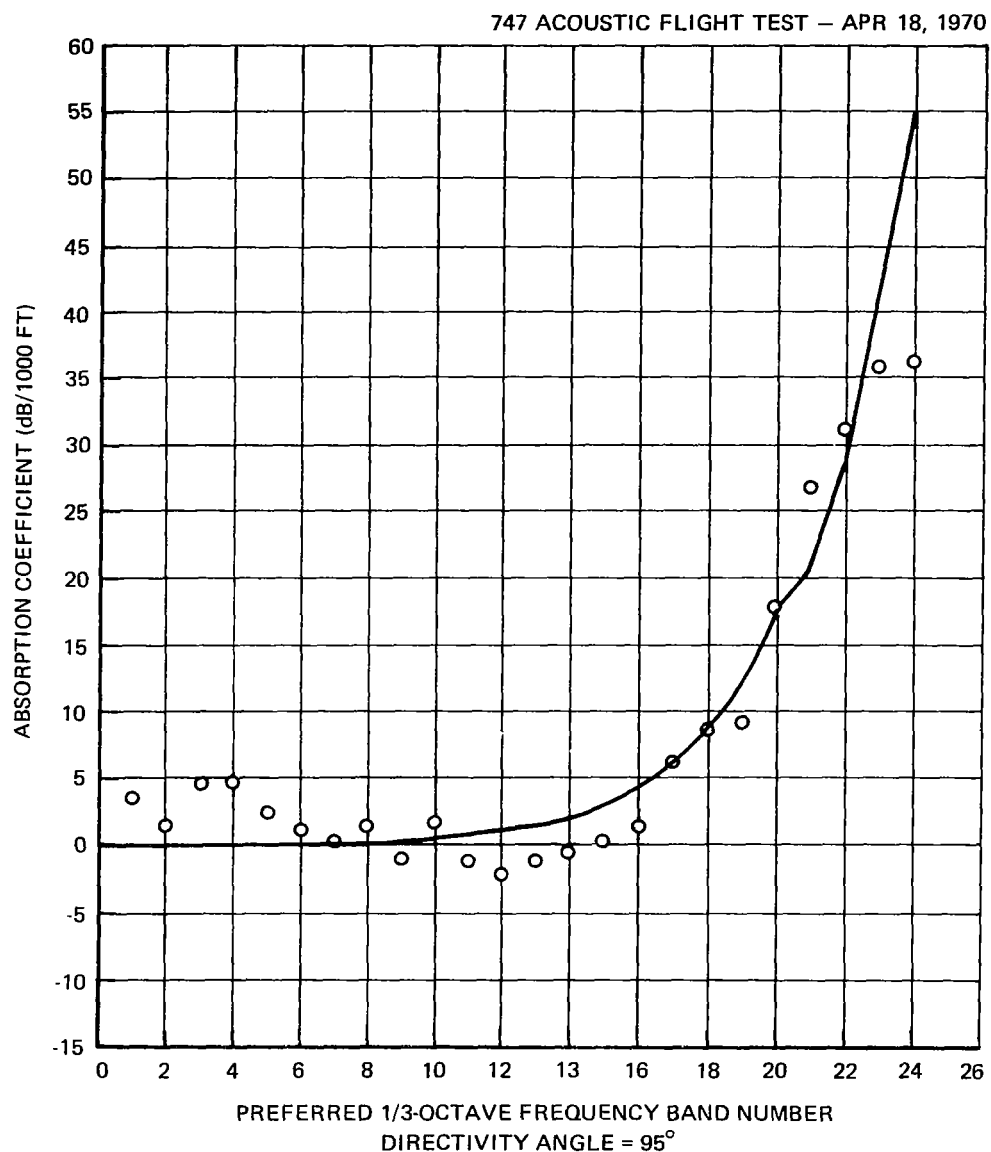


Figure 4. Experimental Values of Absorption Coefficient vs Frequency for Condition 12 (Solid curve represents ARP 866 values for average meteorological conditions)

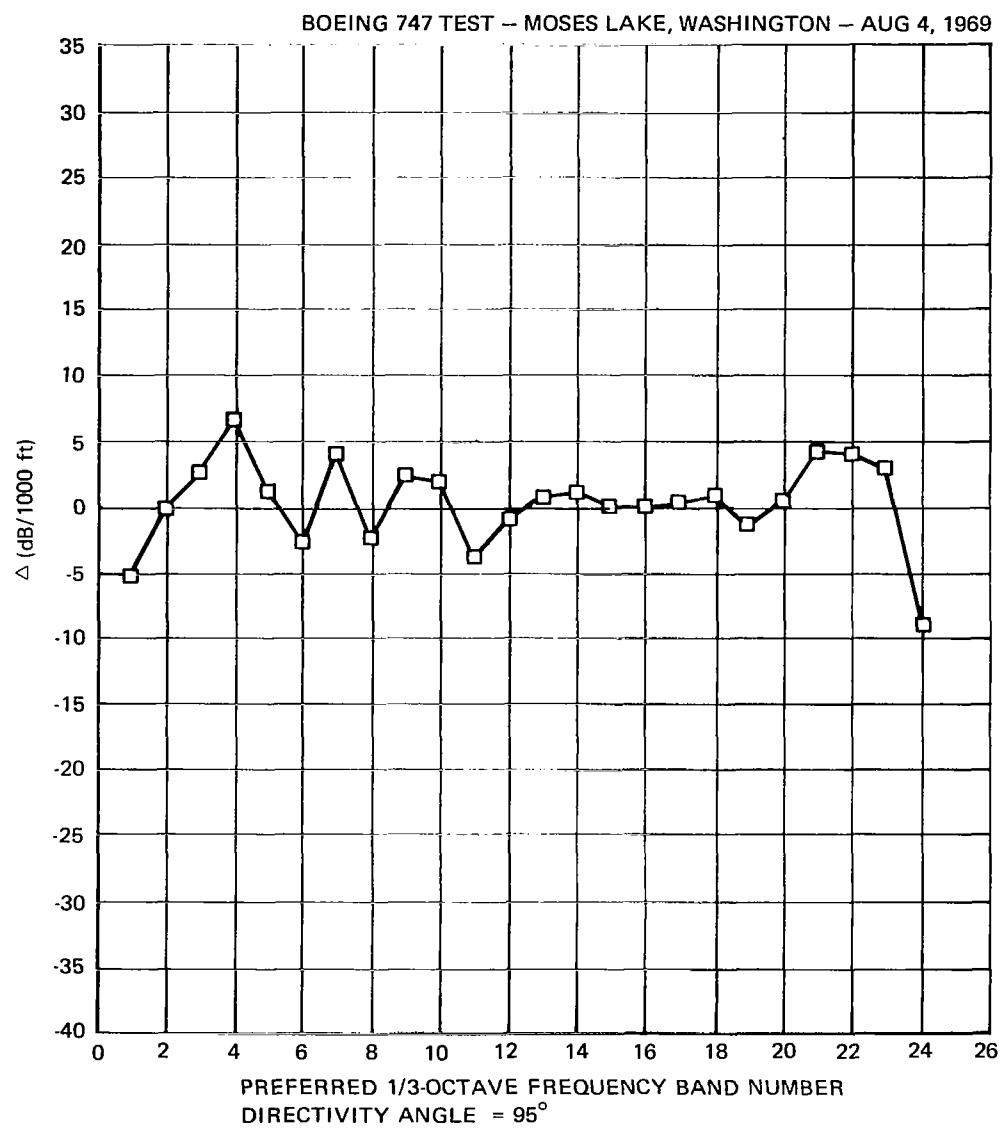


Figure 5. Differences (Δ) Between Experimental and ARP 866 Absorption Coefficients for a Stratified Atmosphere—Condition 14.01

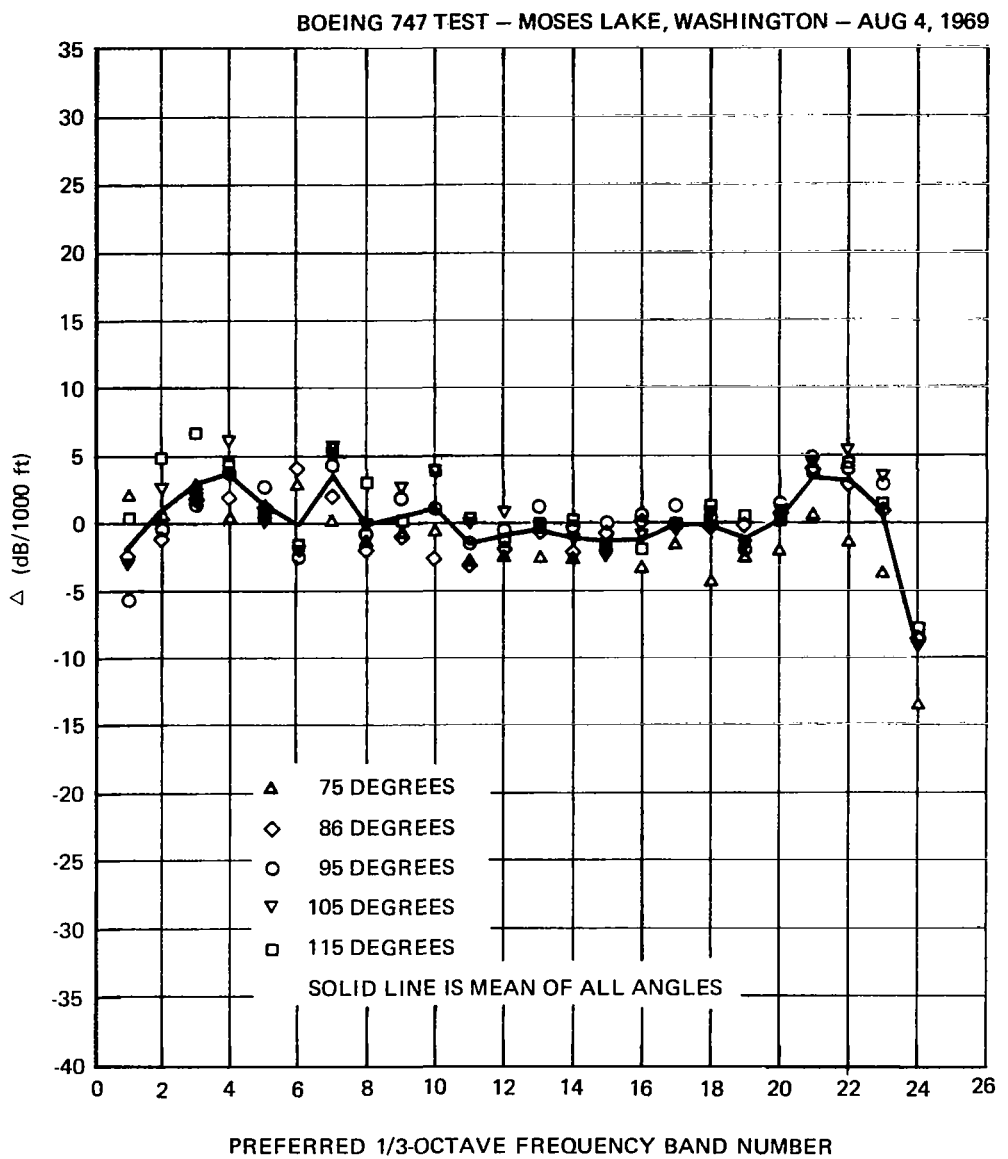


Figure 6. Summary Plot of Differences (Δ) Between Experimental and ARP 866 Absorption Coefficients for All Angles—Condition 14.01

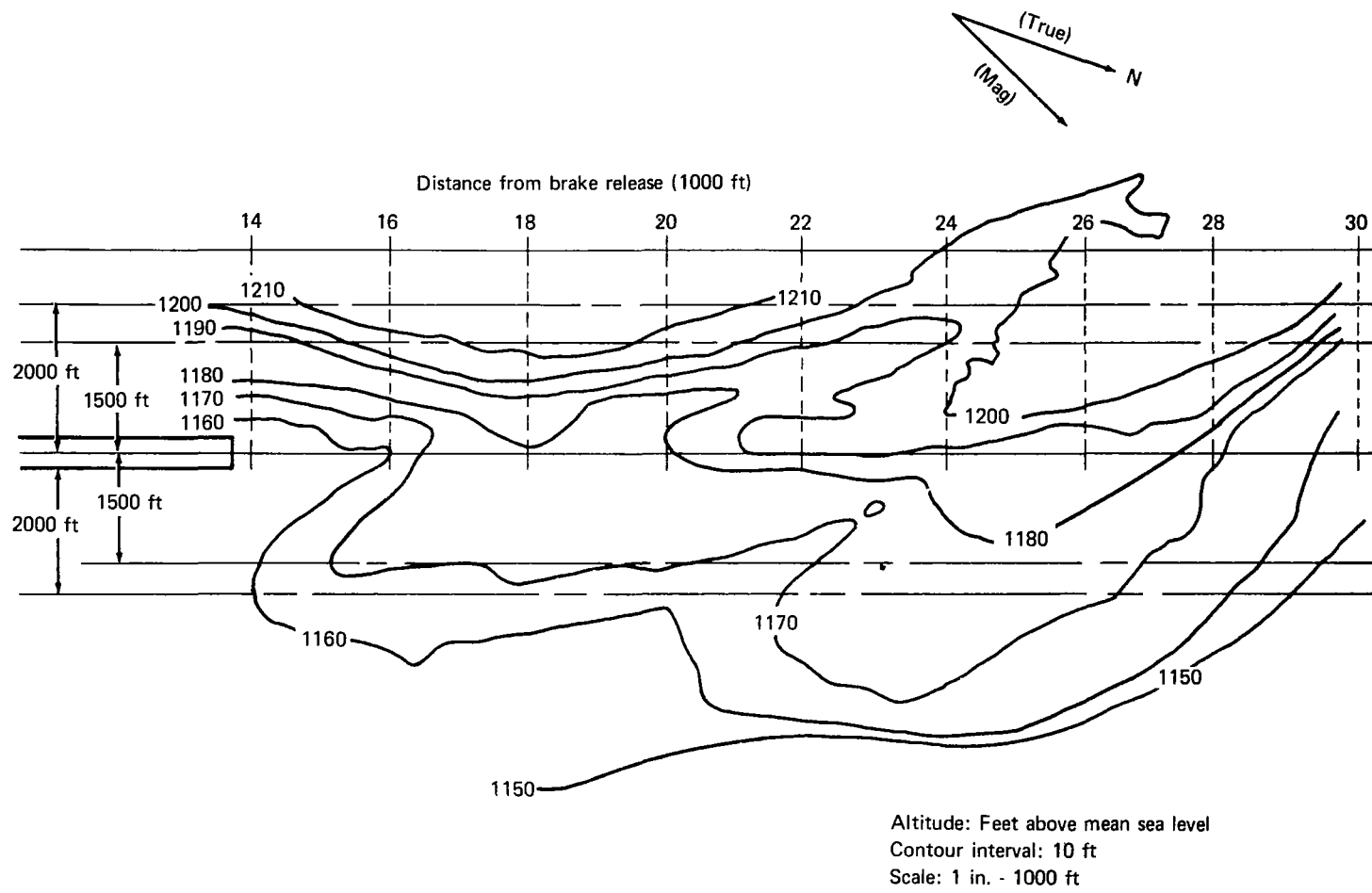


Figure 7. Topographical Map of Grid Area, North End of Runway 14L-32R, Grant County Airport

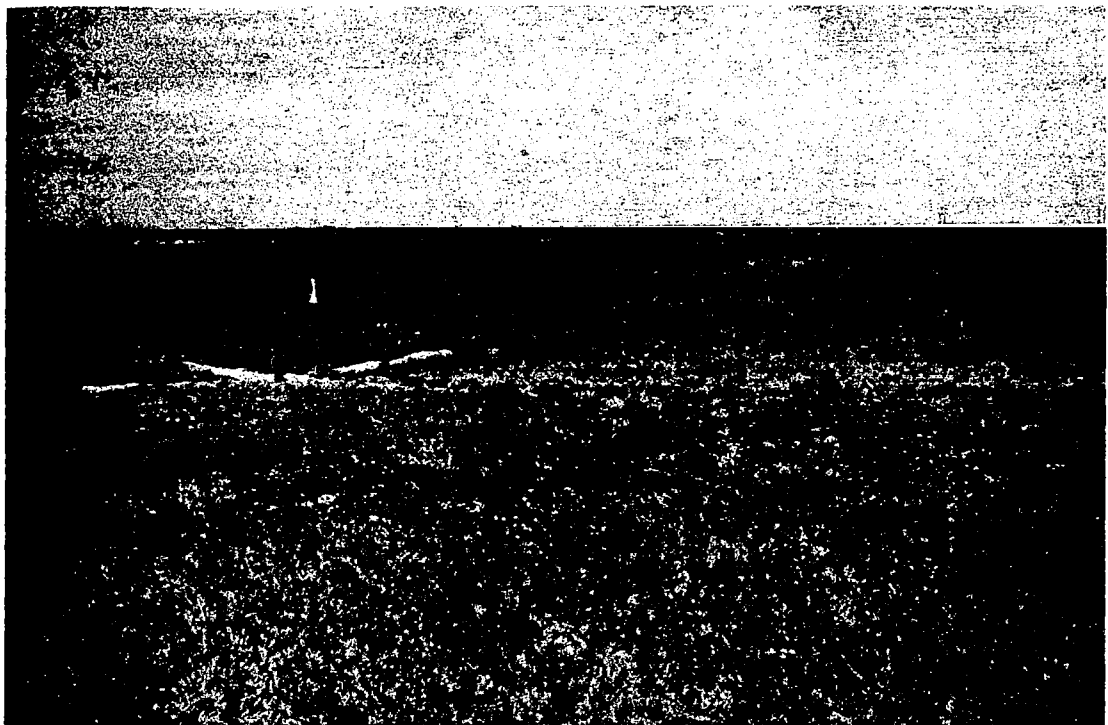


Figure 8. Typical Terrain, Grant County Airport, Moses Lake, Washington

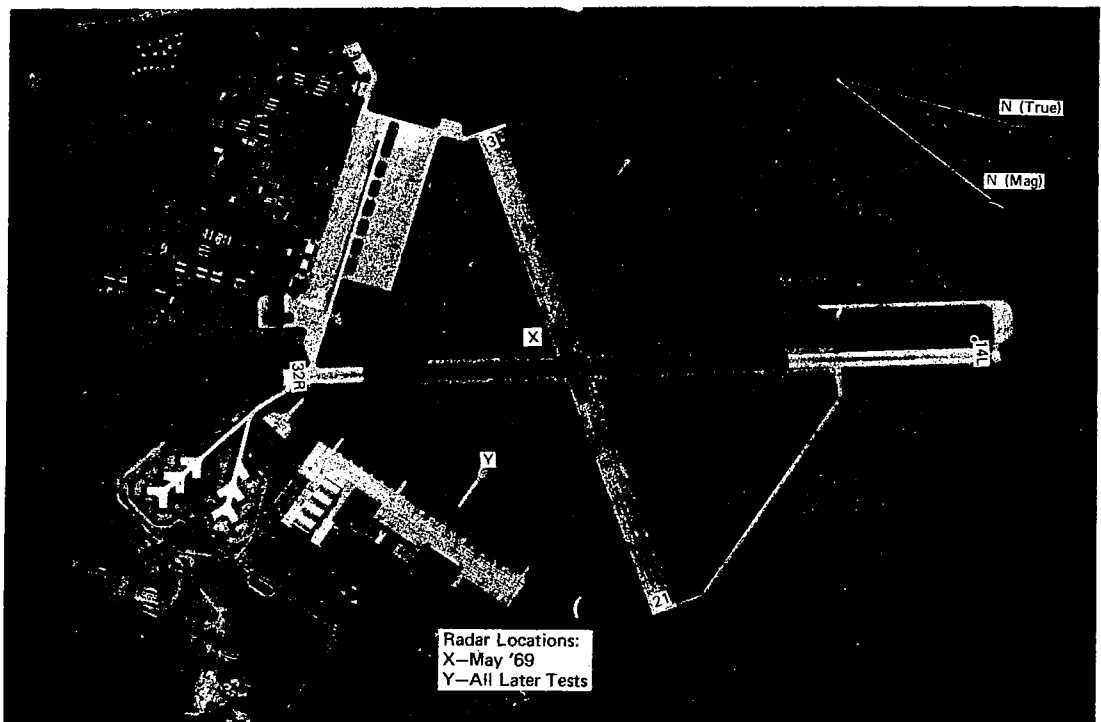
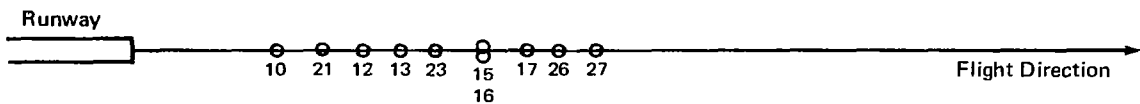
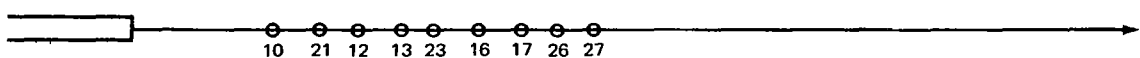


Figure 9. Aerial View of Airport and Facilities, Grant County Airport

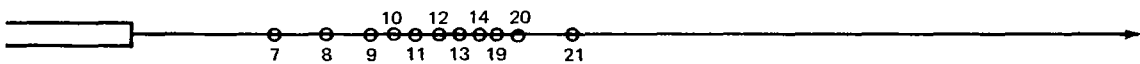


(a) Series 15 and 17, May 1969 (707) (Microphone height 1.2 m)

True N
Mag N



(b) Series 14, August 4, 1969 (747) (Microphone height 1.5 m)



(c) April 18, 1970 (747) (Microphone height 1.2 m)



(d) October 22, 1970 (747) (Microphone height 1.2 m)

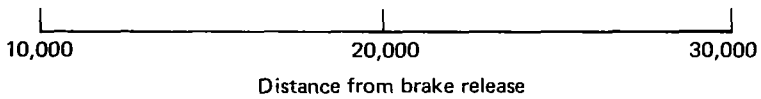


Figure 10. Microphone Grid Layout

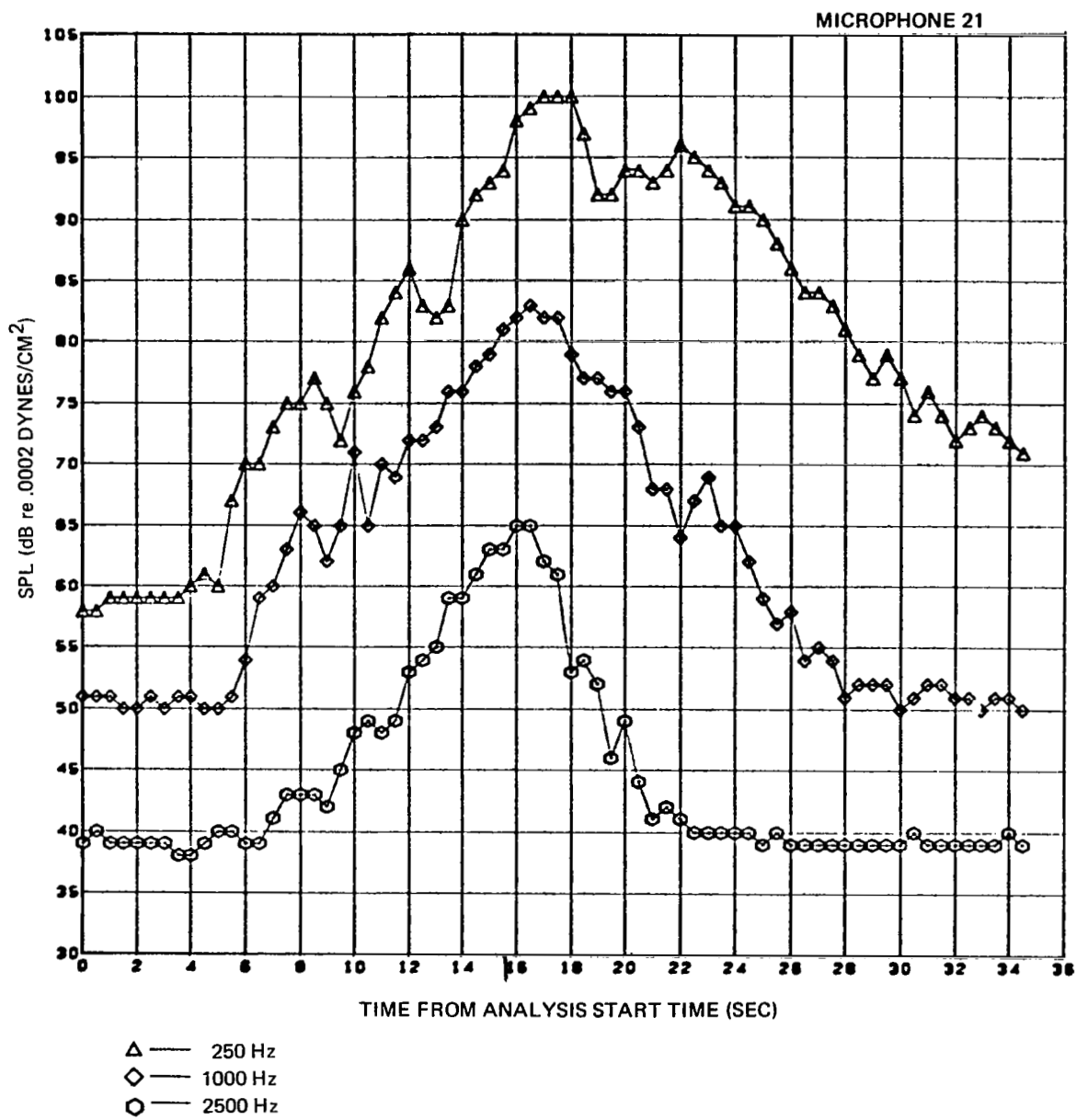


Figure 11. Time History for Test 17.11 on May 18, 1969

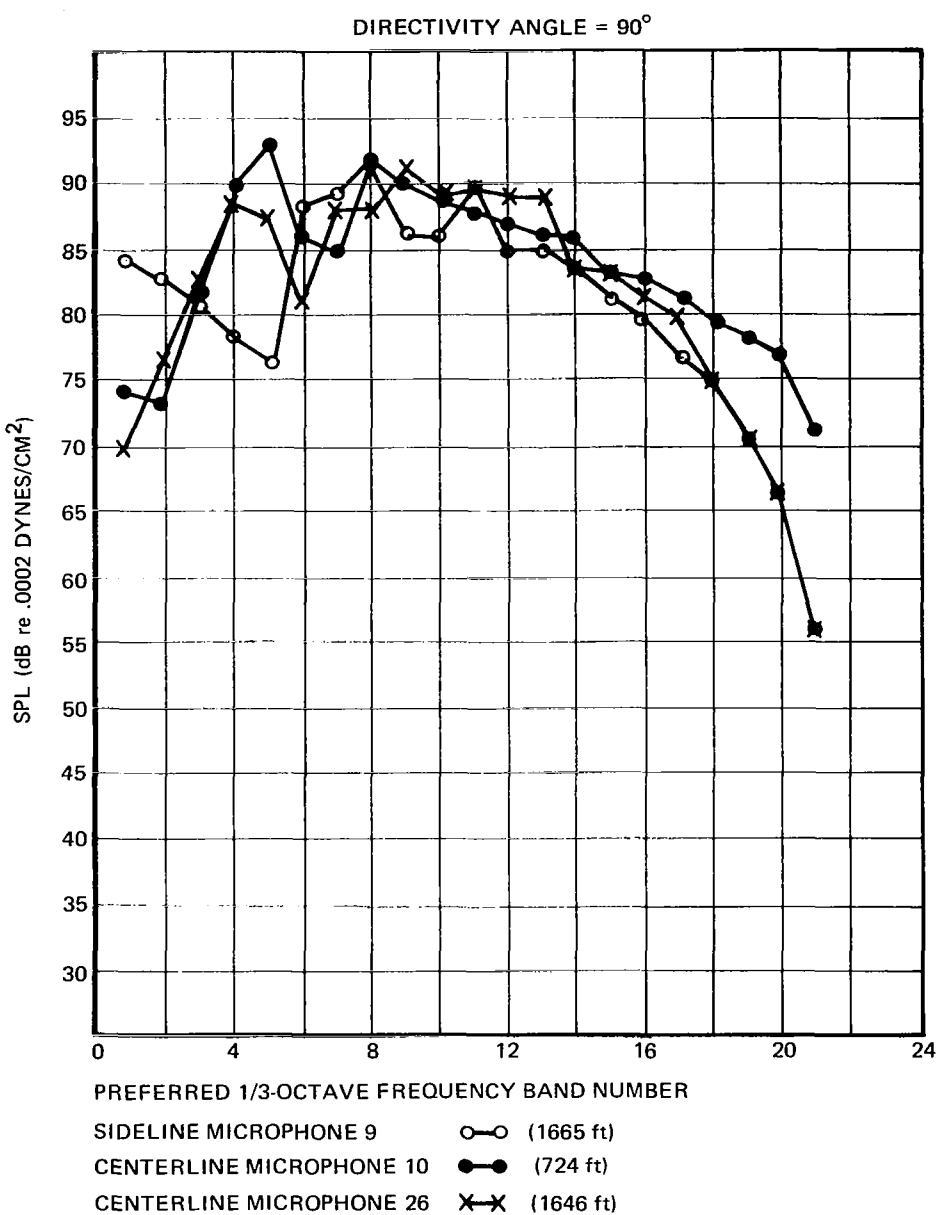


Figure 12. Ground Reflection Effects in Center and Sideline Data for Condition 15.02

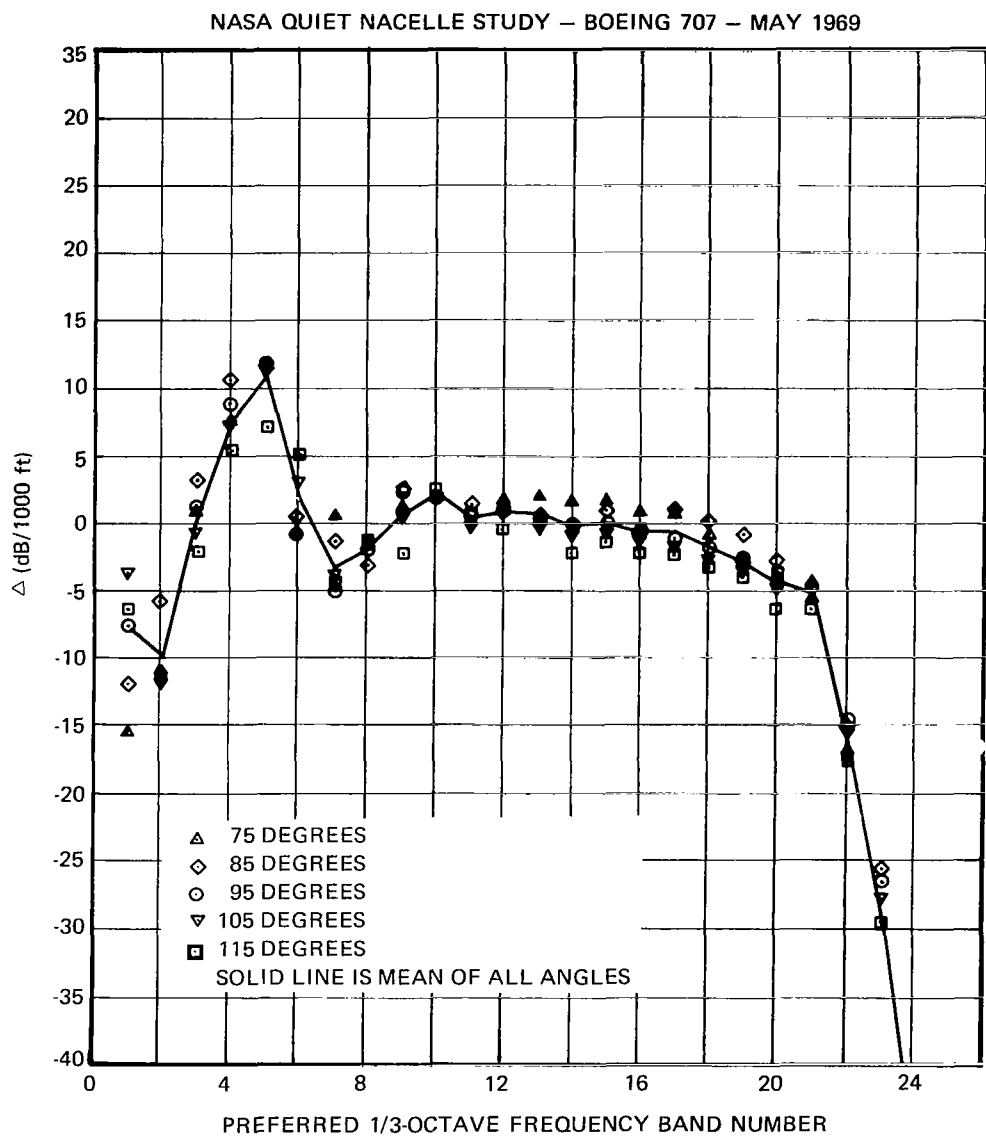


Figure 13. Differences (Δ) Between Experimental and ARP 866 Absorption Coefficients for Condition 15.01 (With Sideline Microphones)

NASA QUIET NACELLE STUDY – BOEING 707 – MAY 1969

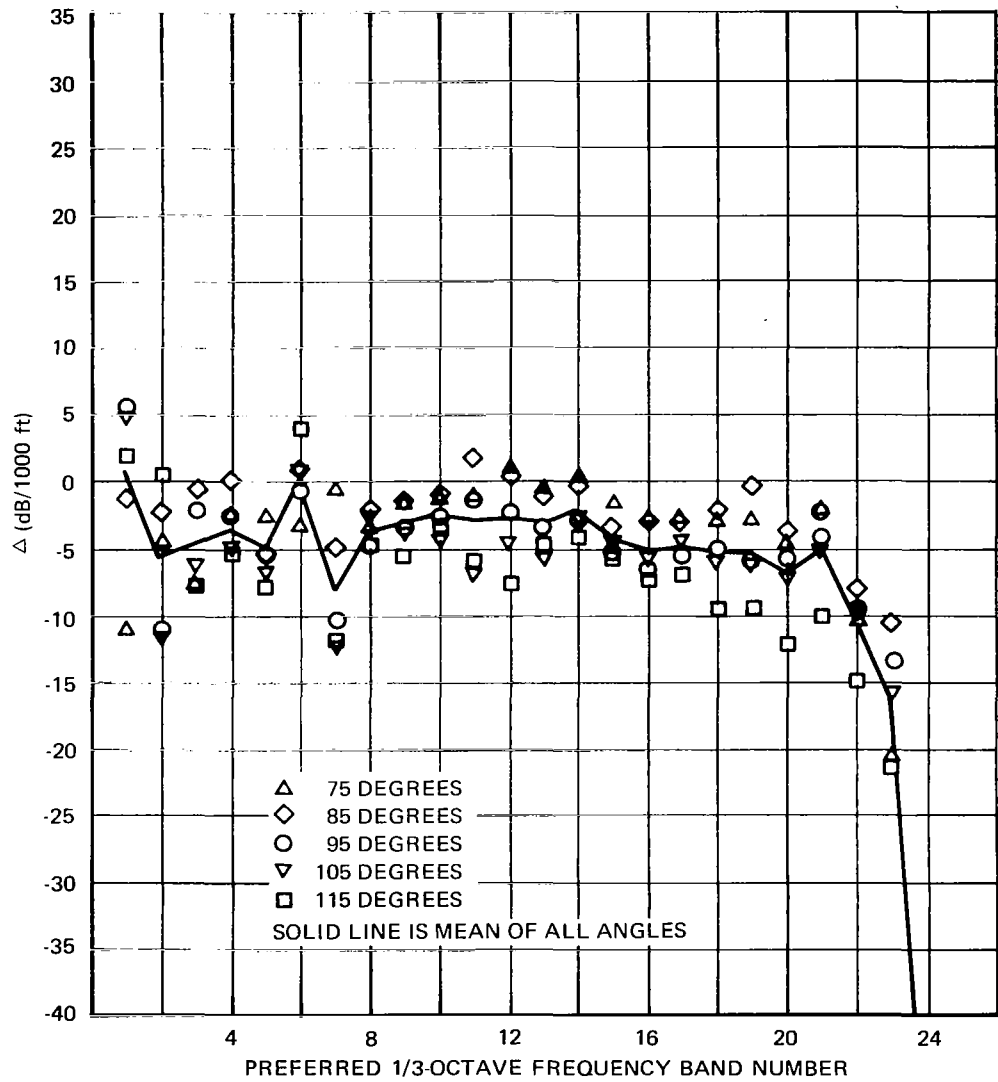


Figure 14. Differences (Δ) Between Experimental and ARP 866 Absorption Coefficients for Condition 15.01 (Without Sideline Microphones)

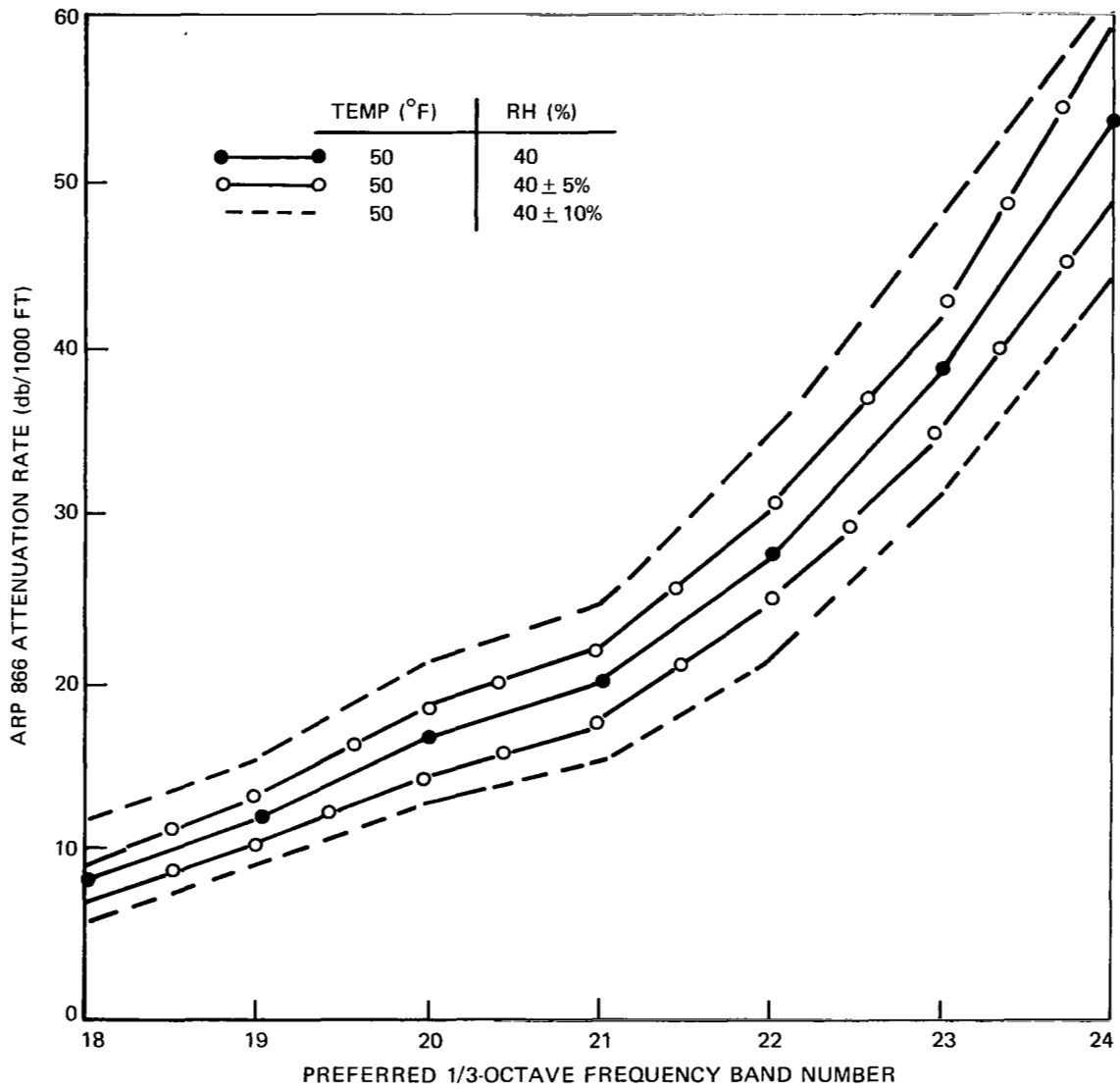
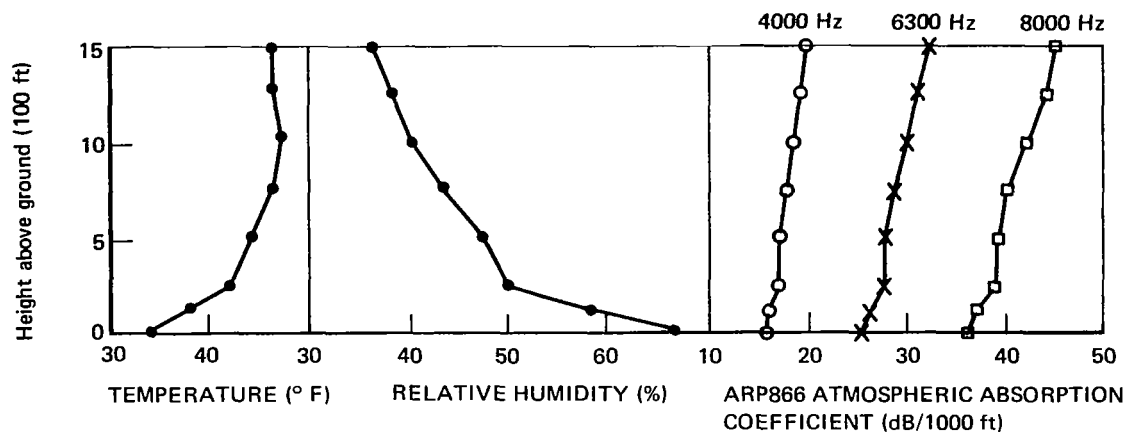


Figure 15. Range of Attenuation Rates for $\pm 5\%$ and $\pm 10\%$ Error in Relative Humidity (ARP 866)



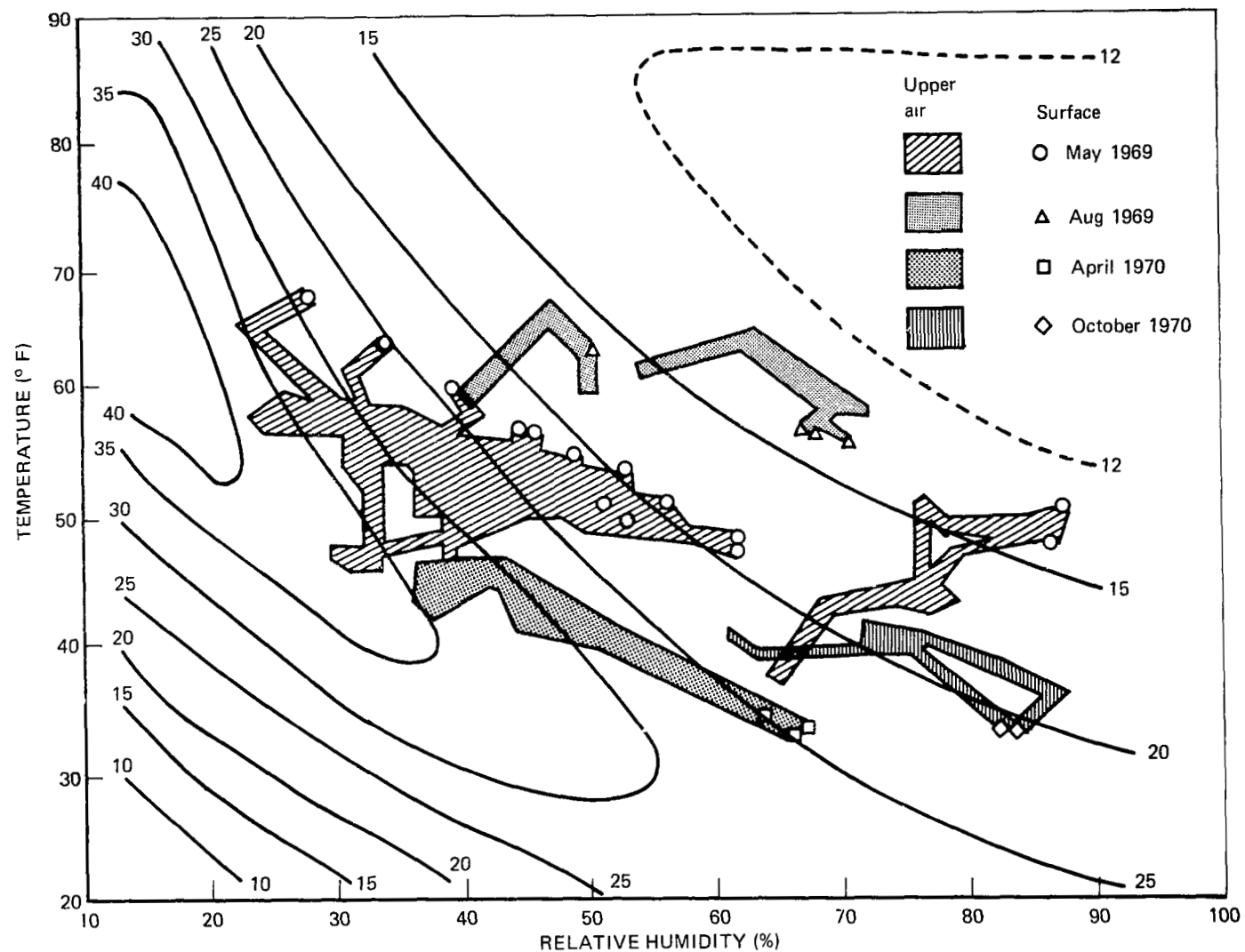


Figure 17. Range of Temperature and Relative Humidity from Surface to Height of Flightpath
(Solid Lines are ARP 866 Absorption Coefficients—6300 Hz, dB/1000 ft)

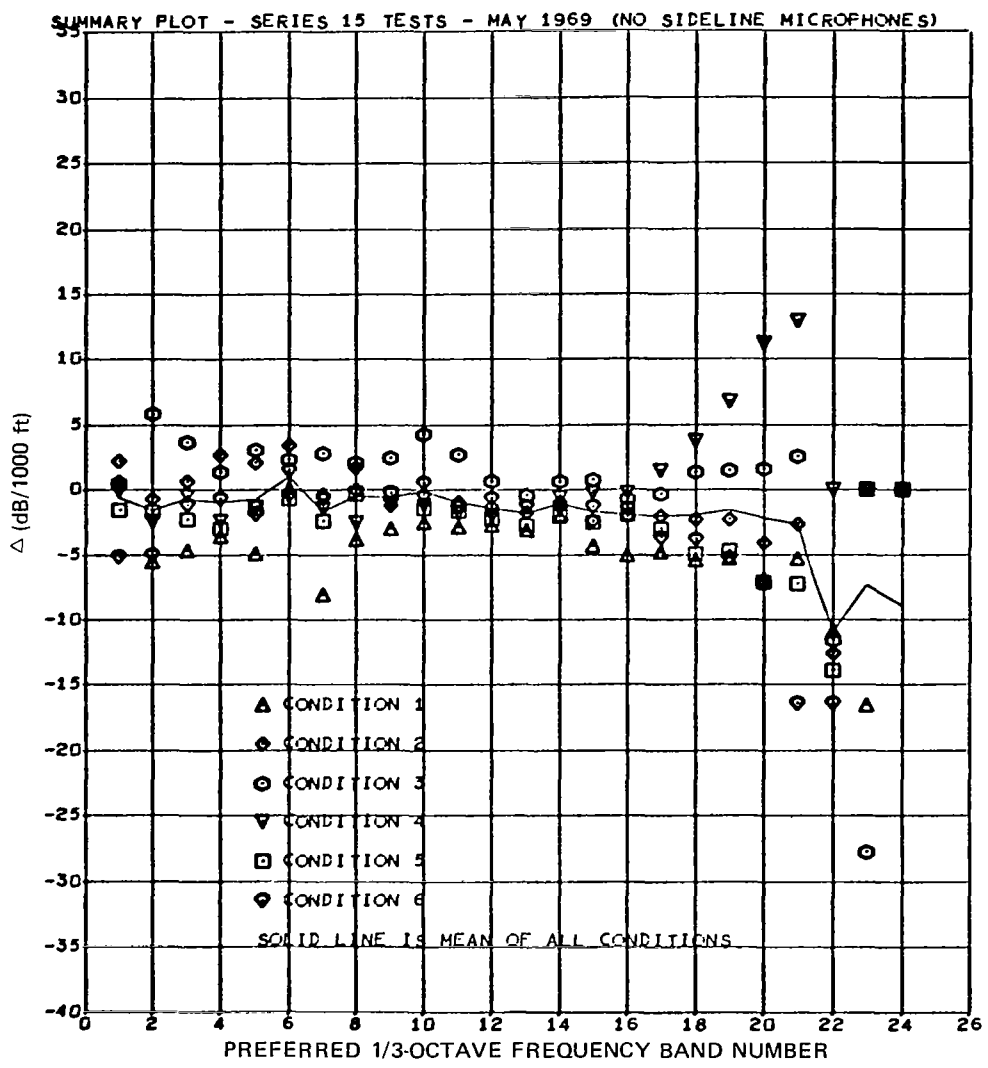


Figure 18. Composite Plots of Differences (Δ) Between Experimental and ARP 866 Absorption Coefficients for each of the Six 707 Tests in Series 15

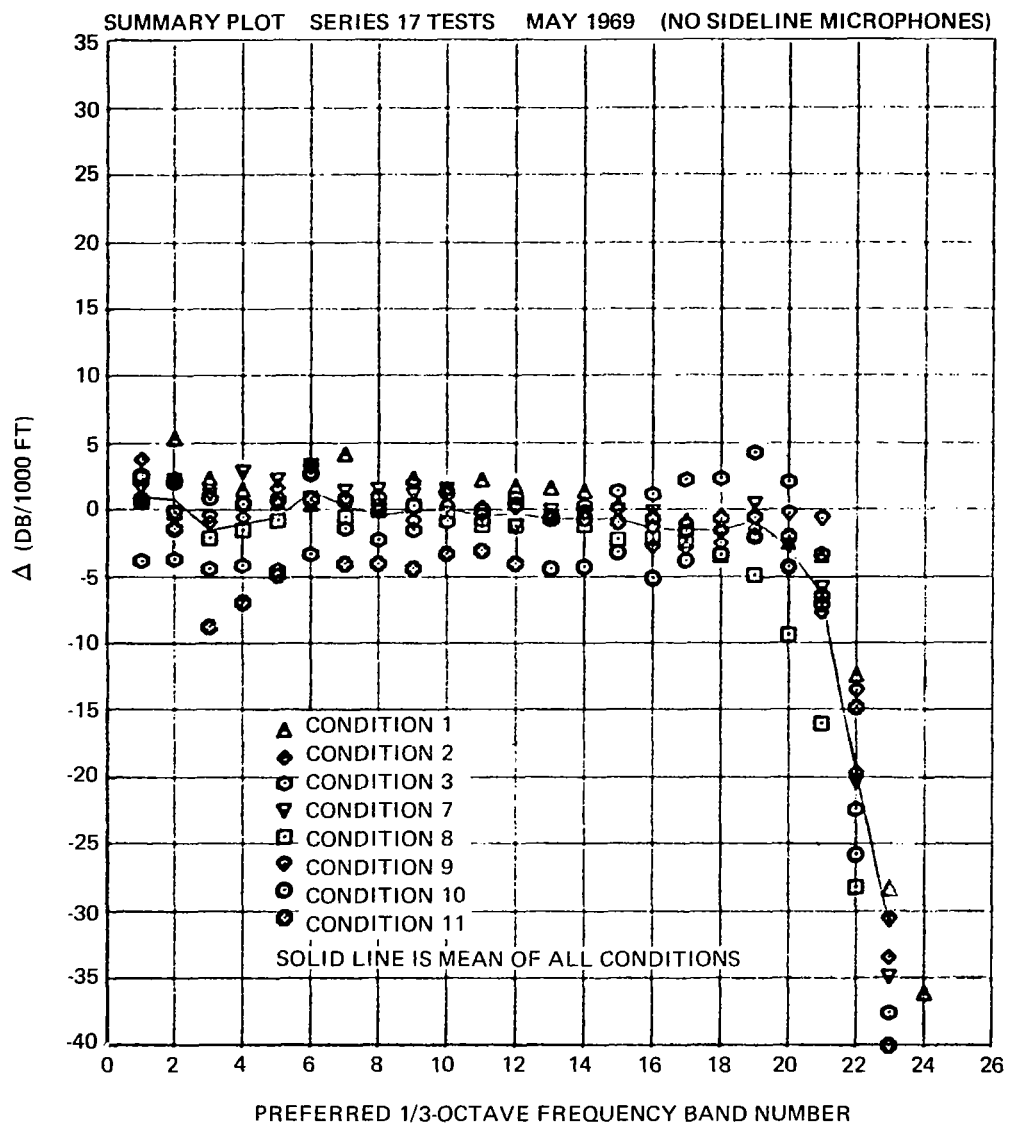


Figure 19. Composite Plots of Differences (Δ) Between Experimental and ARP 866 Absorption Coefficients for Each of the Eight 707 Tests in Series 17

SUMMARY PLOT – SERIES 14 TESTS – AUG 4 1969 (NO SIDELINE MICROPHONES)

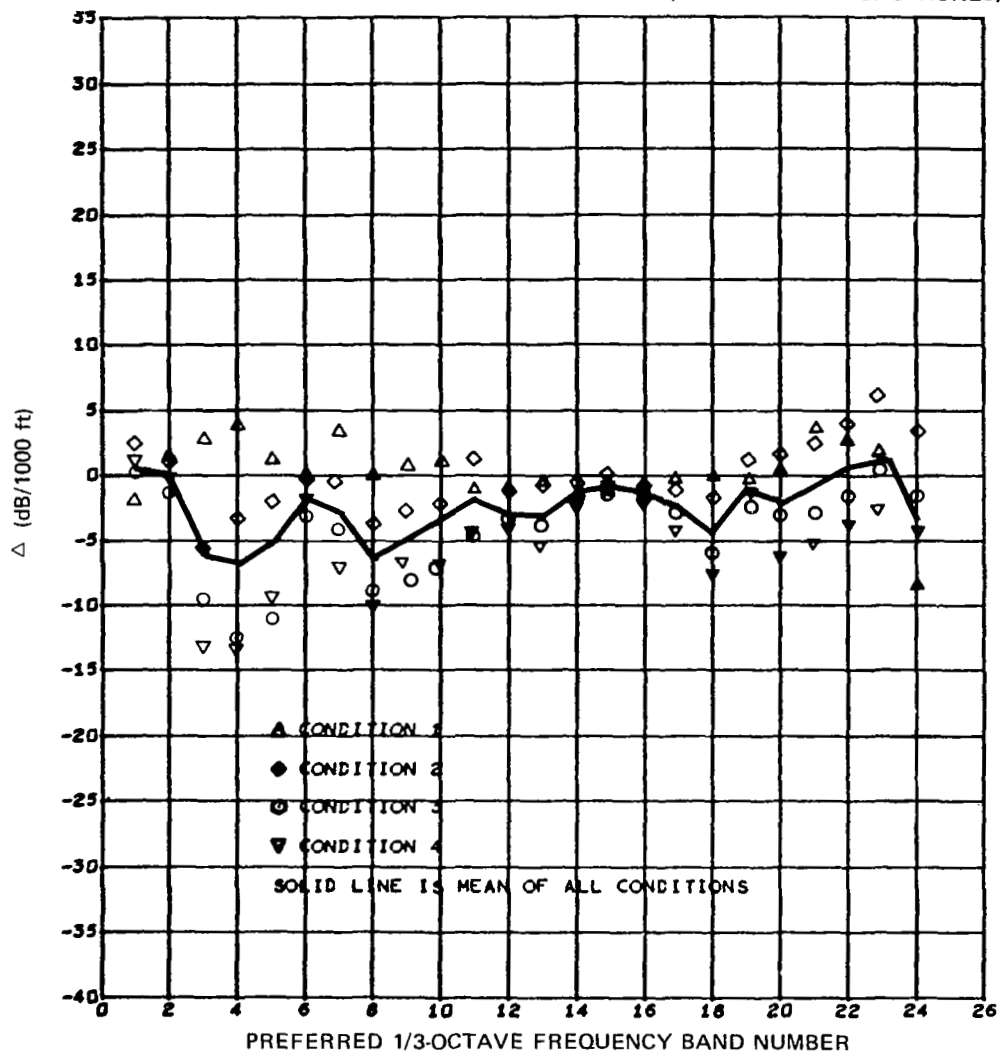


Figure 20. Composite Plots of Differences (Δ) Between Experimental and ARP 866 Absorption Coefficients for Each of the Four 747 Tests, August 4, 1969

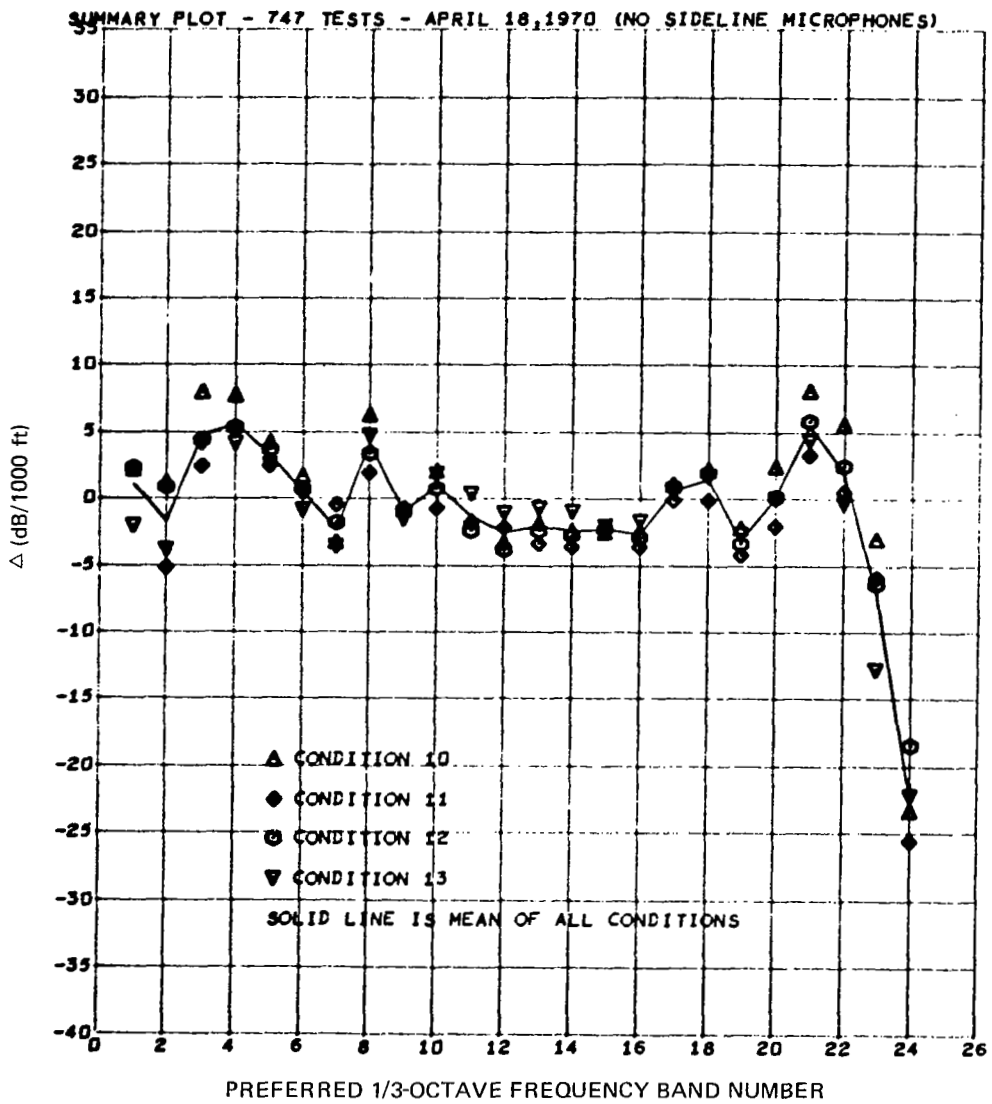


Figure 21. Composite Plots of Differences (Δ) Between Experimental and ARP 866 Absorption Coefficients for Each of the Four 747 Tests, April 18, 1970

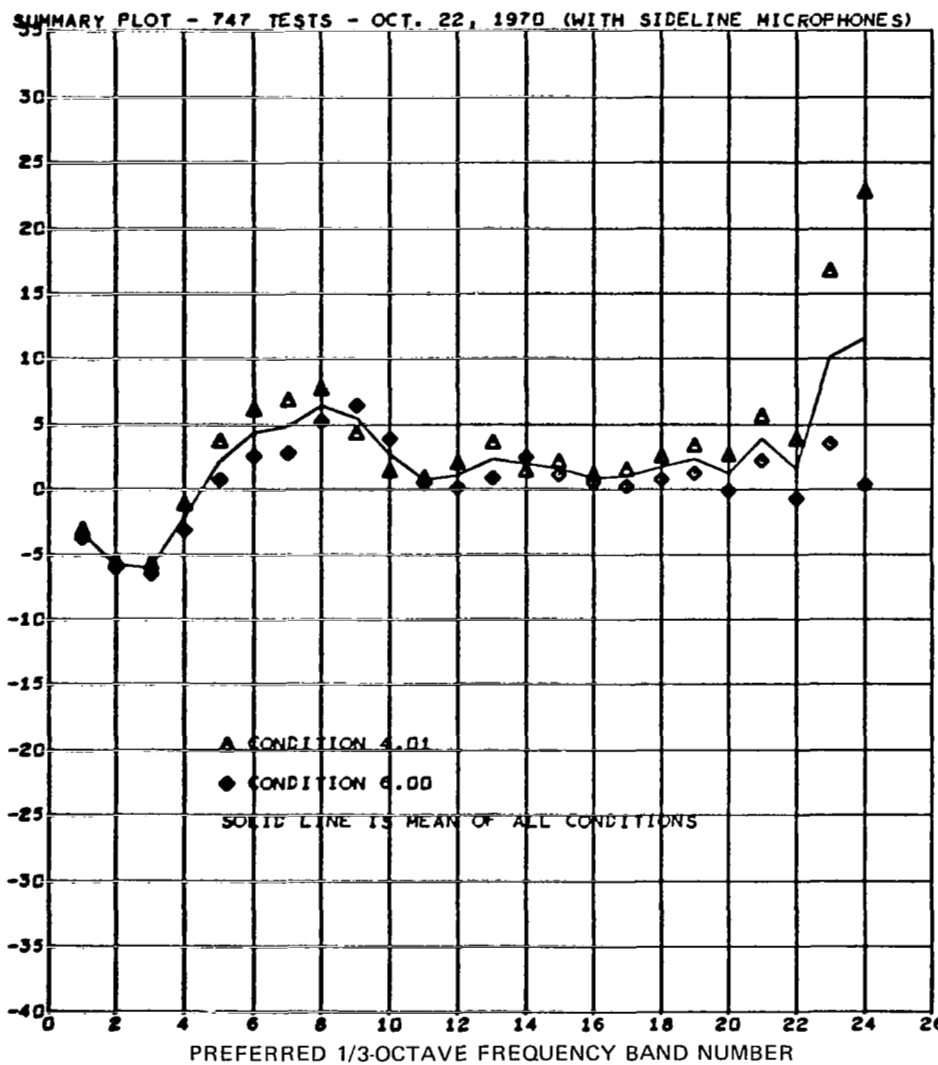


Figure 22. Composite Plots of Differences (Δ) Between Experimental and ARP 866 Absorption Coefficients for Each of the Two 747 Tests, October 22, 1970

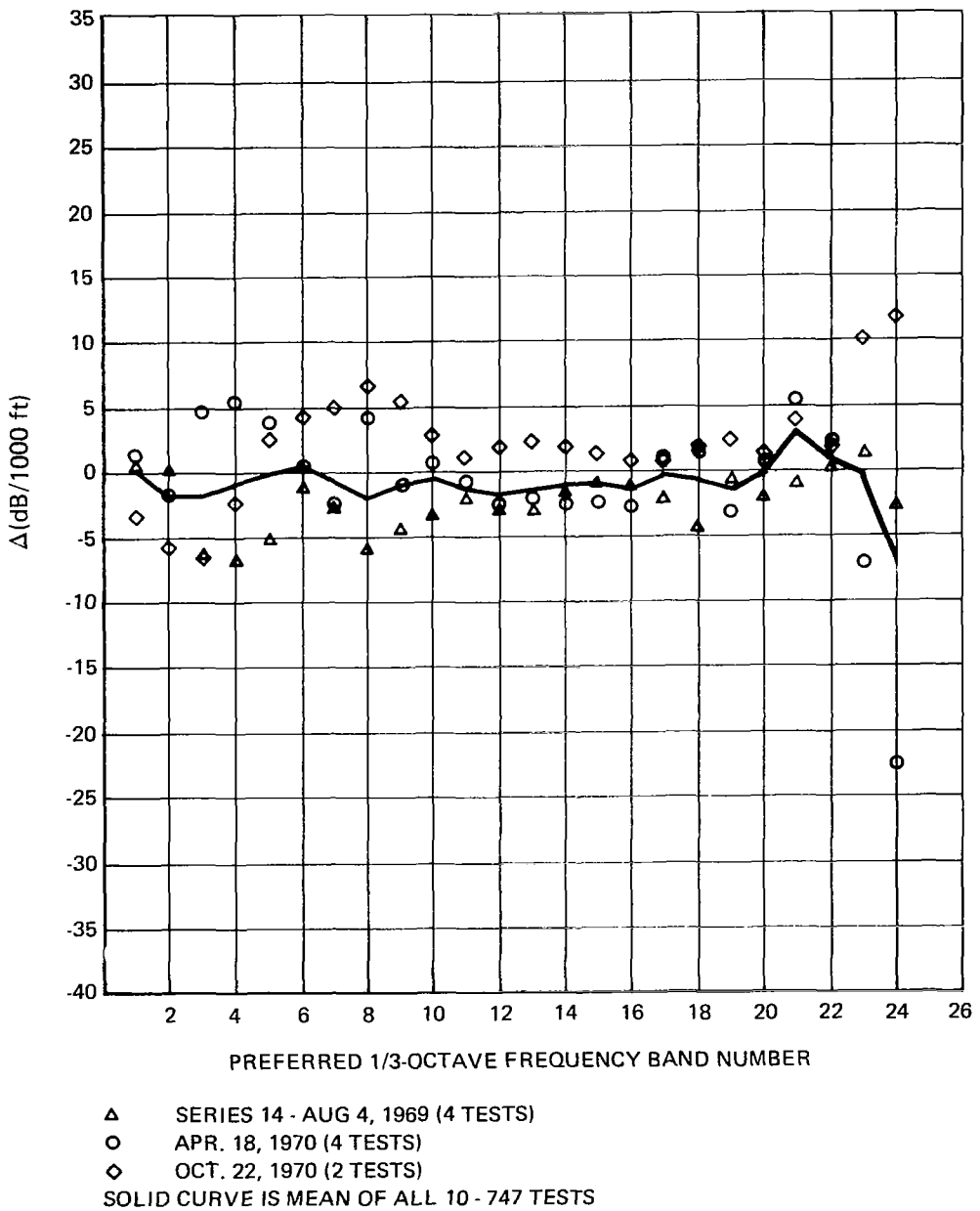


Figure 23. Composite Plot of Differences (Δ) Between Experimental and ARP 866 Absorption Coefficients for 747 Test Series

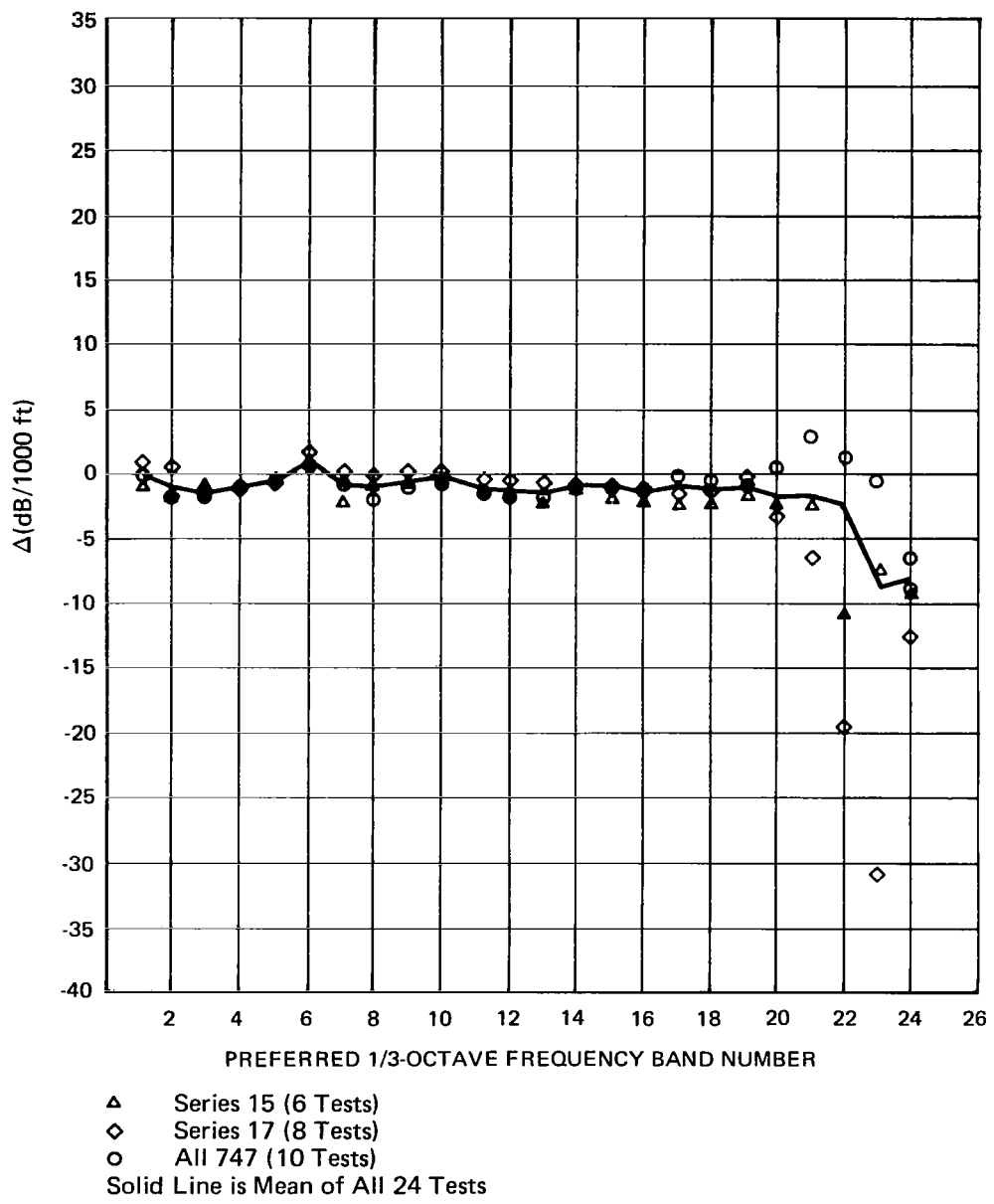


Figure 24. Composite Plot of Differences (Δ) Between Experimental and ARP 866 Absorption Coefficients for Series 15, Series 17, and all 747 Tests

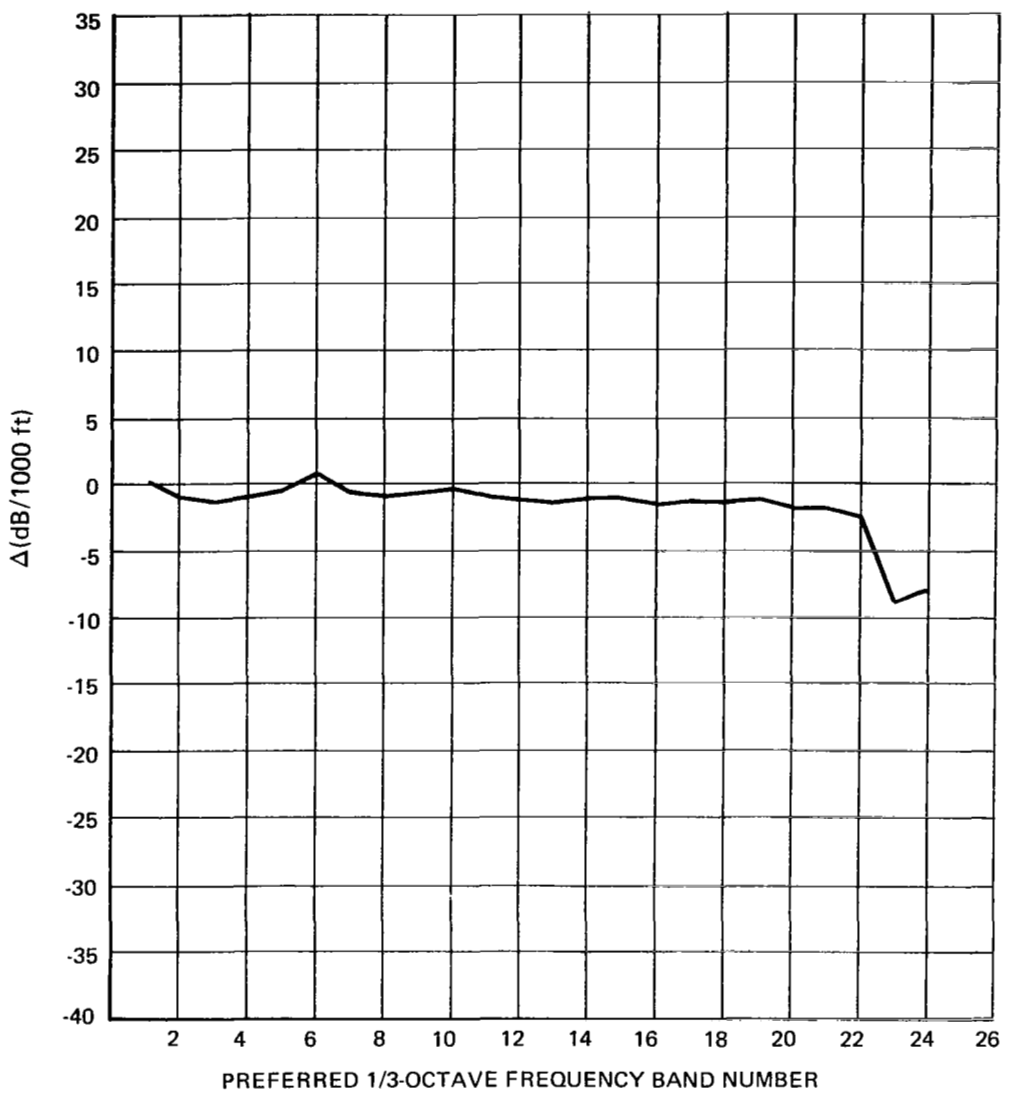


Figure 25. Plot of Overall Mean, All 24 Tests

Appendix A tables and figures follow:

Table A-1. Estimated Sample Variances and Number of Microphones for Test Condition 15.01

1/3-OCT FREQ BAND	DIRECTIVITY ANGLE (DEG)									
	75	93	85	90	95	100	105	110	115	120
1	2.83	3.75	6.24	2.10	1.24	2.48	2.97	2.38	2.22	1.64
2	7.93	8.64	8.00	3.75	1.21	1.07	4.28	2.27	1.47	7.37
3	5.77	5.62	7.46	3.80	2.46	2.14	2.19	4.73	5.82	8.63
4	5.62	5.22	9.52	6.79	5.92	3.46	2.81	2.05	2.98	11.22
5	1.83	.65	.84	3.61	15.19	12.71	5.73	2.21	1.25	1.52
6	8.44	3.11	1.19	3.15	7.33	6.09	5.79	2.21	.40	.25
7	.47	1.75	5.56	7.51	8.55	5.13	3.20	3.84	3.42	3.86
8	2.76	4.70	3.30	1.24	1.73	2.28	2.62	1.32	.59	.38
9	1.54	.53	.04	2.44	2.59	2.88	3.73	2.08	1.63	3.61
10	1.35	2.31	2.61	3.04	3.63	1.85	1.91	.25	.42	.55
11	.73	.87	1.12	1.34	1.36	1.81	3.69	3.21	.76	.74
12	2.25	2.12	1.47	.77	.45	.28	.57	2.83	2.56	2.51
13	1.19	1.92	2.54	1.86	1.18	.45	.13	.67	.84	.60
14	4.98	7.26	11.00	6.21	3.10	5.22	5.44	2.13	3.87	7.71
15	1.68	1.61	2.04	.80	.66	1.40	2.16	2.13	1.92	1.97
16	2.00	.91	1.69	1.52	2.03	1.39	1.03	1.05	1.18	1.78
17	3.46	2.92	2.04	2.92	3.56	1.83	1.02	.79	.94	1.34
18	1.66	1.26	1.16	.79	.83	.46	.65	.39	.28	.44
19	.83	.72	.85	.42	.77	.73	.52	.28	.40	.66
20	.67	.64	1.05	1.22	1.62	1.85	1.55	1.63	3.61	3.24
21	.31	.48	1.06	1.10	1.21	1.06	.95	1.11	3.34	3.92
22	2.95	2.92	3.03	2.73	2.75	2.33	1.61	2.35	3.90	4.34
23	3.54	3.96	5.05	3.55	2.71	3.23	3.66	3.62	4.15	5.44
24	1.06	1.37	1.73	1.77	1.10	.86	.83	.87	.91	.54
	3	2	3	3	3	3	3	3	3	3

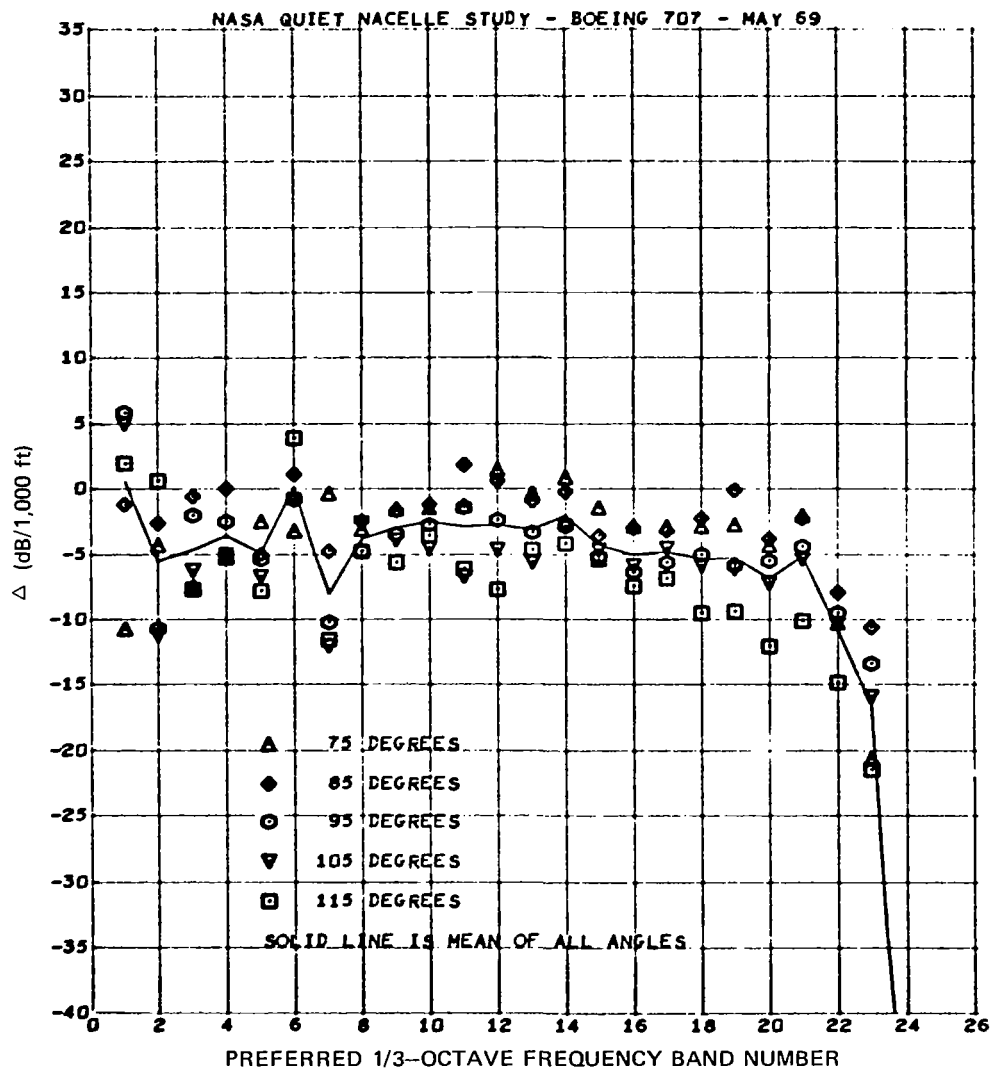


Figure A-1. Summary Plot of Differences (Δ) Between Experimental and ARP 866 Absorption Coefficients for Test Condition 15.01

Table A-2. Estimated Sample Variances and Number of Microphones for Test Condition 15.02

1/3-OCT FREQ BAND	DIRECTIVITY ANGLE (DEG)										
	75	41	85	97	95	100	105	110	115	120	
1	25.08	12.29	5.43	1.83	3.98	3.10	4.35	2.95	7.32	3.50	
2	2.52	.43	2.95	5.25	6.77	5.80	9.22	9.07	7.35	3.47	
3	1.26	2.14	1.034	3.06	.63	.91	4.22	10.00	6.48	9.39	
4	1.78	3.97	15.67	4.83	8.24	2.69	3.34	3.55	1.64	4.04	
5	3.16	4.06	9.77	1.47	5.49	.40	1.83	2.35	1.56	1.50	
6	9.14	7.05	3.25	6.31	6.56	3.85	3.98	5.24	2.34	.76	
7	.92	.67	4.42	4.44	6.57	7.42	11.64	12.17	10.18	12.50	
8	1.53	2.00	4.07	6.68	3.99	3.03	3.10	.90	2.63	.70	
9	4.17	1.95	2.00	6.00	8.91	9.93	11.17	8.94	3.84	1.74	
10	2.19	2.97	5.09	3.44	3.54	2.93	2.60	2.23	1.05	2.11	
11	3.84	3.73	2.72	5.05	4.13	3.44	3.58	2.46	2.02	2.31	
12	1.24	1.43	2.61	2.86	2.23	2.56	2.04	3.45	3.94	3.43	
13	1.13	2.07	3.01	1.48	.59	.99	.55	1.02	2.36	2.70	
14	1.59	.54	.56	1.46	1.89	2.33	2.09	2.11	2.21	1.28	
15	.63	.49	1.28	1.06	.31	.45	.81	1.70	1.85	.76	
16	1.11	.21	.70	.57	.59	.60	.30	.10	.76	.52	
17	1.01	.33	.14	.17	.39	.40	.28	.16	.78	1.81	
18	.51	.42	.44	.06	.51	.15	.15	.49	1.29	1.67	
19	.64	.39	.04	.43	.17	.71	.65	1.30	3.82	3.71	
20	.91	.51	.21	.43	.44	.69	2.71	3.38	3.30	3.52	
21	2.78	.74	.07	.24	1.58	1.18	.82	1.26	2.17	1.84	
22	2.89	2.41	1.67	2.38	2.46	2.41	1.27	1.02	2.39	.46	

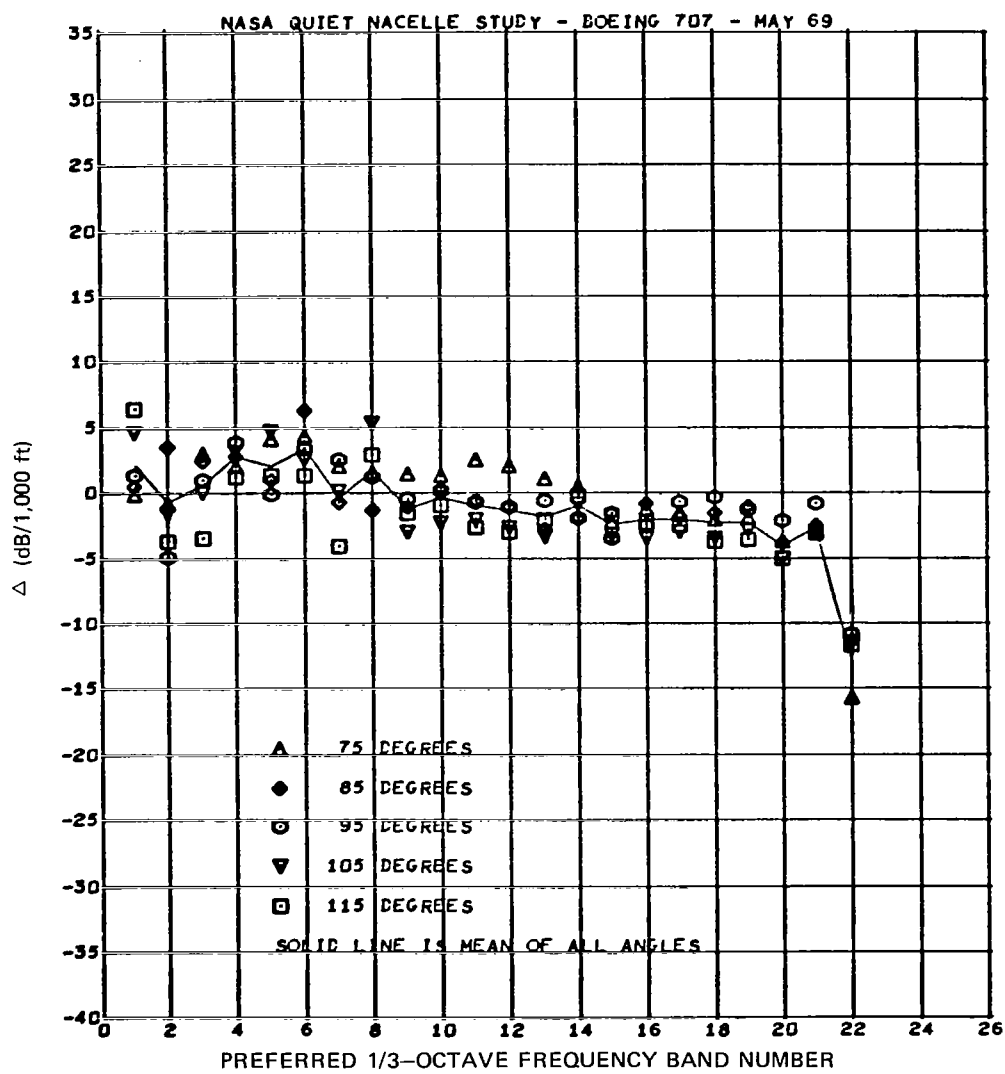


Figure A-2. Summary Plot of Differences (Δ) Between Experimental and ARP 866 Absorption Coefficients for Test Condition 15.02

Table A-3. Estimated Sample Variances and Number of Microphones for Test Condition 15.03

1/3-OCT FREQ BAND	DIRECTIVITY ANGLE (DEG)									
	75	81	85	90	95	100	105	110	115	120
1	14.53	12.57	2.47	3.67	15.83	5.56	2.97	6.37	14.14	.52
2	1.51	3.55	1.35	4.90	12.95	7.71	8.63	4.50	5.09	2.25
3	1.77	2.15	3.82	.72	.84	1.08	1.73	2.33	1.69	7.97
4	1.05	2.20	1.83	.89	4.84	.21	1.42	4.83	4.10	1.06
5	2.80	.92	.93	1.59	7.51	8.85	4.90	2.35	1.52	3.23
6	.97	1.17	4.07	1.32	3.53	8.10	2.55	2.12	1.83	2.63
7	.82	1.04	5.45	1.75	.58	2.07	1.93	4.51	4.58	.26
8	1.31	1.78	8.16	2.87	1.19	.48	.14	.14	1.38	4.15
9	1.33	1.45	1.76	1.56	.97	1.27	1.18	.31	1.71	.53
10	1.76	.25	1.02	1.34	1.13	.30	.89	.89	1.77	1.63
11	1.04	1.50	.73	1.10	1.03	.54	1.25	2.22	1.40	1.16
12	1.71	1.54	1.63	1.19	.96	.40	1.46	1.64	2.16	.93
13	.17	.27	.03	.15	.61	.43	.86	.80	.19	.44
14	1.57	.74	.40	.44	.85	.63	.86	.86	2.70	1.71
15	.20	1.78	.90	.41	.29	.15	.36	1.00	2.64	.64
16	1.16	1.14	1.59	.59	.50	.15	.16	.90	2.23	.36
17	1.56	1.45	2.02	.69	.23	.55	.80	1.41	3.32	1.10
18	1.38	1.43	1.57	.55	.35	.44	1.21	1.21	1.52	1.45
19	.58	2.29	1.81	.72	1.13	.22	.46	1.13	1.42	1.27
20	1.87	4.00	1.59	.72	.99	.35	.60	1.54	2.08	2.17
21	.93	1.96	1.50	1.05	1.27	.61	.63	.96	1.10	3.19
22	8.66	8.49	7.79	7.71	7.95	9.30	8.92	9.70	11.71	12.15
23	.31	1.17	2.51	2.13	1.44	1.50	1.19	3	3	3

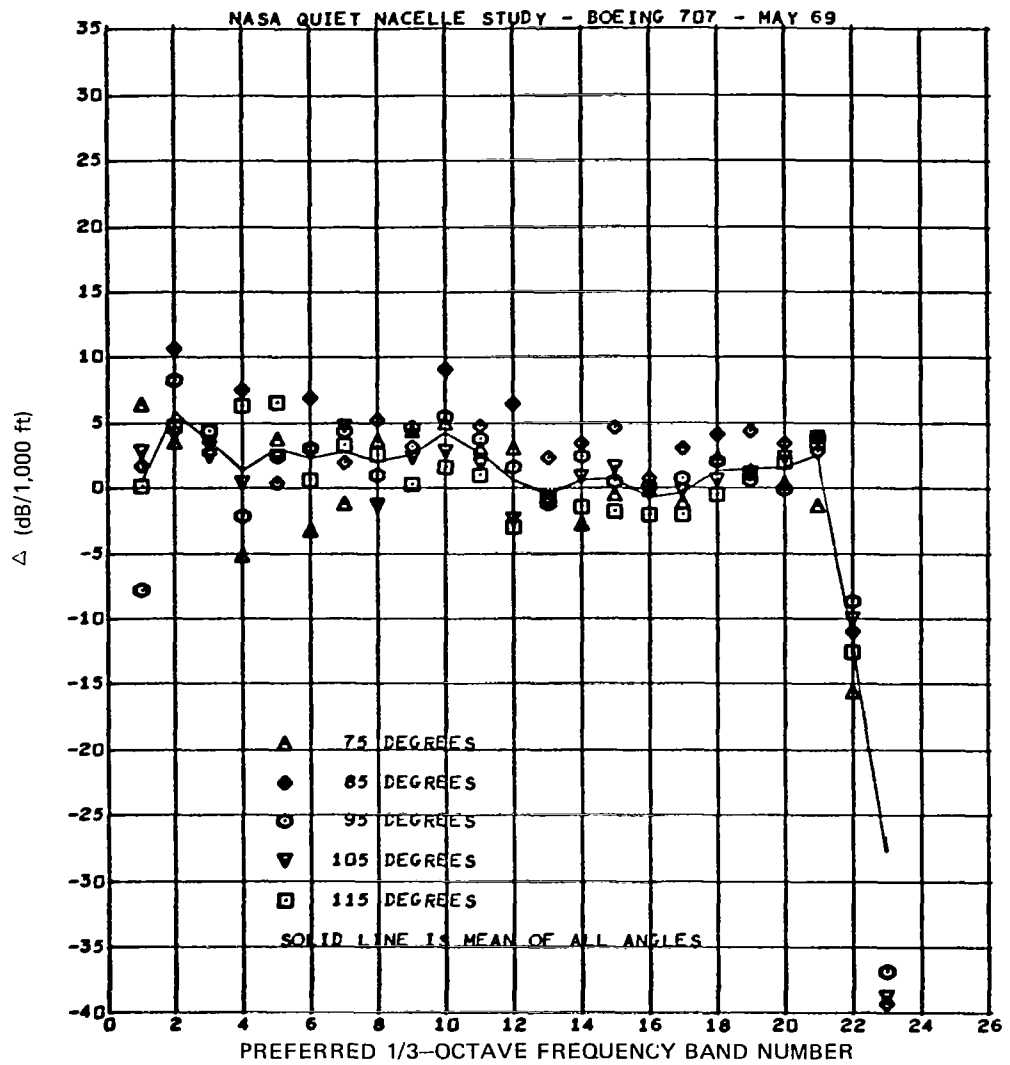


Figure A-3. Summary Plot of Differences (Δ) Between Experimental and ARP 866 Absorption Coefficients for Test Condition 15.03

Table A-4. Estimated Sample Variances and Number of Microphones for Test Condition 15.04

1/3-OCT FREQ BAND	DIRECTIVITY ANGLE (DEG)										
	75	80	85	90	95	100	105	110	115	120	
1	3.71	8.21	.53	4.05	1.22	5.36	6.54	7.34	2.65	3.34	
	4	4	4	4	4	4	4	4	4	4	
2	6.74	5.76	4.22	3.63	15.12	10.12	4.44	13.86	2.80	2.52	
	4	4	4	4	4	4	4	4	4	4	
3	19.72	8.08	2.59	3.08	19.18	19.14	25.80	9.39	8.23	28.89	
	4	4	4	4	4	4	4	4	4	4	
4	2.09	8.54	4.66	8.16	6.68	8.41	8.90	4.21	.30	3.45	
	4	4	4	4	4	4	4	4	4	4	
5	7.78	10.52	6.72	.29	8.99	11.01	1.05	1.90	1.44	.24	
	4	4	4	4	4	4	4	4	4	4	
6	7.80	.74	.80	1.72	2.59	2.12	.38	1.46	2.45	8.19	
	4	4	4	4	4	4	4	4	4	4	
7	4.19	2.92	9.03	12.82	15.77	16.14	10.55	22.94	1.04	1.08	
	4	4	4	4	4	4	4	4	4	4	
8	7.40	2.61	5.93	4.76	3.02	4.03	1.20	.46	.28	4.50	
	4	4	4	4	4	4	4	4	4	4	
9	3.05	2.85	6.32	18.98	8.27	8.04	10.89	19.02	5.47	3.44	
	4	4	4	4	4	4	4	4	4	4	
10	1.82	3.26	.82	13.20	7.70	6.00	3.10	5.70	.52	.29	
	4	4	4	4	4	4	4	4	4	4	
11	6.33	9.63	2.74	18.50	5.87	.84	1.50	6.07	.11	.62	
	4	4	4	4	4	4	4	4	4	4	
12	8.44	8.08	2.43	21.52	7.42	.85	4.54	15.07	.08	.70	
	4	4	4	4	4	4	4	4	4	4	
13	3.71	7.18	1.32	7.64	7.47	.43	1.77	8.04	.51	1.72	
	4	4	4	4	4	4	4	4	4	4	
14	4.57	4.54	1.22	15.32	10.58	2.52	2.62	2.29	.37	2.17	
	4	4	4	4	4	4	4	4	4	4	
15	2.87	3.25	.79	18.00	12.09	2.98	3.99	4.42	.31	2.38	
	4	4	4	4	4	4	4	4	4	4	
16	2.18	7.89	1.67	19.39	13.38	5.17	5.49	3.45	.20	.48	
	4	4	4	4	4	4	4	4	4	4	
17	1.38	3.71	2.69	18.38	4.05	.77	3.91	4.77	.40	.30	
	4	4	4	4	4	4	4	4	4	4	
18	.79	3.93	1.44	15.62	2.55	.91	3.29	8.37	2.64	.72	
	4	4	4	4	4	4	4	4	4	4	
19	.88	1.42	3.17	14.27	1.34	1.03	5.19	12.06	3.67	2.08	
	4	4	4	4	4	4	4	4	4	4	
20	.99	.80	.87	7.16	2.98	1.94	4.98	10.58	5.02	.48	
	4	4	4	4	4	4	4	4	4	3	
21	1.22	.36	.08	1.14	.07	.04	.30	.17	.15		
	3	3	3	3	3	3	3	3	3		

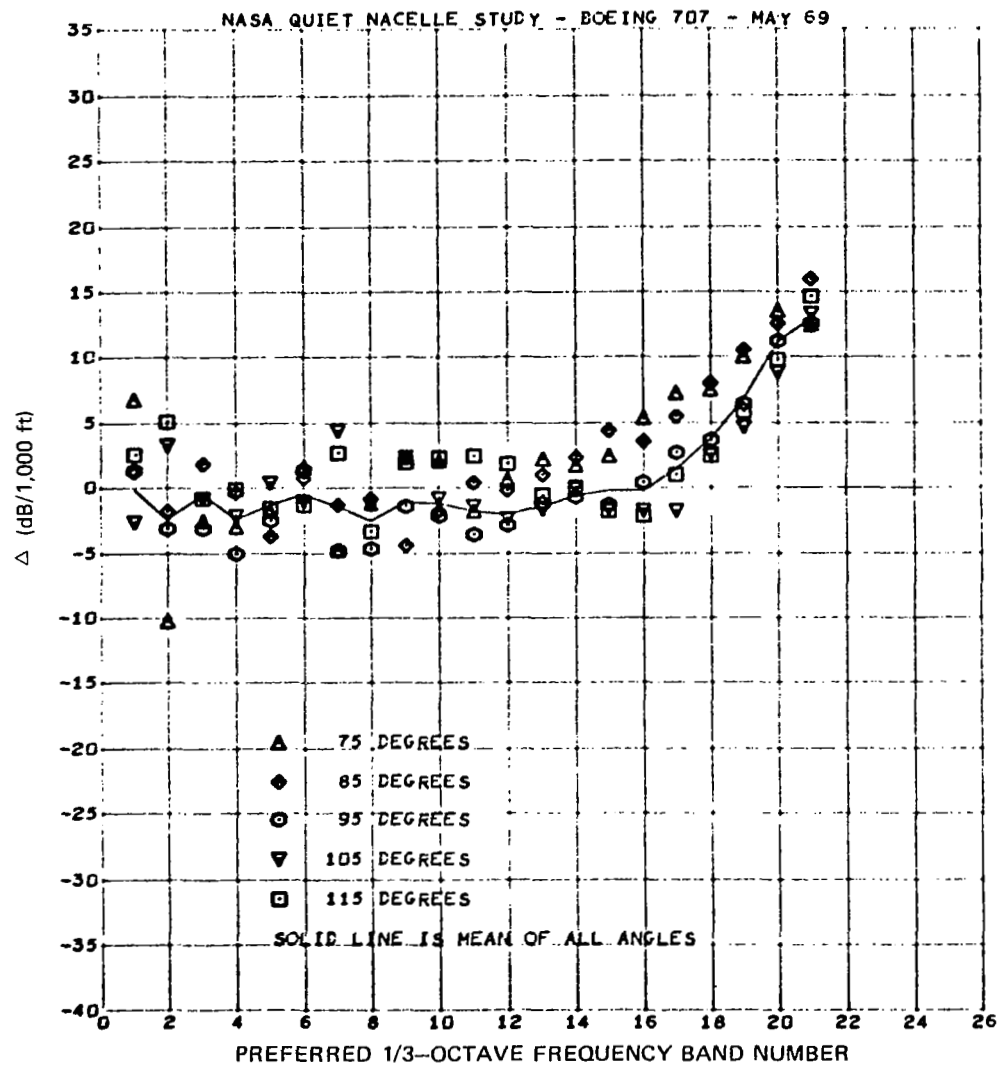


Figure A-4. Summary Plot of Differences (Δ) Between Experimental and ARP 866 Absorption Coefficients for Test Condition 15.04

Table A-5. Estimated Sample Variances and Number of Microphones for Test Condition 15.05

1/3-OCT FREQ BAND	DIRECTIVITY ANGLE (DEG)									
	75	80	85	90	95	100	105	110	115	120
1	1.11	5.95	4.96	16.28	2.28	1.89	.36	.58	.02	.90
2	4.55	2.90	.26	25.40	1.92	5.33	16.56	14.14	.95	1.71
3	7.20	.21	7.77	1.59	7.41	7.90	1.92	.26	1.42	4.51
4	4.39	2.87	3.92	2.92	5.27	.35	.44	1.10	3.52	.12
5	14.65	3.33	2.65	1.44	3.33	1.79	5.53	4.41	2.71	.98
6	11.14	1.90	5.74	4.30	8.27	5.64	1.49	4.79	7.22	2.16
7	6.18	4.61	7.79	12.45	12.57	4.12	.91	.92	.27	.57
8	5.59	3.56	1.44	2.56	2.41	4.24	3.47	6.88	1.95	.30
9	8.43	1.20	.38	2.49	1.21	2.53	2.09	.03	.35	.74
10	4.49	5.77	3.24	3.72	3.27	3.95	.67	3.59	5.66	2.41
11	6.17	8.56	2.14	11.91	5.52	2.92	3.62	2.25	5.18	1.13
12	5.62	7.93	5.02	8.21	10.61	3.89	4.34	2.29	3.08	1.82
13	2.68	2.29	3.99	2.95	4.96	3.81	4.65	6.05	3.41	1.54
14	1.23	2.57	2.95	4.49	5.41	3.56	4.95	2.84	1.13	1.18
15	1.29	3.43	3.42	4.61	4.82	4.43	6.95	2.40	4.37	3.90
16	.37	2.92	2.56	5.05	6.63	2.19	3.49	3.36	4.69	3.38
17	2.15	2.66	3.54	4.68	3.77	3.92	6.39	2.14	5.76	3.86
18	1.65	1.52	2.79	4.24	5.88	3.53	6.09	6.30	3.72	3.43
19	1.83	1.11	1.20	4.32	6.68	3.70	6.50	7.26	3.94	3.63
20	3.08	2.29	1.83	2.59	5.28	2.61	6.21	5.64	1.81	5.25
21	4.18	2.08	4.02	5.02	5.15	3.11	5.68	4.77	3.61	3.38
22	.37	.82	1.23	.84	1.65	.84	2.85	1.21	1.63	1.69

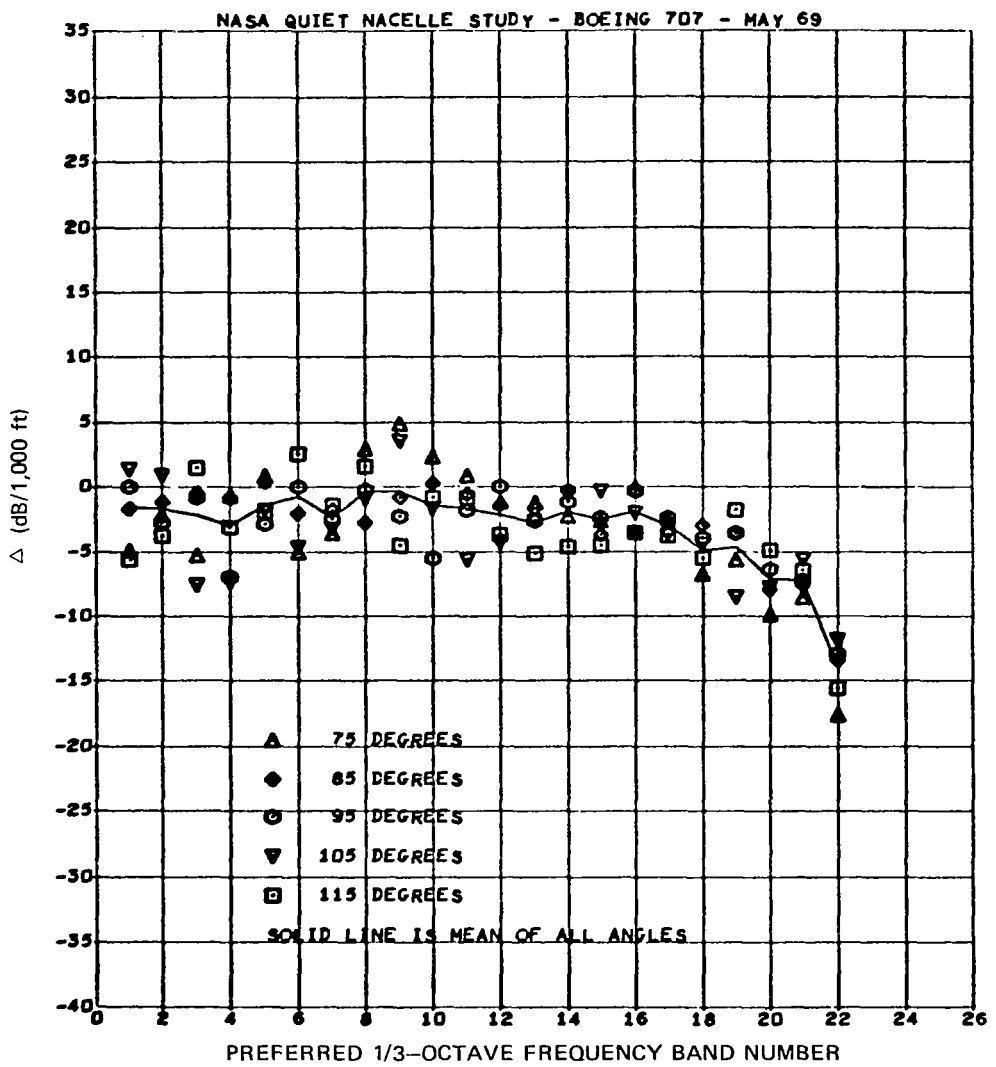


Figure A-5. Summary Plot of Differences (Δ) Between Experimental and ARP 866 Absorption Coefficients for Test Condition 15.05

Table A-6. Estimated Sample Variances and Number of Microphones for Test Condition 15.06

1/3-OCT FREQ BAND	DIRECTIVITY ANGLE (DEG)									
	75	81	85	90	95	100	115	119	115	120
1	3.89	30.23	68.67	8.47	6.67	21.26	4.13	11.74	7.23	1.89
2	14.63	7.24	7.30	5.82	.04	14.56	28.53	39.61	1.39	1.40
3	.99	12.05	11.10	5.05	1.67	.75	3.63	12.14	15.26	32.89
4	4.53	4.82	1.15	3.59	10.95	9.55	2.72	1.78	9.82	8.65
5	9.03	4.35	3.73	5.95	6.16	3.49	1.39	2.75	5.40	10.32
6	4.95	5.55	8.26	2.09	3.97	3.10	2.62	9.51	2.57	.75
7	3.08	6.15	6.79	2.29	10.31	9.93	6.31	19.94	15.21	3.07
8	12.93	6.72	3.63	4.22	8.71	.90	3.19	3.94	2.38	7.16
9	5.10	1.71	7.22	7.45	16.12	7.62	14.92	5.52	2.40	4.52
10	6.89	4.01	6.55	4.89	5.13	.98	1.41	1.94	1.21	5.99
11	10.77	7.20	8.46	7.09	7.79	2.34	3.76	6.50	6.56	7.03
12	4.42	3.00	3.42	3.03	2.42	2.99	2.93	5.78	5.88	4.78
13	3.92	2.53	3.49	3.83	5.35	5.61	3.11	3.42	6.04	4.85
14	6.00	5.92	6.09	3.33	1.92	4.31	1.33	2.48	2.11	4.36
15	1.48	1.18	3.77	5.45	5.58	6.79	3.59	3.76	4.18	5.40
16	2.07	1.97	3.39	4.67	4.04	3.64	1.39	3.96	5.37	4.06
17	2.30	.76	2.10	4.92	2.72	2.40	1.35	3.78	5.95	5.36
18	.83	.87	1.30	4.30	7.44	5.50	3.32	3.94	5.97	4.99
19	.29	.21	1.25	2.99	4.60	2.01	2.05	4.21	5.73	4.32
20	1.35	.50	.85	1.23	1.75	1.30	.77	4.04	5.54	6.63
21	31.7F	34.19	41.21	44.77	51.81	51.58	55.70	52.01	42.66	40.97
22	9.41	9.27	13.73	16.59	18.3F	18.18	19.69	22.34	13.81	11.35

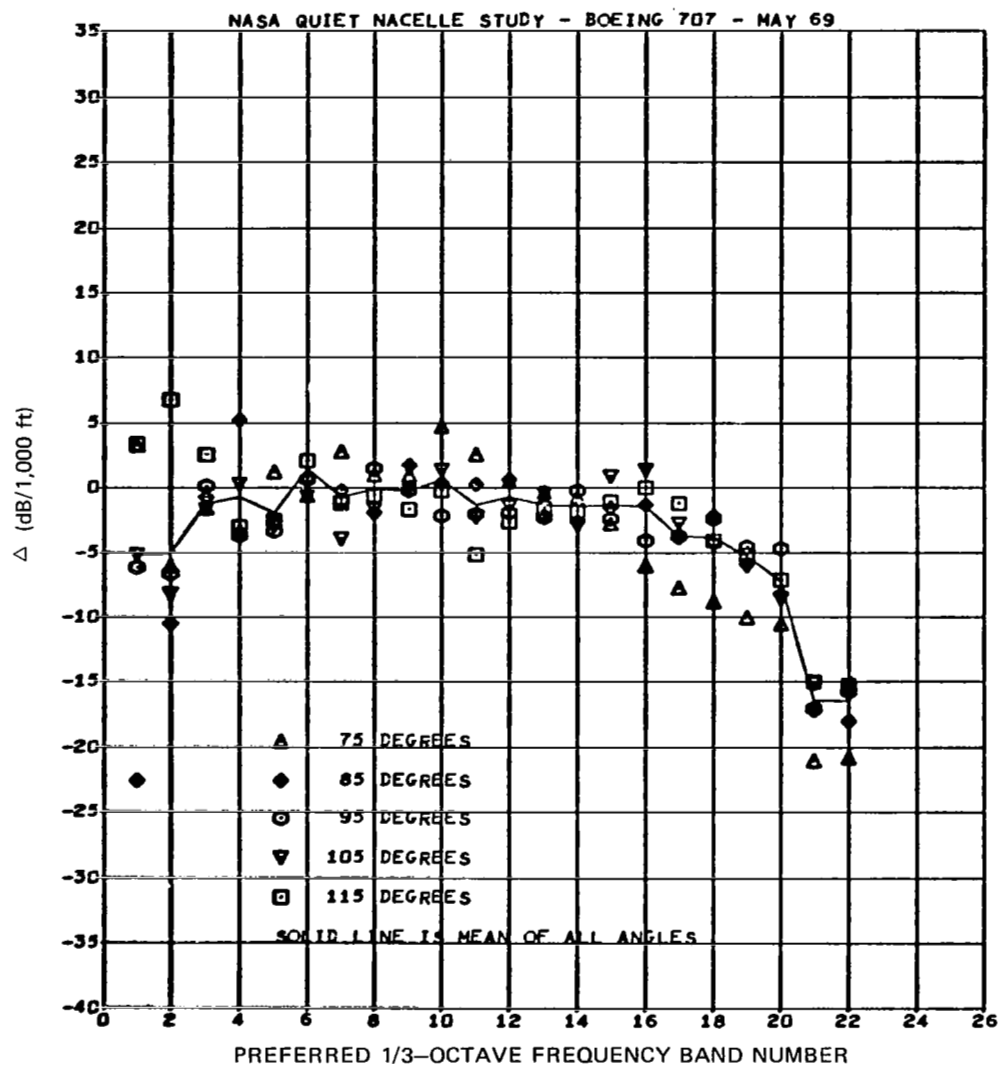


Figure A-6. Summary Plot of Differences (Δ) Between Experimental and ARP 866 Absorption Coefficients for Test Condition 15.06

Table A-7. Estimated Sample Variances and Number of Microphones for Test Condition 17.01

1/3-OCT FREQ BAND	DIRECTIVITY ANGLE (DEG)										
	75	90	85	90	95	100	105	110	115	120	
1	9.49	4.73	3.63	2.59	1.41	1.32	2.08	2.25	3.91	4.00	
	19	10	11	10	10	10	10	10	11	10	
2	5.55	5.93	6.54	5.47	4.33	2.99	2.78	2.35	2.78	3.48	
	10	10	10	10	11	10	10	10	11	10	
3	3.74	5.59	8.01	11.33	14.57	17.54	26.18	27.05	21.15	10.98	
	10	10	10	10	10	10	10	10	10	10	
4	4.65	5.59	7.49	7.61	8.29	11.20	11.88	12.02	16.82	16.84	
	10	10	10	10	10	10	10	10	10	10	
5	5.72	4.52	5.86	5.51	5.15	4.70	3.65	3.36	5.87	8.07	
	10	10	10	10	10	10	10	10	10	10	
6	8.44	4.04	3.74	1.93	.68	.27	.84	1.47	1.81	2.72	
	10	10	10	10	10	10	10	10	10	10	
7	3.00	4.42	6.28	7.18	8.25	10.47	7.47	2.78	1.01	1.54	
	10	10	10	10	10	10	10	10	10	10	
8	3.27	4.55	3.69	3.90	5.64	6.76	3.64	9.98	9.96	7.72	
	10	10	10	10	10	10	10	10	10	10	
9	3.77	4.97	4.77	4.12	3.54	2.86	1.45	.83	.89	1.26	
	10	10	10	10	10	10	10	10	10	10	
10	2.07	4.34	6.57	5.99	4.10	3.82	4.36	4.38	5.99	4.85	
	10	10	10	10	10	10	10	10	10	10	
11	3.00	4.23	4.88	4.78	4.47	2.83	3.50	4.55	2.32	1.51	
	10	10	10	10	10	10	10	10	10	10	
12	2.81	3.27	4.94	5.09	4.36	3.85	2.98	2.44	2.38	1.82	
	10	10	10	10	10	10	10	10	10	10	
13	2.41	3.25	3.54	4.15	5.23	5.65	4.83	3.51	2.17	1.59	
	10	10	10	10	10	10	10	10	10	10	
14	1.69	2.31	4.89	6.79	6.59	6.10	5.54	4.91	3.39	2.44	
	10	10	10	10	10	10	10	10	10	10	
15	1.48	1.62	1.96	2.60	3.38	3.56	3.41	4.14	3.92	3.84	
	10	10	10	10	10	10	10	10	10	10	
16	1.82	1.46	1.09	1.36	1.99	2.93	2.89	2.85	2.83	2.12	
	10	10	10	10	10	10	10	10	10	10	
17	.69	.52	.75	1.16	1.72	2.74	2.24	1.67	1.74	2.11	
	10	10	10	10	10	10	10	10	10	10	
18	.98	.94	.69	1.19	2.38	2.39	2.78	3.45	3.14	3.55	
	10	10	10	10	10	10	10	10	10	10	
19	2.38	1.75	1.90	2.82	4.15	4.28	5.30	6.34	4.21	4.42	
	10	10	10	10	10	10	10	10	10	10	
20	6.41	4.01	1.86	1.64	2.60	2.61	3.25	4.99	5.39	6.15	
	10	10	10	10	10	10	10	10	10	10	
21	4.74	2.99	2.45	1.54	1.62	3.98	4.00	3.16	3.81	4.06	
	10	10	10	10	10	10	10	10	10	10	
22	9.41	6.96	5.97	5.13	5.06	6.56	7.01	6.91	7.79	8.62	
	10	10	10	10	10	10	10	10	10	10	
23	19.51	15.68	14.43	11.72	9.31	9.73	10.43	10.48	5.39	6.07	
	10	10	10	10	10	10	10	10	10	10	
24	4.44	5.26	6.27	8.02	10.22	12.76	14.03	13.46	16.41	15.73	
	7	7	7	7	7	7	7	7	5	5	

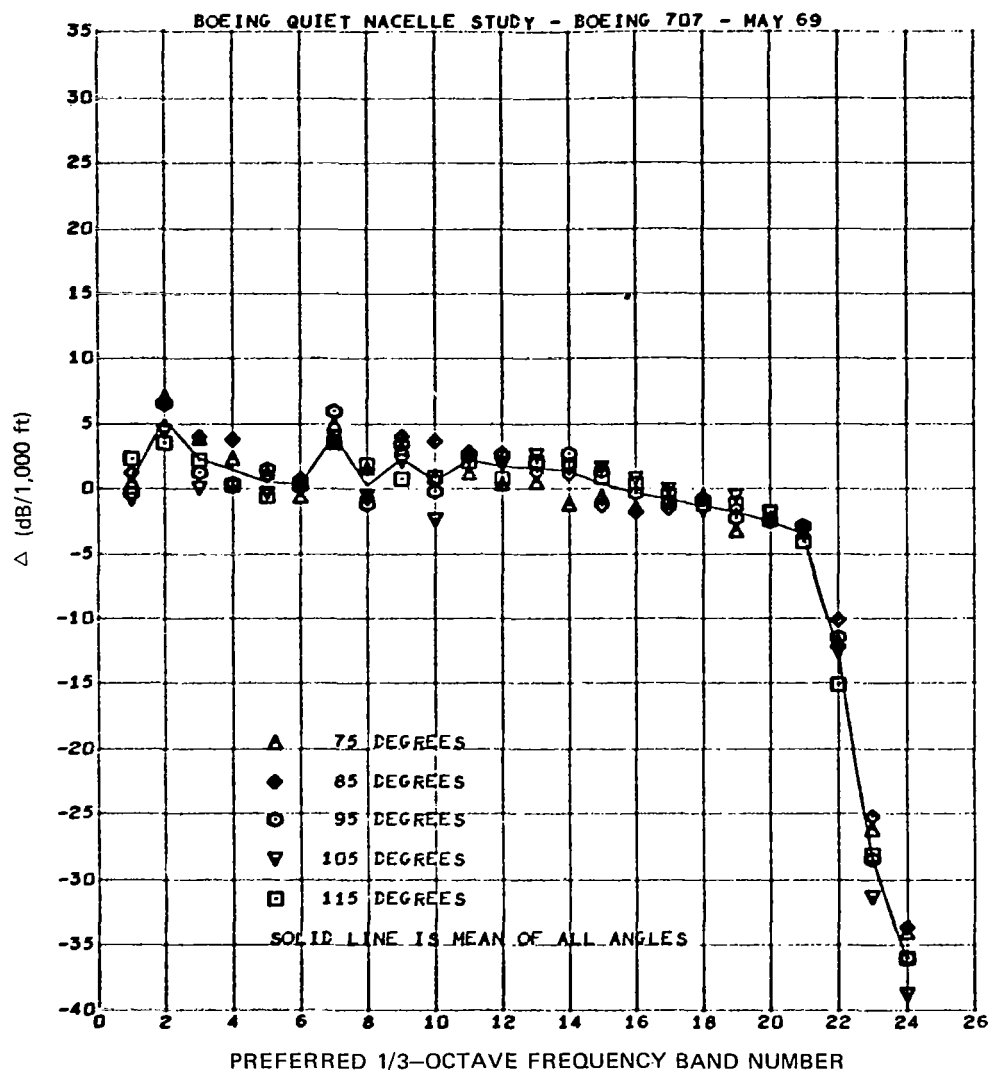


Figure A-7. Summary Plot of Differences (Δ) Between Experimental and ARP 866 Absorption Coefficients for Test Condition 17.01

Table A-8. Estimated Sample Variances and Number of Microphones for Test Condition 17.02

1/3-OCT FREQ BAND	DIRECTIVITY ANGLE (DEG)									
	75	80	85	90	95	100	105	110	115	120
1	3.90	5.02	2.31	3.47	4.03	3.26	1.49	3.21	.96	2.46
	10	10	10	10	10	10	10	10	10	10
2	2.21	4.00	4.97	3.43	1.52	1.84	2.37	4.77	4.24	2.59
	10	10	10	10	10	10	10	10	10	10
3	2.15	1.52	2.57	3.27	2.54	2.81	2.48	5.91	4.01	3.21
	10	10	10	10	10	10	10	10	10	10
4	.65	.60	1.23	1.62	1.87	1.13	1.52	1.98	3.30	3.97
	10	10	10	10	10	10	10	10	10	10
5	3.25	1.39	.72	1.08	.51	.15	.83	2.15	1.15	1.16
	10	10	10	10	10	10	10	10	10	10
6	2.67	2.19	2.07	2.37	2.40	2.35	1.76	1.68	1.16	.65
	10	10	10	10	10	10	10	10	10	10
7	1.56	.83	1.09	1.49	2.34	2.16	1.92	.83	.99	1.85
	10	10	10	10	10	10	10	10	10	10
8	1.11	1.79	1.58	.96	1.22	1.34	1.69	3.53	3.59	3.41
	10	10	10	10	10	10	10	10	10	10
9	1.58	1.27	.35	1.29	1.46	1.20	1.54	.60	.89	.87
	10	10	10	10	10	10	10	10	10	10
10	1.85	1.61	1.87	2.22	2.09	1.40	1.44	2.11	3.38	3.67
	10	10	10	10	10	10	10	10	10	10
11	.95	1.14	1.32	.93	.84	1.46	1.04	.88	2.17	.61
	10	10	10	10	10	10	10	10	10	10
12	.81	1.66	1.51	1.57	.62	1.76	2.87	3.11	2.61	2.06
	10	10	10	10	10	10	10	10	10	10
13	.96	.78	1.31	1.18	1.76	2.18	1.12	.80	1.13	1.20
	10	10	10	10	10	10	10	10	10	10
14	.74	.85	1.51	.54	.79	.94	.80	.95	.76	1.63
	10	10	10	10	10	10	10	10	10	10
15	1.44	1.22	1.36	.65	1.30	2.55	1.05	.90	.49	1.64
	10	10	10	10	10	10	10	10	10	10
16	1.61	1.06	2.18	1.35	1.09	.74	.66	1.65	.67	.66
	10	10	10	10	10	10	10	10	10	10
17	1.34	2.27	1.64	.74	.51	.69	1.39	2.11	1.92	1.69
	10	10	10	10	10	10	10	10	10	10
18	2.22	1.23	2.12	1.73	1.55	2.03	2.33	2.14	.75	.92
	10	10	10	10	10	10	10	10	10	10
19	2.08	2.26	3.15	2.27	2.79	2.98	2.65	2.77	1.72	3.09
	10	10	10	10	10	10	10	10	10	10
20	3.59	3.13	3.73	2.73	3.31	3.83	4.95	5.72	5.27	5.80
	10	10	10	10	10	10	10	10	10	10
21	5.65	5.38	4.65	6.19	6.28	9.25	9.75	12.04	9.07	9.42
	10	10	10	10	10	10	10	10	10	10
22	13.81	13.71	13.35	14.53	15.34	17.66	14.17	12.58	12.18	11.05
	10	10	10	10	10	10	10	10	10	9
23	18.48	20.14	19.83	20.56	22.00	20.40	20.27	20.95	21.44	25.06
	5	5	5	5	5	5	5	5	4	4

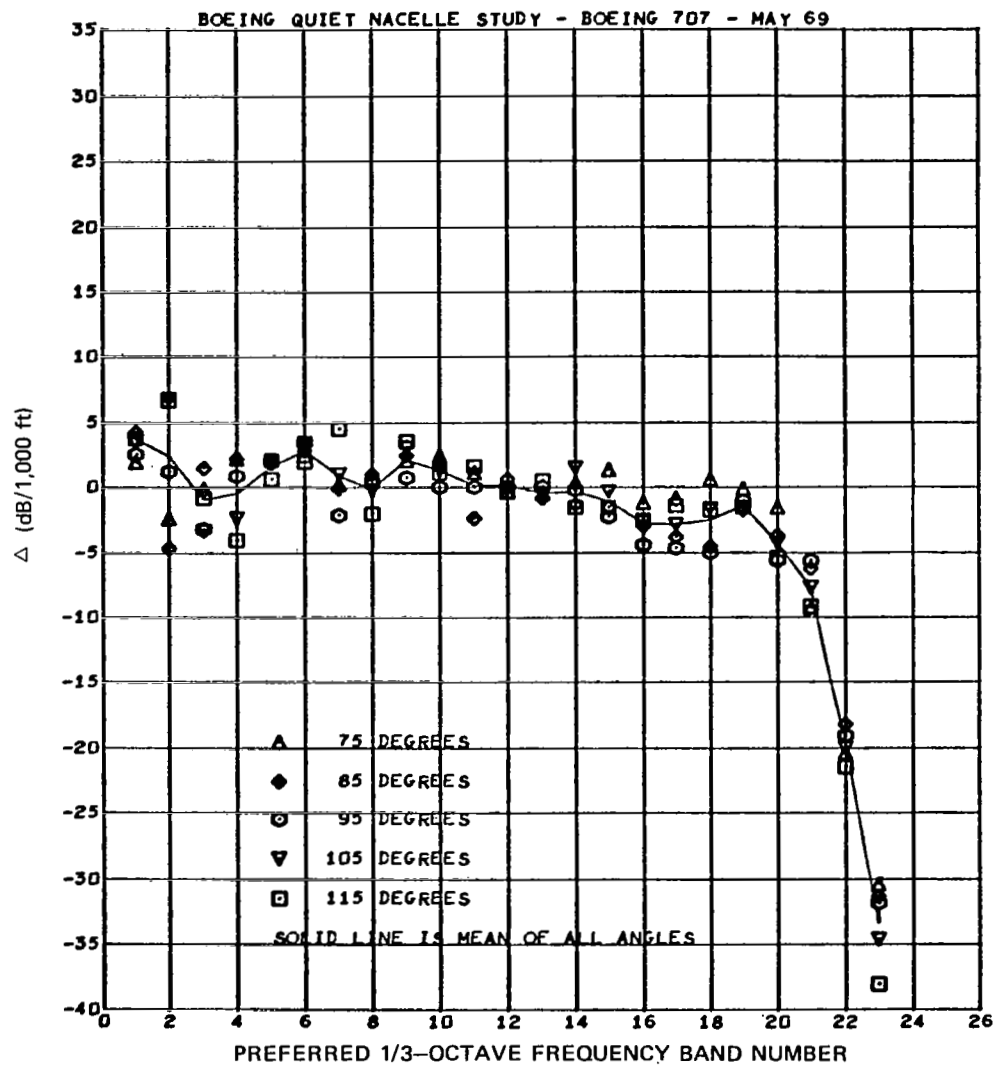


Figure A-8. Summary Plot of Differences (Δ) Between Experimental and ARP 866 Absorption Coefficients for Test Condition 17.02

Table A-9. Estimated Sample Variances and Number of Microphones for Test Condition 17.03

1/3-OCT FREQ BAND	DIRECTIVITY ANGLE (DEG)										
	75	83	85	90	95	100	105	110	115	120	
1	25.52	27.11	21.55	17.98	16.07	11.52	9.33	6.02	5.75	3.49	
	10	10	10	10	10	10	10	10	10	10	
2	4.35	4.56	3.2	4.89	8.67	7.63	7.34	14.15	17.69	18.62	
	10	10	10	10	10	10	10	10	10	10	
3	1.68	4.08	6.28	4.88	6.47	5.85	6.11	11.41	14.07	16.62	
	10	10	10	10	10	10	10	10	10	10	
4	4.79	3.16	3.78	3.31	5.24	5.07	6.13	7.76	6.40	8.33	
	10	10	10	10	10	10	10	10	10	10	
5	4.47	5.51	9.62	11.14	9.58	7.86	7.64	7.68	5.34	4.63	
	10	10	10	10	10	10	10	10	10	10	
6	12.32	11.59	14.62	12.91	14.25	13.17	9.16	10.77	2.16	1.89	
	10	10	10	10	10	10	10	10	10	10	
7	3.89	2.33	1.94	1.36	2.26	2.92	4.98	9.90	12.55	15.13	
	10	10	10	10	10	10	10	10	10	10	
8	3.62	6.31	6.64	6.86	5.77	4.61	3.99	5.24	6.34	3.41	
	10	10	10	10	10	10	10	10	10	10	
9	.40	1.05	1.75	1.60	1.05	.98	3.30	6.79	10.25	13.61	
	10	10	10	10	10	10	10	10	10	10	
10	2.21	1.52	.73	.75	1.62	2.65	4.61	6.36	4.83	5.35	
	10	10	10	10	10	10	10	10	10	10	
11	1.68	2.03	1.75	1.41	2.00	2.30	3.86	5.91	5.56	5.60	
	10	10	10	10	10	10	10	10	10	10	
12	1.37	.58	.86	1.47	1.70	1.08	3.03	4.32	3.19	4.17	
	10	10	10	10	10	10	10	10	10	10	
13	2.64	2.13	1.19	.85	.69	.91	1.16	1.85	3.06	3.79	
	10	10	10	10	10	10	10	10	10	10	
14	4.73	3.97	2.17	.85	.42	.77	.82	.37	1.80	2.07	
	10	10	10	10	10	10	10	10	10	10	
15	4.52	3.52	3.31	2.27	1.23	.82	.89	2.09	2.68	3.07	
	10	10	10	10	10	10	10	10	10	10	
16	6.32	4.37	3.52	4.53	2.15	.78	.19	.32	1.36	1.92	
	10	10	10	10	10	10	10	10	10	10	
17	9.03	5.89	2.85	2.42	2.30	1.38	.98	.67	.68	3.11	
	10	10	10	10	10	10	10	10	10	10	
18	6.02	6.73	4.56	6.10	4.14	2.29	1.52	1.39	.46	1.12	
	10	10	10	10	10	10	10	10	10	10	
19	4.48	3.26	4.66	5.97	4.68	3.47	1.91	1.10	1.41	3.99	
	10	10	10	10	10	10	10	10	10	10	
20	1.70	2.04	2.42	.98	1.07	1.35	1.75	1.99	2.96	4.21	
	10	10	10	10	10	10	10	10	10	10	
21	4.56	4.73	5.96	6.54	5.54	3.66	3.85	5.14	7.28	9.34	
	10	10	10	10	10	10	10	10	10	10	
22	8.09	7.52	5.52	5.25	4.75	5.79	6.91	6.36	5.42	5.20	
	10	10	10	10	10	10	10	10	10	10	
23	6.25	4.43	3.78	4.33	5.31	4.84	5.49	5.50	4.27	1.42	
	10	10	10	10	10	10	10	10	10	10	
24	17.23	7.93	3.33	3.22	3.56	5.92	10.44	1.49	.36	.31	
	10	10	10	10	10	10	10	10	10	10	

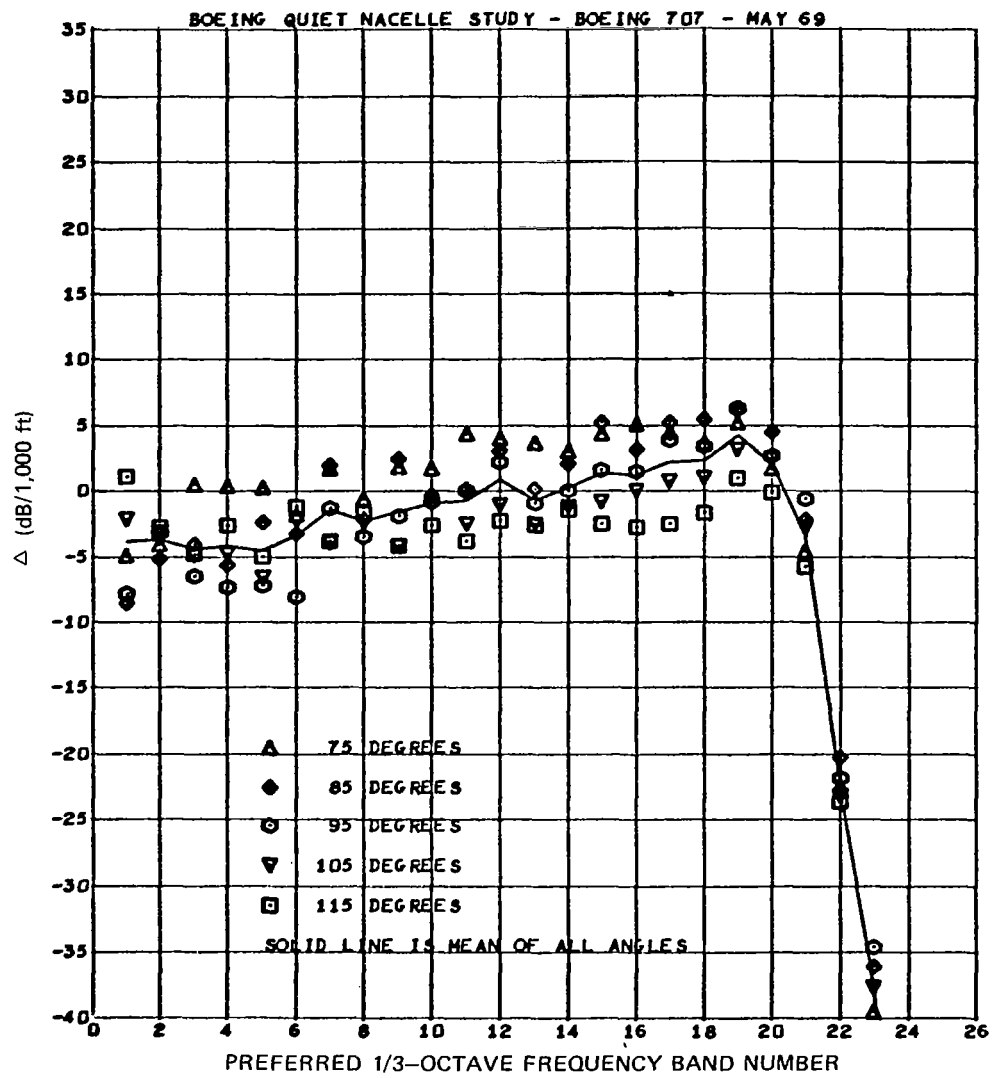


Figure A-9. Summary Plot of Differences (Δ) Between Experimental and ARP 866 Absorption Coefficients for Test Condition 17.03

Table A-10. Estimated Sample Variances and Number of Microphones for Test Condition 17.07

1/3-OCT FREQ BAND	DIRECTIVITY ANGLE (DEG)										
	75	93	85	90	95	100	105	110	115	120	
1	2.84	4.17	4.68	8.54	6.30	4.64	6.31	5.08	2.98	3.08	5
2	6.72	17.51	1.49	5.54	3.11	3.25	3.06	2.34	2.40	2.65	5
3	5.42	3.62	2.93	3.09	3.52	2.23	3.53	7.86	10.96	6.60	5
4	.60	.60	.33	.29	.55	.61	1.72	1.92	2.65	4.33	5
5	1.58	1.25	1.21	1.08	1.03	.89	.32	.84	2.47	2.06	5
6	2.35	1.16	2.16	4.17	1.67	.78	.44	2.03	2.17	.95	5
7	.80	1.27	1.39	1.23	2.03	3.93	5.51	2.59	.87	1.72	5
8	1.99	1.47	1.84	1.42	1.27	2.27	2.91	2.18	2.50	3.18	5
9	1.12	.92	2.21	3.19	2.94	3.38	2.15	1.27	.54	.68	5
10	.81	1.67	3.35	4.81	3.14	1.15	.23	.30	.99	2.26	5
11	.45	1.05	.69	.89	1.71	.96	.06	.18	.13	.16	5
12	1.01	1.16	.13	.47	1.02	1.50	1.62	1.89	1.48	1.15	5
13	.25	.41	.34	1.21	.73	.39	.32	.96	.85	1.36	5
14	.16	1.42	.82	.74	.92	.38	.76	.69	1.34	3.19	5
15	.16	1.18	.96	.81	.53	.45	.74	.82	1.40	2.37	5
16	.25	.48	.22	.34	1.13	1.16	2.15	2.10	2.10	4.70	5
17	1.14	.83	.45	.67	.53	.17	.78	2.15	2.86	2.71	5
18	.28	.33	.15	.31	1.67	1.96	.40	1.03	1.10	1.47	5
19	.59	.76	.21	.21	1.18	2.30	2.34	1.56	1.45	1.62	5
20	1.35	1.26	.63	.55	.15	.68	1.03	3.03	4.18	2.38	5
21	3.63	1.32	1.57	1.64	2.31	2.12	2.32	4.06	4.94	4.75	5
22	7.39	6.07	6.23	6.81	7.85	9.42	10.73	11.98	11.54	11.52	5
23	6.74	6.19	7.46	9.27	9.75	9.47	4.94	3.50	1.63	3.02	3

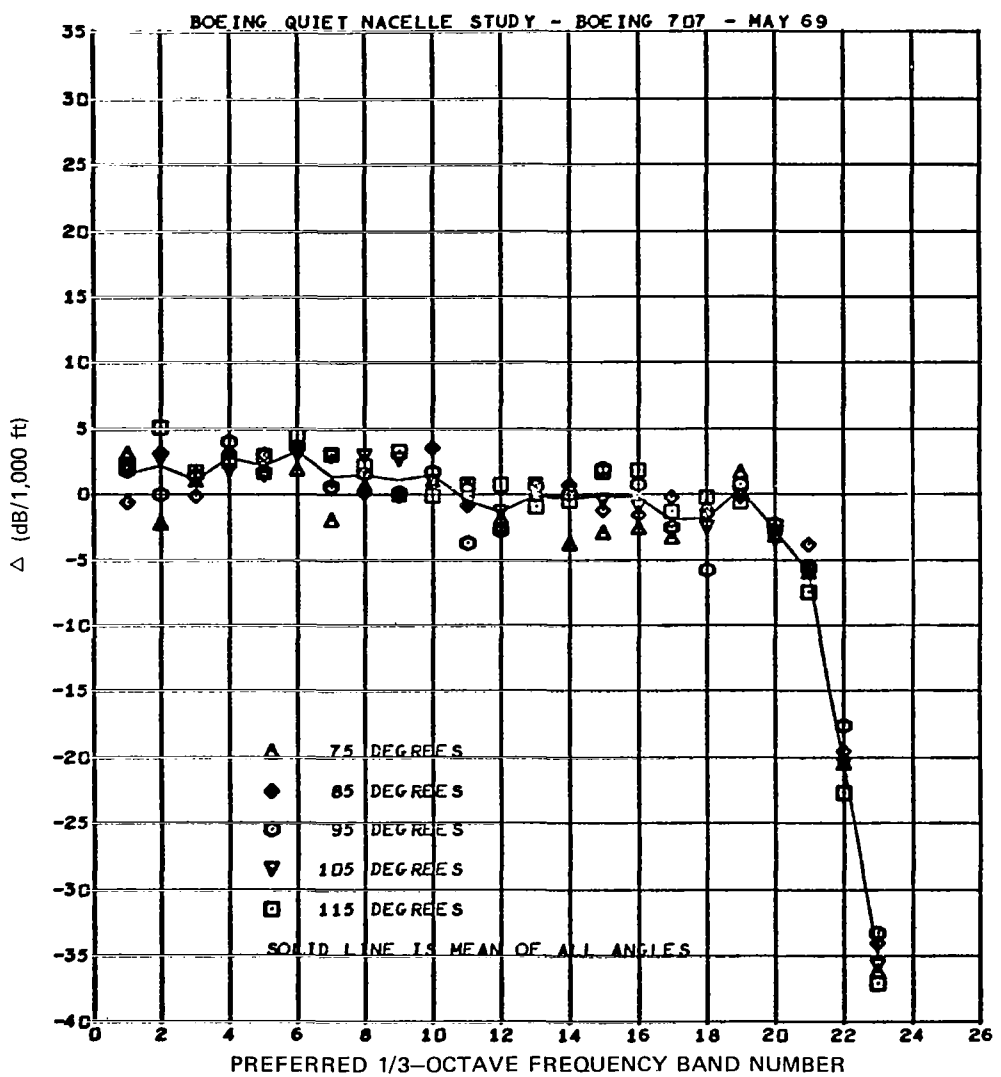


Figure A-10. Summary Plot of Differences (Δ) Between Experimental and ARP 866 Absorption Coefficients for Test Condition 17.07

Table A-11. Estimated Sample Variances and Number of Microphones for Test Condition 17.08

1/3-OCT FREQ BAND	DIRECTIVITY ANGLE (DEG)									
	75	43	85	91	95	100	105	110	115	120
1	1.83	2.38	.21	1.77	3.41	1.49	2.01	1.12	2.95	8.53
2	.72	.31	1.68	2.41	2.84	1.32	.69	1.30	2.32	3.92
3	.16	1.78	.77	.76	1.35	.93	3.31	4.00	1.44	1.93
4	1.22	.25	1.26	.77	1.52	1.08	1.52	.54	.18	.99
5	.55	1.11	1.53	.76	1.78	2.16	.88	.85	1.04	1.45
6	1.19	1.63	1.26	1.77	1.53	.45	2.12	1.53	1.01	.73
7	.96	.79	1.23	.68	1.88	1.69	1.95	1.12	.95	2.18
8	.98	1.54	1.35	1.49	1.70	.77	.31	.49	.55	1.24
9	.72	.51	.68	1.24	1.26	1.61	.64	.43	2.28	2.20
10	.82	.76	.94	1.49	1.77	1.48	1.60	2.08	.80	.12
11	.36	.76	1.66	1.91	2.41	.40	.81	1.96	2.25	1.66
12	.56	.77	1.54	2.23	2.36	.55	1.29	1.47	1.78	.64
13	.75	2.24	1.14	.76	2.33	1.08	.94	1.59	1.43	1.99
14	1.81	.11	.76	.29	1.03	.34	.09	1.42	.51	1.17
15	2.45	.34	1.12	.25	1.48	1.43	.71	3.26	1.30	1.92
16	1.43	1.55	.91	1.11	3.18	1.24	.10	2.46	.91	.85
17	.51	1.70	.88	.61	2.27	2.38	2.29	1.21	1.48	.94
18	1.94	3.42	1.01	.58	2.23	2.04	1.54	.92	1.33	.78
19	3.15	1.18	1.18	.45	2.53	.41	1.47	.75	1.04	2.28
20	3.46	3.93	4.15	1.86	.07	1.19	1.68	2.39	4.74	6.16
21	3.42	1.75	2.13	2.00	1.98	3.14	3.97	5.88	8.38	9.84
22	4.72	5.72	7.43	7.17	5.01	4.61	6.07	9.31	5.32	4.20

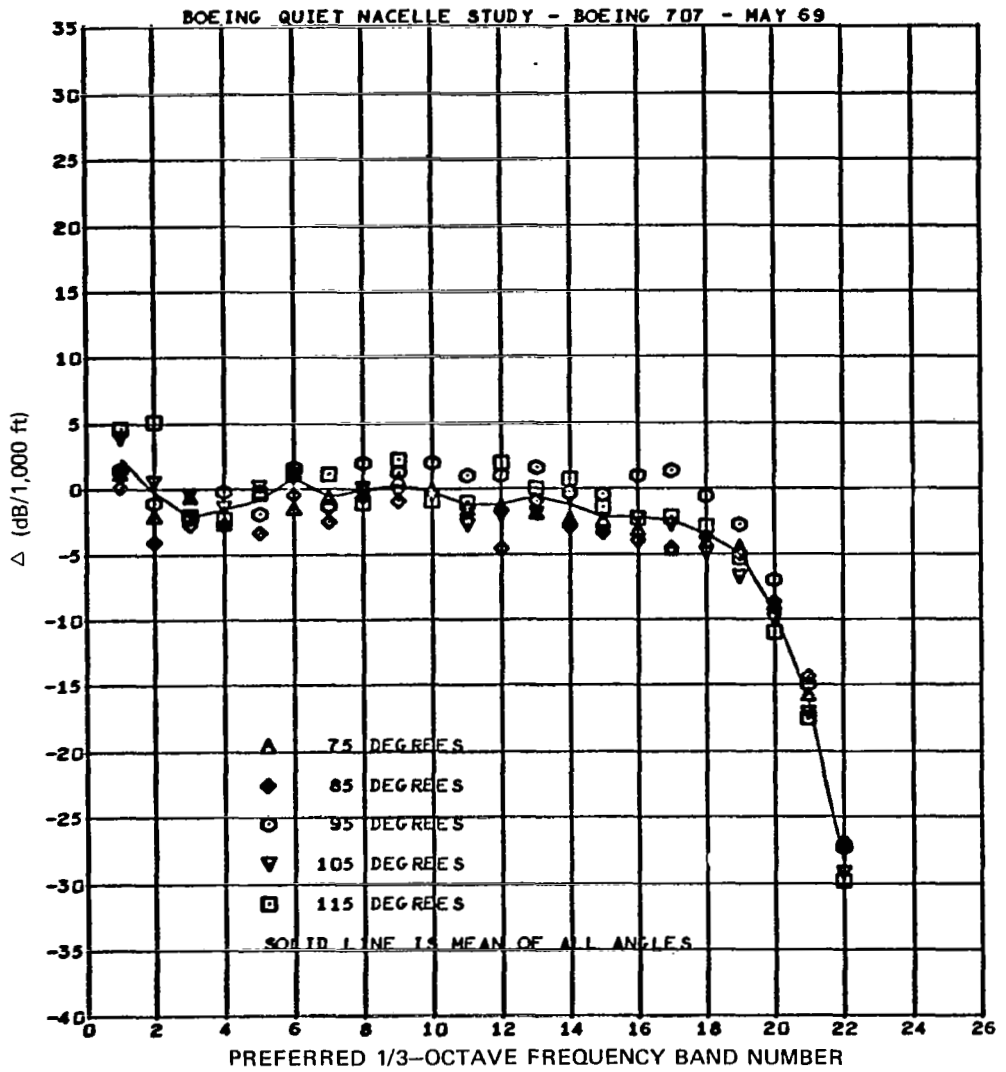


Figure A-11. Summary Plot of Differences (Δ) Between Experimental and ARP 866 Absorption Coefficients for Test Condition 17.08

Table A-12. Estimated Sample Variances and Number of Microphones for Test Condition 17.09

1/3-OCT FREQ BAND	DIRECTIVITY ANGLE (DEG)									
	75	81	85	90	95	100	105	110	115	120
1	2.23	3.13	2.22	1.15	2.94	2.87	2.90	1.47	2.78	1.73
2	1.31	.77	1.35	2.11	3.16	.66	1.61	2.70	1.38	1.54
3	1.10	.93	1.79	1.60	1.67	4.20	3.77	3.17	1.94	2.12
4	1.55	3.66	2.38	1.27	.39	.77	1.20	2.61	2.02	3.72
5	1.89	1.47	1.12	.65	.63	1.33	.49	.54	1.31	.41
6	4.09	.83	.32	.87	.62	.25	1.05	.73	.30	.74
7	2.60	2.33	2.17	1.90	2.06	3.53	2.72	.75	.40	1.23
8	4.21	2.23	2.10	1.18	1.15	.38	.49	.22	.66	2.05
9	1.41	1.73	1.89	.89	.63	.96	.93	1.29	.43	.40
10	2.86	2.45	1.32	.64	.54	.28	.68	.46	.69	1.21
11	3.23	1.66	.94	1.08	.93	1.01	.88	1.14	1.47	.83
12	2.29	.93	1.08	1.77	1.23	.75	.25	.58	.65	.95
13	1.80	2.74	2.11	1.15	1.14	1.16	.97	1.21	2.38	1.27
14	1.42	2.27	2.48	1.44	.81	.38	.61	1.04	1.54	1.41
15	1.27	1.04	1.36	2.28	1.43	1.92	1.20	.41	1.84	1.40
16	.54	1.39	.89	1.31	2.56	1.17	.70	1.43	1.90	3.33
17	.45	.34	.87	1.13	2.03	1.40	1.00	.81	.68	1.93
18	.90	.82	.71	.68	1.21	1.25	.49	.89	.78	.95
19	.56	.21	.26	1.27	1.62	.84	.47	1.46	2.31	3.19
20	1.51	.62	.24	1.46	1.21	1.58	1.09	1.32	.94	.91
21	1.62	1.35	1.94	2.16	.99	1.12	2.15	2.77	3.91	5.77
22	7.39	6.21	6.43	5.9	5.83	5.11	7.49	8.43	9.36	11.16
23	12.21	16.83	19.88	21.88	23.90	26.09	25.51	22.42	9.35	8.82
	4	4	4	4	4	4	4	4	3	3

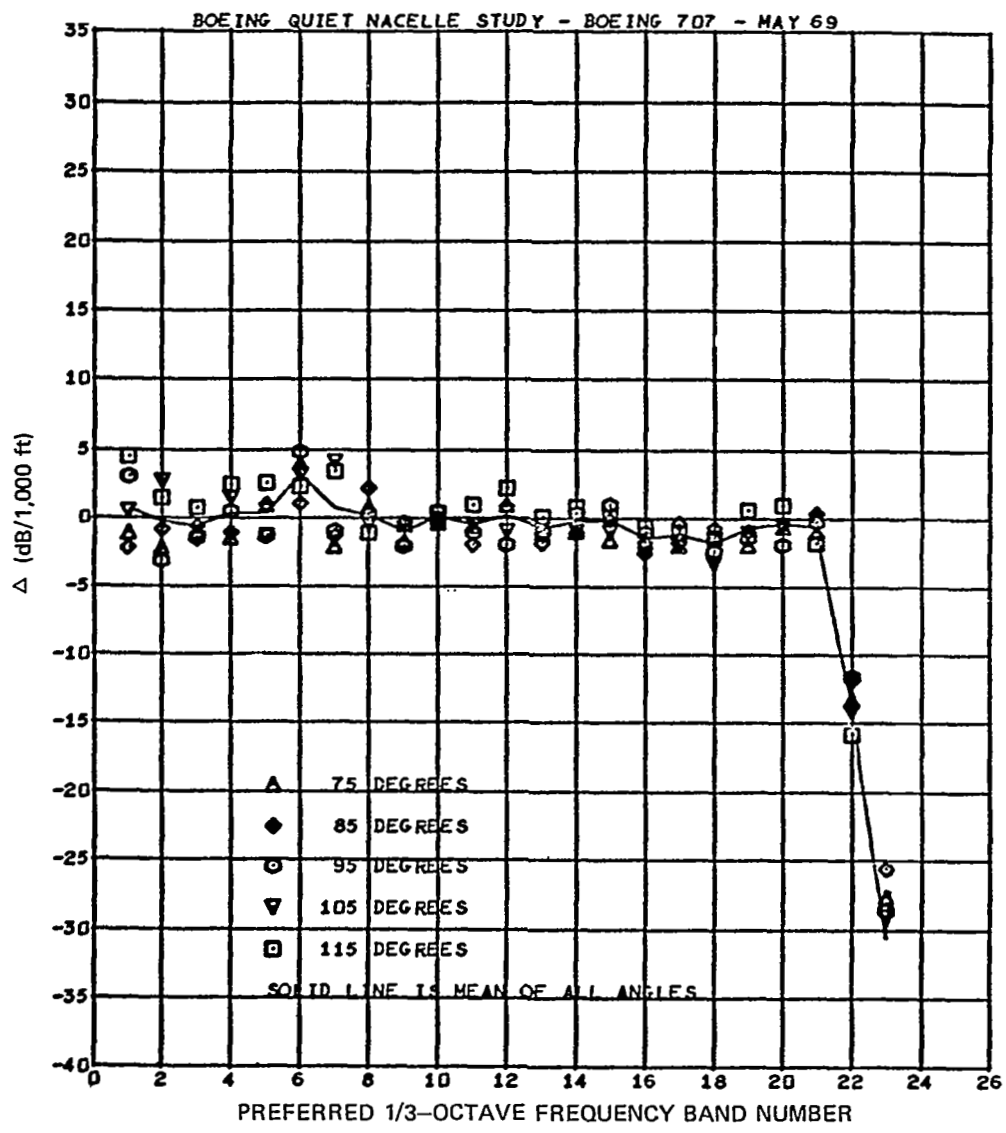


Figure A-12. Summary Plot of Differences (Δ) Between Experimental and ARP 866 Absorption Coefficients for Test Condition 17.09

Table A-13. Estimated Sample Variances and Number of Microphones for Test Condition 17.10

1/3-OCT FREQ BAND	DIRECTIVITY ANGLE (DEG)									
	75	81	85	91	95	101	105	111	115	121
1	4.19	2.34	.52	2.85	2.21	6.10	7.89	4.83	.95	1.28
2	1.52	2.46	2.41	3.24	2.73	2.59	2.46	1.36	1.34	2.28
3	2.51	1.75	1.54	1.30	1.13	1.30	3.76	4.32	5.32	5.77
4	1.33	2.13	1.92	2.31	1.49	2.44	1.68	1.21	1.49	1.27
5	2.81	.84	.96	2.74	.79	.32	.75	1.23	.45	.34
6	.69	.53	.72	.67	.17	.81	1.33	1.86	1.18	1.34
7	2.39	1.77	2.71	4.96	2.35	2.27	4.89	6.36	1.31	1.13
8	1.13	.91	.89	.88	2.17	2.51	1.89	1.42	1.55	.79
9	.83	.34	1.18	1.21	1.19	2.16	3.56	2.66	1.00	.36
10	1.23	1.46	1.76	.66	.34	1.30	1.16	1.29	2.69	1.35
11	1.67	2.34	1.74	.94	.78	1.99	2.87	1.85	1.86	.94
12	.51	.27	.46	.24	.55	1.31	2.36	2.12	1.59	.31
13	.41	.96	1.38	1.66	.48	.40	.90	1.61	1.45	.91
14	1.17	1.38	1.42	.84	.35	.52	.55	1.22	2.19	1.70
15	.43	1.35	1.96	2.47	1.35	1.76	.94	2.18	2.62	1.31
16	.74	.42	.72	1.26	.79	1.18	1.39	1.31	.85	1.21
17	.77	.71	.76	1.21	.94	1.82	3.71	3.72	3.98	1.36
18	1.85	1.11	1.19	2.31	1.74	.75	2.15	1.78	1.97	.36
19	1.44	.74	.79	1.48	1.19	1.38	1.89	2.41	1.84	.97
20	1.27	.39	.83	1.14	.73	1.39	4.81	4.17	5.39	5.42
21	11.01	11.99	12.14	11.23	12.06	11.92	12.71	15.48	19.12	21.11
22	13.92	15.21	16.11	14.62	13.89	14.63	13.68	16.17	17.96	16.22
23	8.57	19.94	14.53	13.82	17.58	19.18	6.03	3.62	2.62	2.43

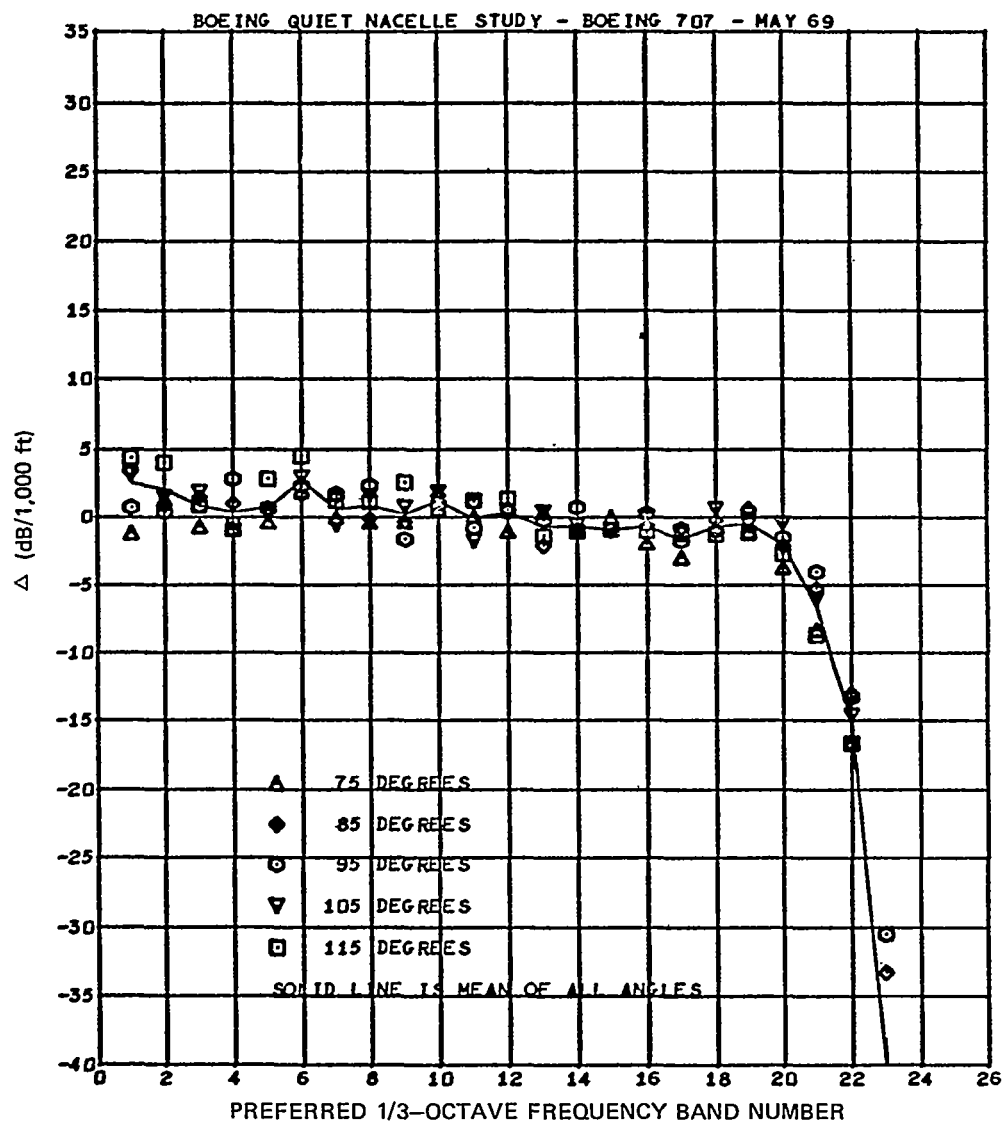


Figure A-13. Summary Plot of Differences (Δ) Between Experimental and ARP 866 Absorption Coefficients for Test Condition 17.10

Table A-14. Estimated Sample Variances and Number of Microphones for Test Condition 17.11

1/3-OCT FREQ BAND	DIRECTIVITY ANGLE (DEG)									
	75	85	95	96	95	100	115	110	115	120
1	2.37	2.25	3.79	5.52	5.81	4.66	4.19	4.55	2.37	2.03
2	7.29	12.23	15.37	11.86	7.41	9.29	3.54	2.46	4.87	2.99
3	10.76	12.72	11.97	11.64	12.23	14.38	16.56	17.10	19.34	17.29
4	4.70	2.74	1.12	1.13	3.21	5.39	8.37	13.51	18.50	22.32
5	3.94	5.25	6.57	4.44	2.73	2.73	4.30	3.74	6.95	8.01
6	1.10	1.12	1.35	3.20	1.61	.47	1.53	2.31	2.14	3.23
7	9.04	9.42	10.49	10.48	10.21	6.27	2.26	4.16	3.01	1.17
8	3.15	2.83	2.14	1.22	1.51	4.05	9.30	11.32	8.13	6.97
9	4.22	5.76	7.36	6.14	3.58	2.03	2.25	3.21	1.31	2.10
10	4.88	4.47	4.14	2.97	.84	.61	1.32	2.56	2.65	2.42
11	4.90	5.97	6.05	4.89	3.35	1.46	1.43	1.28	1.31	1.86
12	2.34	2.07	1.92	2.45	2.16	1.51	1.69	2.13	1.24	.83
13	1.35	2.37	2.71	2.71	2.86	1.20	1.42	1.70	1.52	1.04
14	2.64	2.11	3.14	2.78	3.74	2.47	1.44	.68	.87	2.43
15	1.26	.79	1.23	2.42	3.13	2.77	1.39	2.11	1.75	1.79
16	1.51	1.51	1.26	1.87	2.02	1.29	.36	1.73	1.91	4.14
17	1.18	.57	.38	2.08	3.42	2.74	1.35	1.91	2.13	4.01
18	1.60	1.74	1.74	1.55	3.35	3.28	1.93	1.45	2.45	3.70
19	.78	2.06	4.74	6.03	4.70	4.68	4.16	3.06	2.64	3.73
20	1.01	.54	1.94	3.03	3.58	4.06	4.69	5.91	7.94	9.47
21	1.14	2.02	3.35	5.81	5.24	6.32	7.36	6.85	6.57	8.28
22	2.78	5.30	7.23	7.13	8.56	8.49	7.00	6.18	6.13	6.47
23	4.68	6.16	8.12	9.55	6.74	4.18	3.14	4.48	6.80	4.32
	4	4	4	4	4	4	4	4	4	3

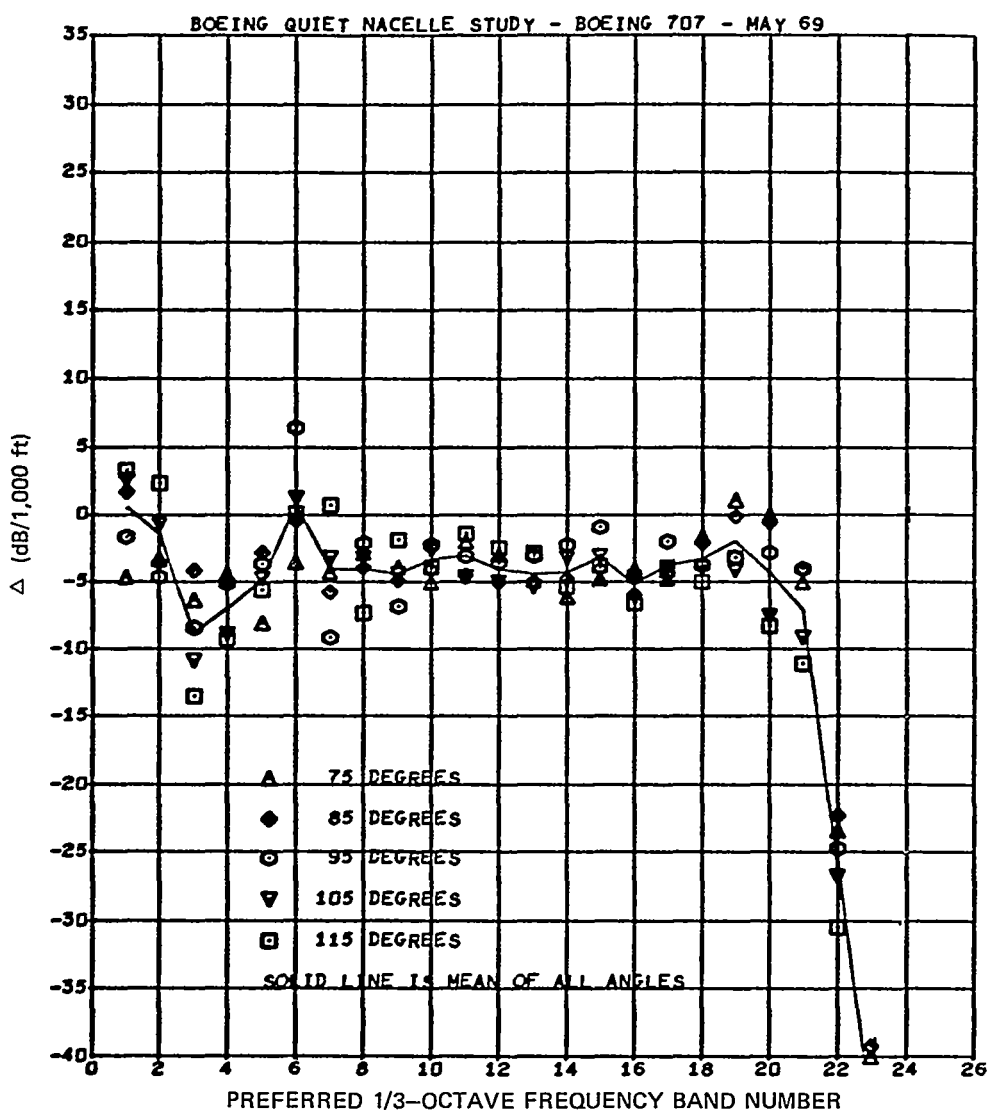


Figure A-14. Summary Plot of Differences (Δ) Between Experimental and ARP 866 Absorption Coefficients for Test Condition 17.11

Table A-15. Estimated Sample Variances and Number of Microphones for Test Condition 14.01

1/3-OCT FREQ BAND	DIRECTIVITY ANGLE (DEG)									
	75	30	85	90	95	100	105	110	115	120
1	12.93	3.56	8	4.36	8	6.77	7.22	13.43	9.85	9.84
2	5.39	5.09	6.54	9.21	9.83	21.03	18.28	19.42	23.83	13.10
3	5.87	5.41	8.26	13.29	18.72	33.09	28.01	37.04	51.14	37.85
4	6.58	7.52	6.47	7.93	7.08	11.56	13.43	17.17	18.82	25.19
5	2.42	2.34	3.06	7.33	5.71	3.39	2.76	2.70	3.46	8.32
6	3.77	4.61	2.28	1.66	2.13	2.04	1.86	3.01	1.85	1.41
7	4.12	4.26	5.38	7.53	12.89	21.07	12.94	6.06	6.30	11.97
8	1.50	3.18	1.29	1.38	1.78	7.84	13.21	15.12	14.14	14.44
9	3.13	3.34	4.51	7.60	9.69	10.42	7.55	5.87	5.91	6.38
10	1.69	2.62	4.49	3.37	1.56	1.70	6.07	11.13	11.69	7.50
11	4.40	3.73	2.79	2.06	4.14	8.29	4.26	4.27	3.61	3.83
12	4.35	3.65	2.55	1.96	1.10	1.46	.91	.90	2.14	2.36
13	8.44	4.24	2.24	1.51	1.50	1.83	1.34	1.60	2.90	3.25
14	6.65	3.40	4.03	1.88	.74	1.61	1.11	1.77	2.63	2.24
15	4.21	2.53	2.46	2.58	2.10	1.56	1.43	1.34	1.46	2.93
16	5.19	2.66	2.18	2.18	.96	1.27	3.00	2.20	1.33	1.35
17	1.01	1.21	2.93	3.99	3.72	3.33	3.14	2.34	1.19	3.19
18	8.03	9.30	11.03	7.83	5.85	8.32	7.90	9.08	7.43	5.46
19	6.39	2.84	1.51	1.05	1.49	1.75	.43	.31	.71	2.05
20	5.00	2.79	2.42	3.06	4.00	5.68	6.44	7.26	5.44	5.11
21	8.70	4.99	3.79	6.29	9.07	12.64	12.87	13.37	11.45	10.10
22	8.14	5.91	3.35	4.85	7.02	9.69	10.35	12.13	11.58	10.73
23	11.61	6.87	5.20	7.15	8.91	11.34	12.45	12.44	13.66	16.68
24	15.65	6.61	3.83	5.08	7.59	10.72	13.49	14.38	5.43	6.89

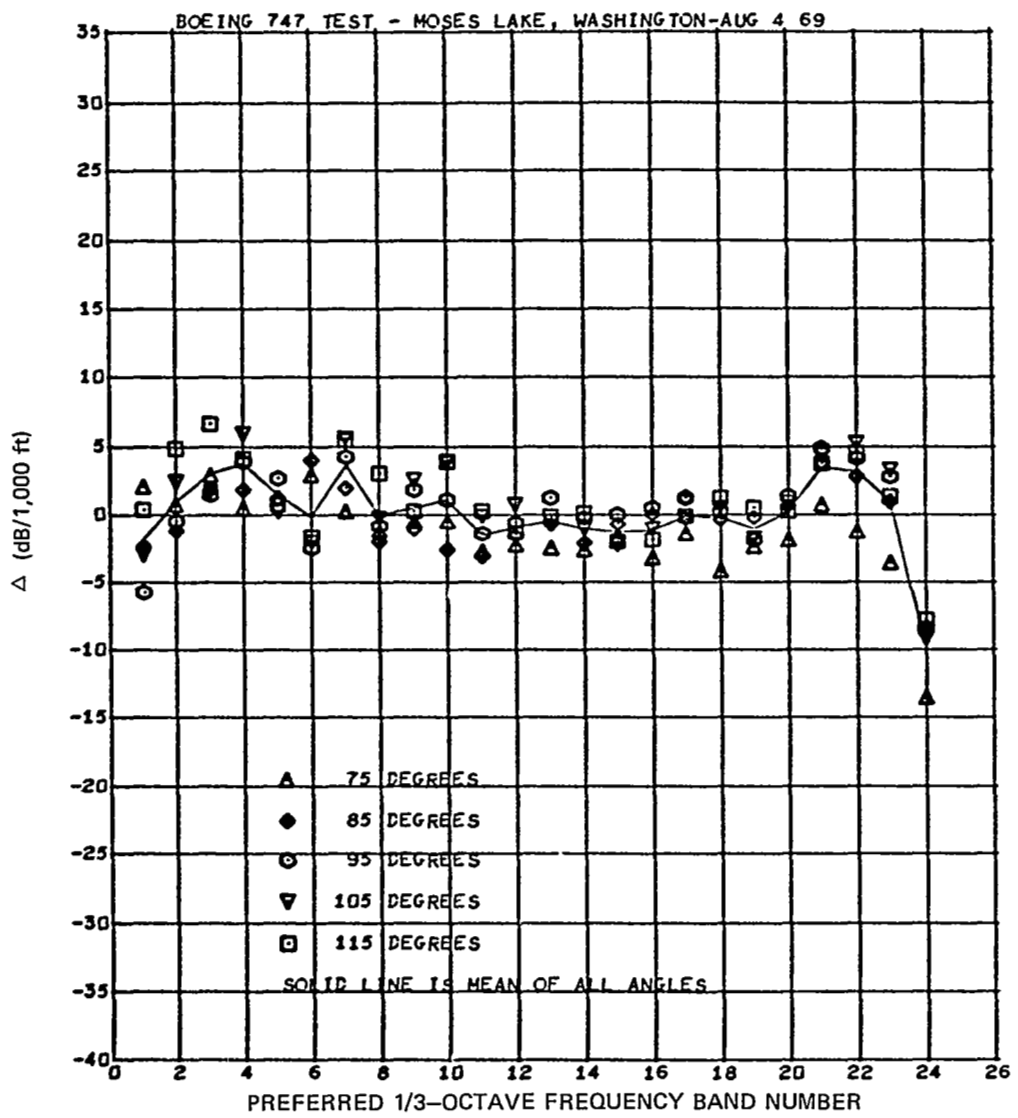


Figure A-15. Summary Plot of Differences (Δ) Between Experimental and ARP 866 Absorption Coefficients for Test Condition 14.01

Table A-16. Estimated Sample Variances and Number of Microphones for Test Condition 14.02

1/3-OCT FREQ BAND	DIRECTIVITY ANGLE (DEG)									
	75	80	85	90	95	100	105	110	115	120
1	20.32	7.39	2.99	2.83	5.44	14.85	9.76	6.63	6.44	8.44
2	4.80	7.84	8.53	9.94	14.41	21.85	21.41	21.72	16.99	10.64
3	2.25	4.21	5.21	10.06	9.40	16.15	18.40	20.62	25.11	30.38
4	2.39	3.35	3.65	4.79	4.64	6.29	7.32	9.29	17.20	24.00
5	1.34	1.56	1.55	1.68	1.34	3.33	4.15	3.46	2.78	7.06
6	3.41	4.36	4.85	.66	1.65	3.53	3.01	4.51	6.17	4.36
7	1.70	2.35	6.47	6.76	8.24	12.02	15.28	15.45	7.59	4.94
8	4.68	1.75	1.91	2.82	2.25	.42	1.74	3.78	4.69	11.24
9	7.73	2.71	1.09	1.74	3.53	7.51	6.53	6.20	5.42	4.12
10	7.24	4.67	3.79	2.58	1.21	2.35	2.01	3.29	5.31	4.87
11	3.54	4.34	5.19	4.58	3.28	1.99	1.08	.85	2.92	1.56
12	2.61	2.41	1.82	.76	.71	1.22	.39	1.02	2.50	1.80
13	3.91	2.18	1.63	1.76	.78	.67	.98	1.02	2.49	4.58
14	1.84	1.50	1.20	1.06	1.04	1.25	1.31	1.07	.52	.25
15	.93	1.00	.85	.58	.60	.77	.62	.69	.73	.66
16	3.66	2.08	.96	1.29	1.01	1.07	.89	.57	.44	1.15
17	1.08	1.71	2.67	3.23	3.17	3.98	2.53	1.16	.78	.94
18	8.74	4.90	3.13	1.21	1.95	6.13	5.13	4.91	4.96	5.98
19	5.27	1.73	.55	.99	.70	1.19	.52	.84	1.98	1.65
20	3.55	1.48	.44	.72	1.62	5.34	3.59	2.77	2.74	2.30
21	3.63	1.32	1.50	3.45	5.24	9.44	9.83	9.53	8.03	6.81
22	7.15	2.25	.71	1.41	2.85	5.62	7.09	7.79	7.73	7.65
23	9.60	2.94	1.11	2.05	3.72	7.54	8.98	10.83	10.47	8.10
24	8.95	3.00	1.29	1.85	4.84	10.32	12.02	11.75	8.09	6.55

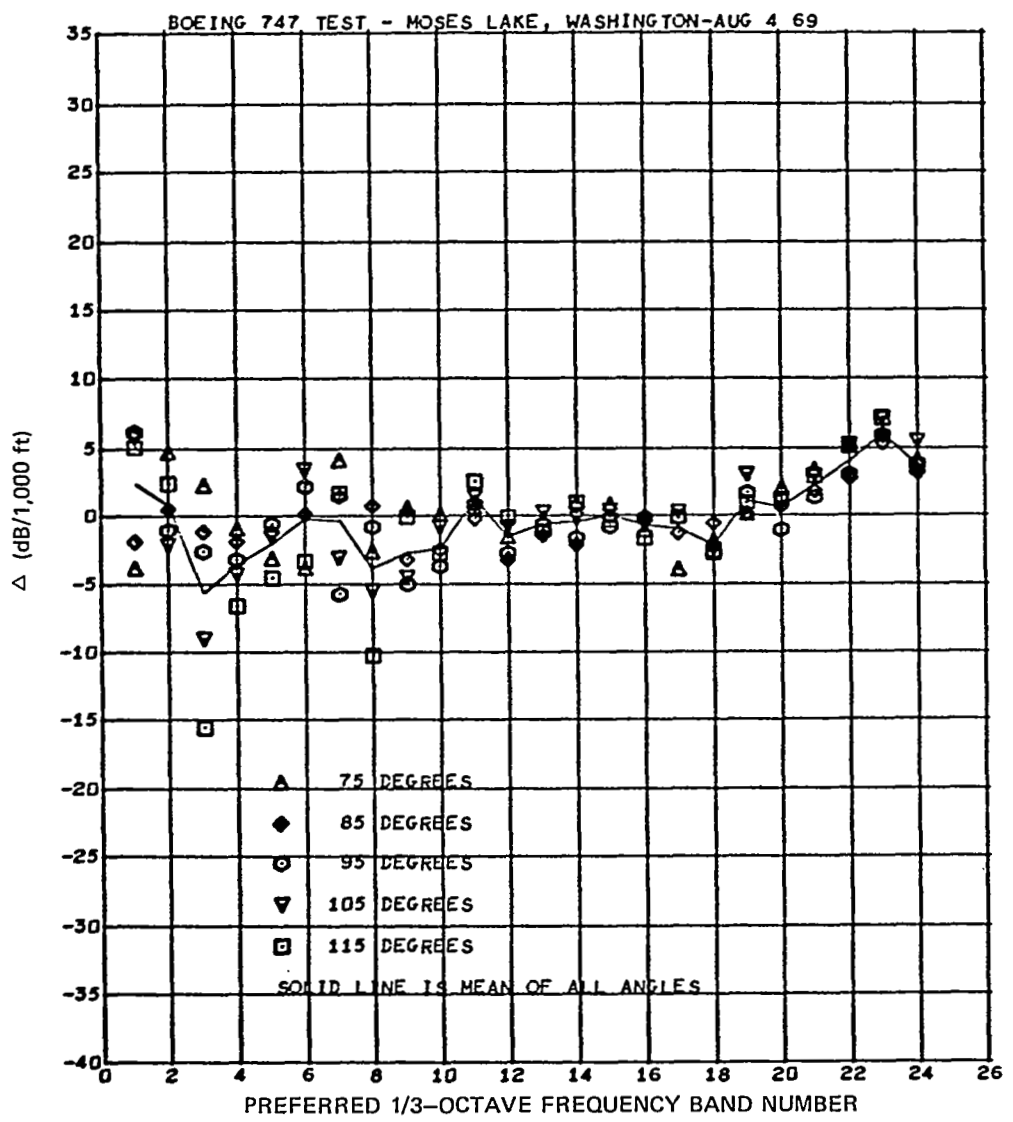


Figure A-16. Summary Plot of Differences (Δ) Between Experimental and ARP 866 Absorption Coefficients for Test Condition 14.02

Table A-17. Estimated Sample Variances and Number of Microphones for Test Condition 14.03

1/3-OCT FREQ BAND	DIRECTIVITY ANGLE (DEG)										
	75	80	85	90	95	100	105	110	115	120	
1	21.24	19.04	12.22	10.45	8.59	7.74	6.25	5.37	2.54	3.58	
2	5.51	6.26	6.96	8.59	12.11	18.97	15.28	10.23	10.85	13.30	
3	11.43	13.62	12.81	16.67	17.66	20.47	22.47	28.48	22.53	22.38	
4	7.05	10.85	20.18	31.59	44.89	62.20	58.60	49.63	44.80	43.80	
5	5.29	1.86	2.39	4.88	7.73	11.43	18.45	28.77	39.43	43.30	
6	4.51	3.66	1.95	.55	.76	4.36	3.69	3.54	5.65	8.07	
7	9.85	13.53	17.26	18.38	17.58	19.49	16.34	15.89	18.05	18.44	
8	3.46	7.20	9.15	14.29	15.56	14.87	12.53	12.15	11.52	12.69	
9	5.53	7.07	9.90	11.19	13.49	17.58	17.65	17.46	16.38	14.30	
10	5.14	4.61	3.91	3.71	4.41	6.82	6.06	6.84	10.21	11.35	
11	8.50	7.11	5.31	3.72	2.93	4.05	3.85	3.90	5.51	8.76	
12	5.08	3.14	1.91	1.32	.91	.85	.42	2.13	1.79	1.55	
13	2.10	1.54	1.82	1.32	1.09	1.64	.86	.89	.45	.75	
14	3.07	1.90	1.11	.78	.95	1.35	1.84	2.62	2.04	1.68	
15	2.77	2.22	1.67	1.39	1.40	1.53	1.49	1.68	1.39	1.20	
16	2.08	1.25	1.51	1.28	1.03	.97	1.98	1.43	1.07	1.00	
17	4.23	4.67	4.34	3.17	2.37	1.75	1.40	1.31	1.09	1.16	
18	4.78	4.55	6.25	5.13	4.59	6.85	6.36	5.75	5.71	5.86	
19	3.07	1.69	1.46	1.05	1.18	1.61	1.67	2.00	1.05	1.41	
20	1.79	2.29	2.92	2.37	3.01	4.12	4.32	4.58	5.16	5.78	
21	5.10	5.12	6.32	7.06	7.98	9.88	9.89	10.27	10.00	9.51	
22	6.75	4.58	4.87	5.92	7.75	9.96	11.22	12.20	13.59	14.97	
23	6.30	4.06	4.37	5.61	7.27	9.77	10.26	16.86	12.19	13.12	
24	6.03	3.40	4.40	6.28	7.96	10.59	12.03	13.27	13.88	14.57	

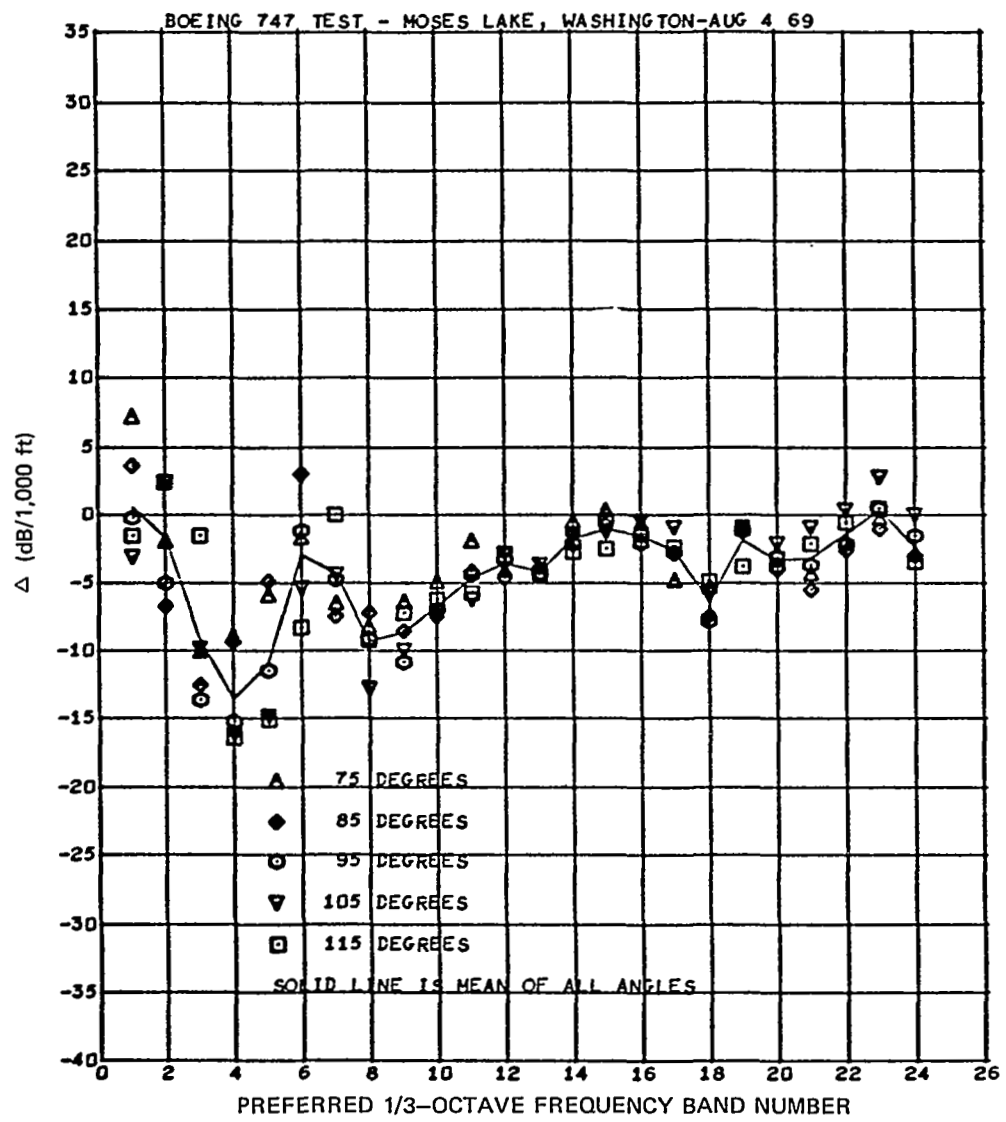


Figure A-17. Summary Plot of Differences (Δ) Between Experimental and ARP 866 Absorption Coefficients for Test Condition 14.03

Table A-18. Estimated Sample Variances and Number of Microphones for Test Condition 14.04

1/3-OCT FREQ BAND	DIRECTIVITY ANGLE (DEG)									
	75	80	85	90	95	100	105	110	115	120
1	7.54	12.63	10.69	7.14	4.69	8.76	5.91	4.25	3.60	3.01
2	12.46	9.82	10.36	9.27	6.61	7.40	7.90	10.99	8.58	5.55
3	7.18	7.19	9.55	13.77	13.18	14.86	17.23	23.67	23.96	23.49
4	2.08	3.93	6.28	11.19	12.34	14.27	16.31	19.06	18.61	18.37
5	4.49	4.70	5.64	7.16	6.16	6.84	10.28	15.77	25.26	31.55
6	8.16	8.45	5.42	3.01	2.06	2.12	2.32	3.66	4.07	3.51
7	6.03	7.69	9.02	7.10	5.80	6.63	7.00	6.73	5.78	5.24
8	1.59	2.99	3.91	4.13	4.23	5.18	4.28	3.99	5.64	8.44
9	2.58	1.07	1.20	1.95	3.09	6.24	6.65	6.23	5.27	7.44
10	2.09	1.86	1.40	1.39	1.18	2.53	3.68	5.35	7.11	8.37
11	3.56	2.00	1.31	.97	1.01	1.43	1.98	3.35	4.86	6.16
12	3.26	2.18	.91	2.02	1.94	1.63	1.93	3.26	3.65	3.31
13	2.53	1.93	2.00	2.29	2.42	3.46	4.19	5.16	4.60	3.40
14	1.32	.91	.71	.66	.91	1.79	1.96	1.98	2.03	1.53
15	1.41	1.27	1.24	1.31	1.08	1.00	1.15	1.78	1.02	.5^n
16	1.90	1.85	1.36	2.23	1.98	1.77	1.23	1.41	1.39	1.23
17	1.59	3.66	3.77	2.63	1.85	1.30	.98	1.19	1.64	1.24
18	2.84	2.12	3.35	3.37	2.55	2.68	3.16	4.04	3.29	1.58
19	1.34	.99	1.06	1.52	1.80	2.39	1.82	1.55	1.69	1.79
20	1.93	1.49	1.59	2.74	3.41	4.36	3.86	3.59	3.55	2.40
21	2.18	2.22	3.95	5.97	6.73	7.57	6.85	5.84	4.76	3.09
22	2.73	2.04	2.68	4.15	5.85	8.71	9.41	9.31	8.09	6.13
23	2.71	2.55	3.73	6.03	7.44	9.46	10.36	11.17	9.21	6.95
24	2.69	2.79	3.87	5.62	6.35	7.72	8.90	10.38	9.62	8.43

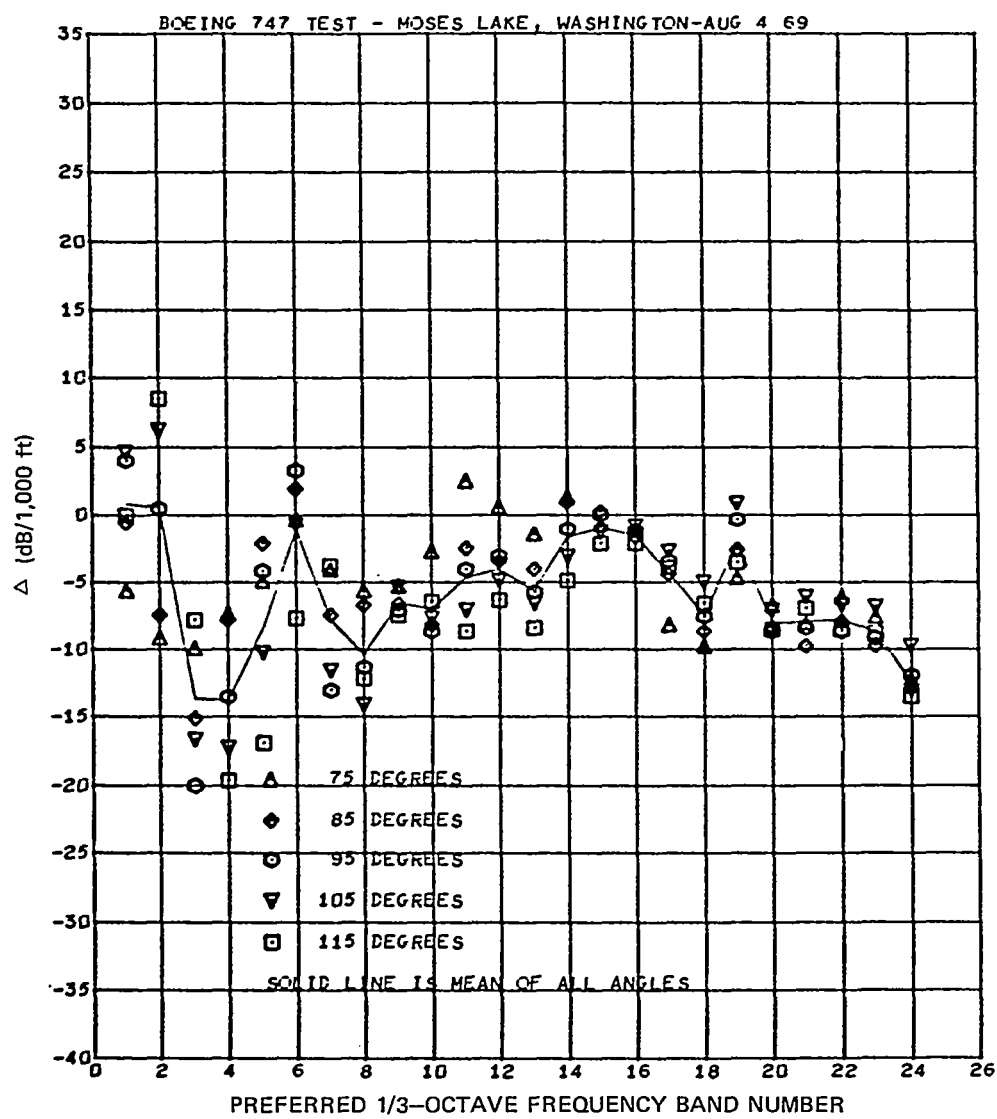


Figure A-18. Summary Plot of Differences (Δ) Between Experimental and ARP 866 Absorption Coefficients for Test Condition 14.04

Table A-19. Estimated Sample Variances and Number of Microphones for Test Condition 10

1/3-OCT FREQ BAND	DIRECTIVITY ANGLE (DEG)									
	75	83	85	90	95	100	105	110	115	120
1	2.87	.86	2.12	2.90	3.02	5.34	5.27	3.93	2.61	3.18
	11	11	11	11	11	11	11	11	11	11
2	1.53	.58	1.16	4.30	4.23	3.04	2.15	1.57	1.46	2.32
	11	11	11	11	11	11	11	11	11	11
3	2.73	2.45	1.53	1.13	.97	1.66	2.11	.68	1.55	3.15
	11	11	11	11	11	11	11	11	11	11
4	.58	1.39	2.11	.81	.88	1.54	1.10	.90	1.49	2.17
	11	11	11	11	11	11	11	11	11	11
5	.29	.47	.59	.85	.52	.67	1.27	.65	.62	1.24
	11	11	11	11	11	11	11	11	11	11
6	1.14	1.22	1.04	.56	.78	1.11	1.17	1.34	.91	.92
	11	11	11	11	11	11	11	11	11	11
7	1.30	1.03	1.26	1.33	.85	1.52	2.46	1.78	1.53	1.90
	11	11	11	11	11	11	11	11	11	11
8	1.21	1.24	.93	1.03	1.26	1.50	1.32	1.31	1.42	.86
	11	11	11	11	11	11	11	11	11	11
9	1.68	1.62	.92	.51	.85	.81	.94	.56	.30	.60
	11	11	11	11	11	11	11	11	11	11
10	.39	.46	.71	.82	.37	1.66	1.30	.76	.79	1.46
	11	11	11	11	11	11	11	11	11	11
11	.79	.36	.46	.51	.75	1.03	1.24	1.29	1.03	.73
	11	11	11	11	11	11	11	11	11	11
12	1.24	.84	.95	.93	.95	1.34	1.46	1.87	1.41	1.15
	11	11	11	11	11	11	11	11	11	11
13	.88	.80	.54	.58	1.17	1.34	1.42	1.00	.65	.47
	11	11	11	11	11	11	11	11	11	11
14	1.26	.89	.78	.83	.66	.53	.34	1.40	1.69	.92
	11	11	11	11	11	11	11	11	11	11
15	.62	.75	.81	.79	.96	1.11	1.10	.94	.72	.26
	11	11	11	11	11	11	11	11	11	11
16	.21	.34	1.15	1.22	1.36	1.25	1.09	1.05	.77	.60
	11	11	11	11	11	11	11	11	11	11
17	.30	.56	1.34	1.66	1.93	2.07	1.41	1.02	1.17	1.11
	11	11	11	11	11	11	11	11	11	11
18	.92	.81	1.04	1.98	3.31	2.16	1.73	1.26	.67	.67
	11	11	11	11	11	11	11	11	11	11
19	.66	.68	.67	1.22	1.61	.98	.64	.86	.88	1.48
	11	11	11	11	11	11	11	11	11	11
20	.23	.41	.97	.94	1.03	.88	.77	.77	.73	.57
	11	11	11	11	11	11	11	11	11	11
21	.25	.29	.81	1.48	1.45	1.18	1.22	1.18	.74	.83
	11	11	11	11	11	11	11	11	11	11
22	.28	.39	1.02	1.63	.65	.59	.43	.28	.13	.14
	11	11	11	11	11	11	11	11	11	11
23	.38	.27	.74	.68	.41	.90	1.45	2.20	3.83	5.43
	11	11	11	11	11	11	11	11	11	11
24	2.55	2.30	3.17	3.88	5.13	5.29	6.35	7.83	8.38	19.39
	8	8	9	9	9	8	8	7	6	6

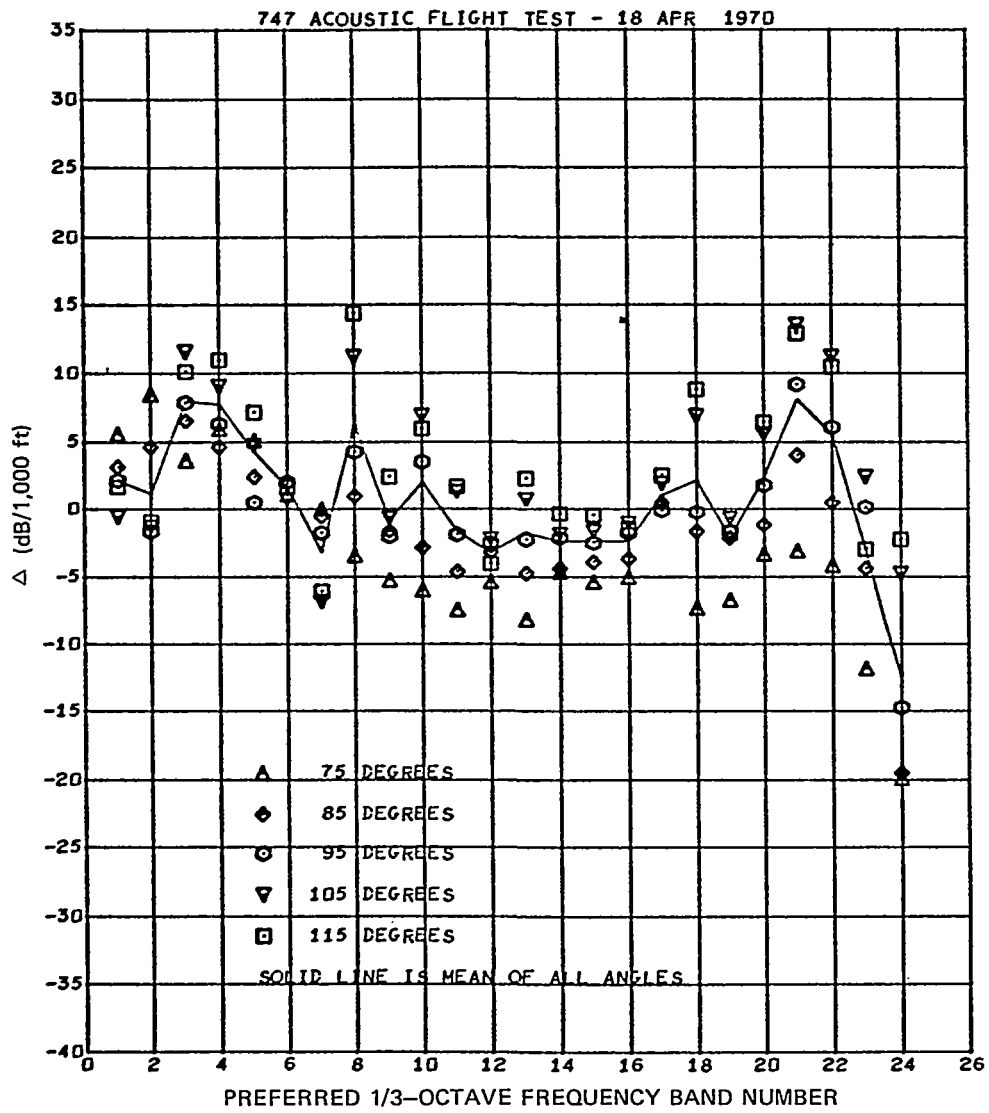


Figure A-19. Summary Plot of Differences (Δ) Between Experimental and ARP 866 Absorption Coefficients for Test Condition 10

Table A-20. Estimated Sample Variances and Number of Microphones for Test Condition 11

1/3-OCT FREQ BAND	DIRECTIVITY ANGLE (DEG)									
	75	81	85	93	95	100	105	110	115	120
1	2.27	3.85	4.47	4.23	3.33	2.45	2.44	2.71	2.25	.96
	11	11	11	11	11	11	11	11	11	11
2	1.92	2.73	1.81	1.22	1.90	3.37	4.12	1.96	1.40	1.54
	11	11	11	11	11	11	11	11	11	11
3	5.63	5.65	3.95	2.85	3.29	3.94	3.18	2.65	3.04	2.69
	11	11	11	11	11	11	11	11	11	11
4	1.18	1.30	1.34	1.25	1.66	1.15	.71	.62	2.56	6.21
	11	11	11	11	11	11	11	11	11	11
5	.53	.72	1.03	.69	.51	.65	.51	.27	1.13	1.36
	11	11	11	11	11	11	11	11	11	11
6	.97	1.53	1.12	1.00	.67	.52	.77	.95	.76	.53
	11	11	11	11	11	11	11	11	11	11
7	.89	.66	.65	.86	1.05	.89	1.13	1.44	1.55	1.13
	11	11	11	11	11	11	11	11	11	11
8	.92	.77	1.02	1.31	1.29	1.38	1.93	2.27	1.14	.40
	11	11	11	11	11	11	11	11	11	11
9	1.67	1.24	1.01	1.04	1.11	1.17	1.15	.96	.62	.45
	11	11	11	11	11	11	11	11	11	11
10	.66	.53	.55	.53	.49	.64	.88	.76	.83	.98
	11	11	11	11	11	11	11	11	11	11
11	.55	.93	1.53	.87	.56	.56	.58	.94	.90	.61
	11	11	11	11	11	11	11	11	11	11
12	2.23	1.43	1.03	1.13	.96	.61	.46	.94	1.02	.59
	11	11	11	11	11	11	11	11	11	11
13	1.26	1.09	.88	.96	.89	.73	1.13	1.54	1.31	.73
	11	11	11	11	11	11	11	11	11	11
14	.49	.78	.84	.69	.53	.52	.51	.56	.89	1.19
	11	11	11	11	11	11	11	11	11	11
15	.34	.46	.68	1.14	1.47	1.55	1.23	.83	.53	.42
	11	11	11	11	11	11	11	11	11	11
16	.59	.40	.32	.52	.97	1.10	.98	.79	.47	.31
	11	11	11	11	11	11	11	11	11	11
17	.41	.54	.55	.73	1.32	1.75	1.46	1.24	.89	.81
	11	11	11	11	11	11	11	11	11	11
18	1.17	1.14	1.25	1.27	2.29	2.20	.98	.72	.65	.64
	11	11	11	11	11	11	11	11	11	11
19	.52	.35	.21	.34	.59	.69	.56	.59	1.47	1.59
	11	11	11	11	11	11	11	11	11	11
20	.21	.29	.39	.42	.63	.81	.62	.50	.52	.60
	11	11	11	11	11	11	11	11	11	11
21	.51	.45	.44	.29	.26	.44	.58	.62	.63	.41
	11	11	11	11	11	11	11	11	11	11
22	.32	.45	.42	.25	.19	.31	.47	.51	.77	.80
	11	11	11	11	11	11	11	11	11	11
23	.50	.53	.61	.67	.85	1.17	2.16	3.02	3.87	4.51
	11	11	11	11	11	11	11	11	11	11
24	2.04	2.04	2.15	2.61	3.32	4.15	5.11	5.68	5.43	5.62
	10	10	10	10	10	10	10	10	9	8

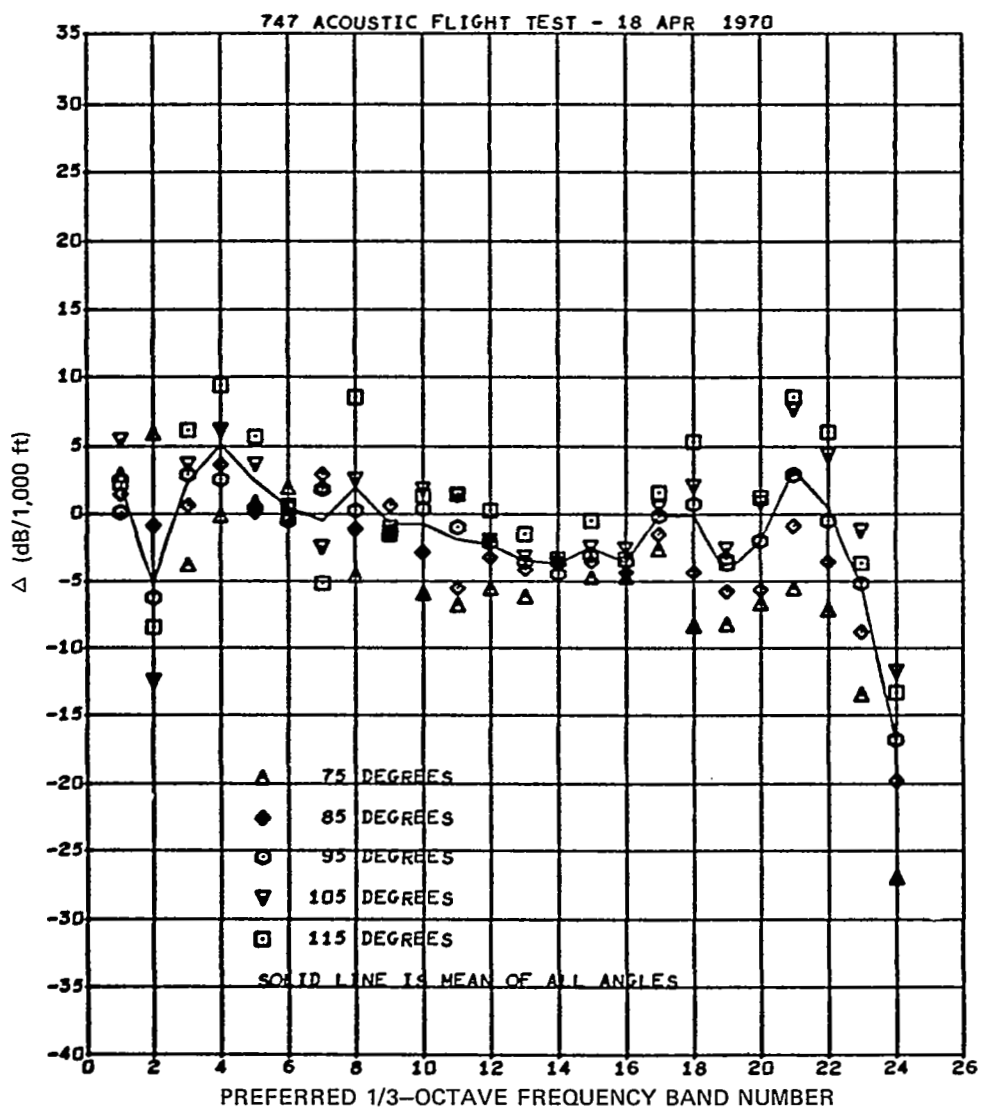


Figure A-20. Summary Plot of Differences (Δ) Between Experimental and ARP 866 Absorption Coefficients for Test Condition 11

Table A-21. Estimated Sample Variances and Number of Microphones for Test Condition 12

1/3-OCT FREQ BAND	DIRECTIVITY ANGLE (DEG)									
	75	80	85	90	95	100	105	110	115	120
1	1.84	1.85	1.33	1.67	2.17	1.99	1.54	1.86	2.13	3.17
	11	11	11	11	11	11	11	11	11	11
2	3.63	5.63	3.96	2.19	3.74	3.27	1.84	.94	1.77	2.51
	11	11	11	11	11	11	11	11	11	11
3	2.23	2.19	2.51	3.34	3.22	2.89	2.16	1.77	1.36	3.28
	11	11	11	11	11	11	11	11	11	11
4	1.14	.58	.43	.42	1.35	2.19	3.06	4.92	5.55	5.10
	11	11	11	11	11	11	11	11	11	11
5	.91	.77	.72	.55	.43	.60	1.06	2.76	3.61	2.73
	11	11	11	11	11	11	11	11	11	11
6	1.73	2.08	1.52	1.58	1.52	1.45	1.47	1.91	1.63	.91
	11	11	11	11	11	11	11	11	11	11
7	1.19	.78	.44	.67	1.21	1.30	1.79	2.20	1.94	1.63
	11	11	11	11	11	11	11	11	11	11
8	.66	.82	.38	1.26	2.08	2.17	3.19	4.56	3.19	1.41
	11	11	11	11	11	11	11	11	11	11
9	1.31	.82	.68	.56	.82	1.05	.88	.92	1.34	2.03
	11	11	11	11	11	11	11	11	11	11
10	.60	1.06	1.45	1.71	2.19	2.01	1.47	1.09	.78	.88
	11	11	11	11	11	11	11	11	11	11
11	1.08	1.67	1.28	1.45	1.51	1.75	1.20	.98	.31	.37
	11	11	11	11	11	11	11	11	11	11
12	1.15	1.23	1.31	1.19	1.18	1.12	.94	.67	.55	.54
	11	11	11	11	11	11	11	11	11	11
13	.75	.71	.83	.60	.74	.86	.65	.52	.46	.66
	11	11	11	11	11	11	11	11	11	11
14	.81	1.41	1.19	.82	.81	.64	.55	.67	1.16	1.21
	11	11	11	11	11	11	11	11	11	11
15	.54	.43	.62	1.30	.39	.53	.46	.58	1.01	1.01
	11	11	11	11	11	11	11	11	11	11
16	.43	.63	1.16	2.42	1.56	1.12	1.01	.56	.37	.81
	11	11	11	11	11	11	11	11	11	11
17	.38	.28	.42	1.69	1.45	1.40	.80	.66	.92	1.73
	11	11	11	11	11	11	11	11	11	11
18	.96	1.86	.82	.97	.92	1.23	2.24	2.29	1.40	.71
	11	11	11	11	11	11	11	11	11	11
19	.20	.20	.74	.62	.68	.61	.45	.82	.94	1.16
	11	11	11	11	11	11	11	11	11	11
20	.24	.61	.28	.34	.38	.45	.48	.66	.84	.78
	11	11	11	11	11	11	11	11	11	11
21	.33	.52	.43	.71	.95	1.04	1.32	1.06	1.03	.98
	11	11	11	11	11	11	11	11	11	11
22	.51	.53	.21	.53	.32	.66	.90	1.21	1.56	1.26
	11	11	11	11	11	11	11	11	11	11
23	2.58	2.56	1.51	1.52	2.21	3.17	4.50	6.11	7.91	4.15
	11	11	11	11	11	11	11	11	11	10
24	4.32	4.06	2.86	3.22	3.64	3.45	3.31	4.15	2.25	.16
	6	7	7	7	7	7	6	6	5	4

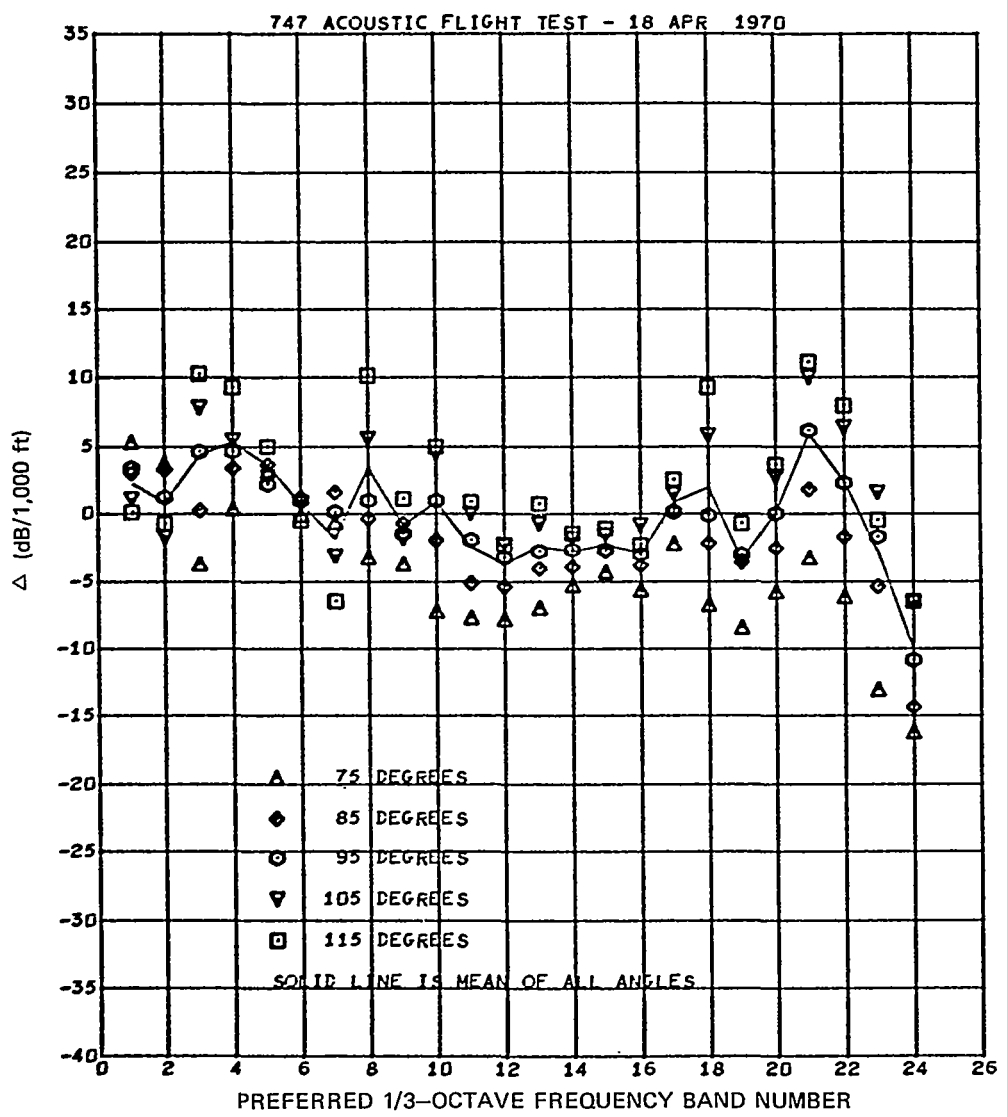


Figure A-21. Summary Plot of Differences (Δ) Between Experimental and ARP 866 Absorption Coefficients for Test Condition 12

Table A-22. Estimated Sample Variances and Number of Microphones for Test Condition 13

1/3-OCT FREQ BAND	DIRECTIVITY ANGLE (DEG)									
	75	80	85	90	95	100	105	110	115	120
1	3.37	2.42	.93	.71	1.82	2.01	1.95	1.73	2.05	3.88
	11	11	11	11	11	11	11	11	11	11
2	2.30	1.69	2.16	3.03	3.95	3.17	2.33	2.49	2.75	3.69
	11	11	11	11	11	11	11	11	11	11
3	1.42	3.37	4.75	5.43	4.50	3.01	2.30	1.06	1.66	3.22
	11	11	11	11	11	11	11	11	11	11
4	1.04	.54	.58	1.21	1.75	2.59	3.55	3.23	2.92	4.85
	11	11	11	11	11	11	11	11	11	11
5	.74	.96	.94	.88	.49	.99	1.20	.81	1.38	1.95
	11	11	11	11	11	11	11	11	11	11
6	2.20	2.02	1.98	1.66	1.88	2.47	2.31	1.48	1.10	.95
	11	11	11	11	11	11	11	11	11	11
7	.90	.94	1.44	1.89	2.12	1.83	2.02	2.10	1.87	1.13
	11	11	11	11	11	11	11	11	11	11
8	1.05	.31	.21	.54	1.37	1.48	2.39	2.44	.73	1.28
	11	11	11	11	11	11	11	11	11	11
9	1.12	2.10	2.41	1.74	1.88	1.79	1.06	1.05	1.46	1.60
	11	11	11	11	11	11	11	11	11	11
10	.82	.96	1.07	.82	.78	.74	.78	.75	1.17	2.12
	11	11	11	11	11	11	11	11	11	11
11	.91	.62	1.27	.99	1.05	1.39	1.85	2.27	1.37	1.87
	11	11	11	11	11	11	11	11	11	11
12	1.69	.83	.75	.73	.45	.26	.68	.74	.49	.46
	11	11	11	11	11	11	11	11	11	11
13	1.08	.64	.66	1.64	1.37	1.16	.84	.45	.32	.46
	11	11	11	11	11	11	11	11	11	11
14	.64	.83	.77	.88	1.39	1.26	.31	1.11	1.44	1.76
	11	11	11	11	11	11	11	11	11	11
15	.52	1.16	.88	.72	.64	.71	1.17	1.19	1.64	1.18
	11	11	11	11	11	11	11	11	11	11
16	.49	.41	.52	.79	.58	.39	.41	1.03	1.08	.61
	11	11	11	11	11	11	11	11	11	11
17	.63	.79	.52	.27	.30	.33	.64	.97	.79	.48
	11	11	11	11	11	11	11	11	11	11
18	.85	1.19	.75	.35	.57	1.32	1.76	1.02	.60	.77
	11	11	11	11	11	11	11	11	11	11
19	.90	.63	.41	.19	.08	.41	.79	1.20	1.63	1.12
	11	11	11	11	11	11	11	11	11	11
20	.61	.42	.29	.14	.22	.21	.35	.45	.47	.46
	11	11	11	11	11	11	11	11	11	11
21	.51	.35	.22	.12	.16	.28	.40	.68	.82	.86
	11	11	11	11	11	11	11	11	11	11
22	.58	.26	.29	.13	.17	.39	.83	1.08	1.51	2.69
	11	11	11	11	11	11	11	11	11	11
23	.74	.53	.82	1.42	1.83	2.70	4.30	5.73	4.62	6.78
	10	10	10	10	10	10	10	10	10	9
24	.86	.75	.68	1.14	1.47	2.19	4.43	1.75	2.81	3.16
	5	5	5	5	5	5	5	4	4	3

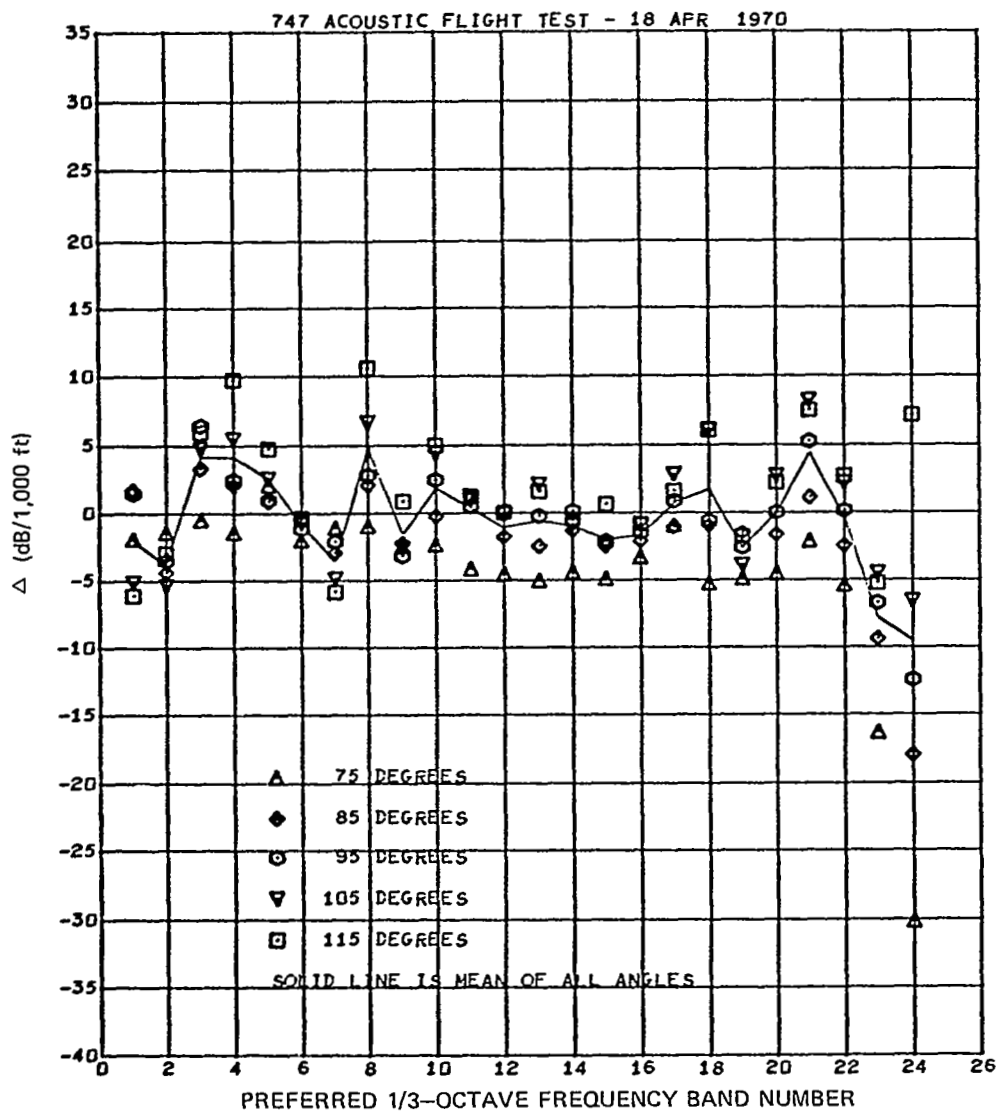


Figure A-22. Summary Plot of Differences (Δ) Between Experimental and ARP 866 Absorption Coefficients for Test Condition 13

Table A-23. Estimated Sample Variances and Number of Microphones for Test Condition 004.1

1/3-OCT FREQ BAND	DIRECTIVITY ANGLE (DEG)									
	75	85	85	90	95	100	105	110	115	120
1	1.87	5.01	3.17	3.18	3.39	2.33	1.87	1.72	2.05	.73
	12	12	12	12	12	12	12	12	12	12
2	5.20	7.80	6.45	5.26	7.67	6.74	7.05	4.77	1.28	.98
	12	12	12	12	12	12	12	12	12	12
3	5.14	3.99	5.44	5.00	5.80	7.07	9.22	13.62	10.04	3.69
	12	12	12	12	12	12	12	12	12	12
4	1.31	.57	.86	.96	2.22	4.40	4.52	4.96	4.34	4.41
	12	12	12	12	12	12	12	12	12	12
5	.92	.59	1.24	2.56	2.10	1.70	2.34	1.47	2.42	3.44
	12	12	12	12	12	12	12	12	12	12
6	2.15	4.80	2.85	2.64	3.92	5.10	3.75	1.74	3.00	2.87
	12	12	12	12	12	12	12	12	12	12
7	3.24	4.17	3.93	3.40	8.42	7.93	5.35	4.69	6.89	5.45
	12	12	12	12	12	12	12	12	12	12
8	2.91	3.45	4.35	5.59	5.39	4.91	3.98	2.43	1.22	3.47
	12	12	12	12	12	12	12	12	12	12
9	5.19	7.50	10.27	7.44	7.70	6.68	6.37	5.41	3.76	3.55
	12	12	12	12	12	12	12	12	12	12
10	2.19	1.24	.87	1.75	3.63	2.48	1.34	1.43	2.30	1.79
	12	12	12	12	12	12	12	12	12	12
11	1.34	2.32	2.23	1.63	3.89	2.76	1.52	1.31	3.09	2.89
	12	12	12	12	12	12	12	12	12	12
12	3.68	3.73	3.95	3.44	7.69	3.39	4.19	1.64	2.55	2.40
	12	12	12	12	12	12	12	12	12	12
13	.86	.76	1.39	2.60	5.47	6.11	4.09	3.66	1.54	.81
	12	12	12	12	12	12	12	12	12	12
14	1.83	.36	.84	1.81	4.16	4.58	4.55	4.70	6.15	5.47
	12	12	12	12	12	12	12	12	12	12
15	1.52	2.41	1.25	.82	2.26	2.63	2.65	1.38	3.08	2.54
	12	12	12	12	12	12	12	12	12	12
16	1.27	.59	.69	1.22	2.88	1.51	1.29	1.86	2.86	4.10
	12	12	12	12	12	12	12	12	12	12
17	2.40	1.28	1.69	2.63	2.76	2.76	1.63	1.35	3.57	2.72
	12	12	12	12	12	12	12	12	12	12
18	1.99	1.93	1.39	3.37	7.39	3.73	1.49	.93	1.25	2.19
	12	12	12	12	12	12	12	12	12	12
19	1.80	.83	2.25	2.51	2.66	2.59	1.41	2.22	1.60	2.59
	12	12	12	12	12	12	12	12	12	12
20	2.81	1.16	3.16	3.26	3.16	2.86	2.57	1.85	1.74	2.55
	12	12	12	12	12	12	12	12	12	12
21	4.48	1.21	2.74	3.07	4.34	4.12	3.66	3.03	1.63	1.65
	12	12	12	12	12	12	12	12	12	12
22	1.10	1.06	7.74	9.17	9.77	.71	.95	1.45	1.87	2.47
	11	11	12	12	12	11	11	10	10	10
23	.15	.15	.11	.20	.31	.32	.48	.80	.82	.58
	7	7	7	7	7	7	7	7	7	7
24	.32	.17	.09	.24	.55	.51	.35	.36	.61	.82
	7	7	7	7	7	7	7	7	7	7

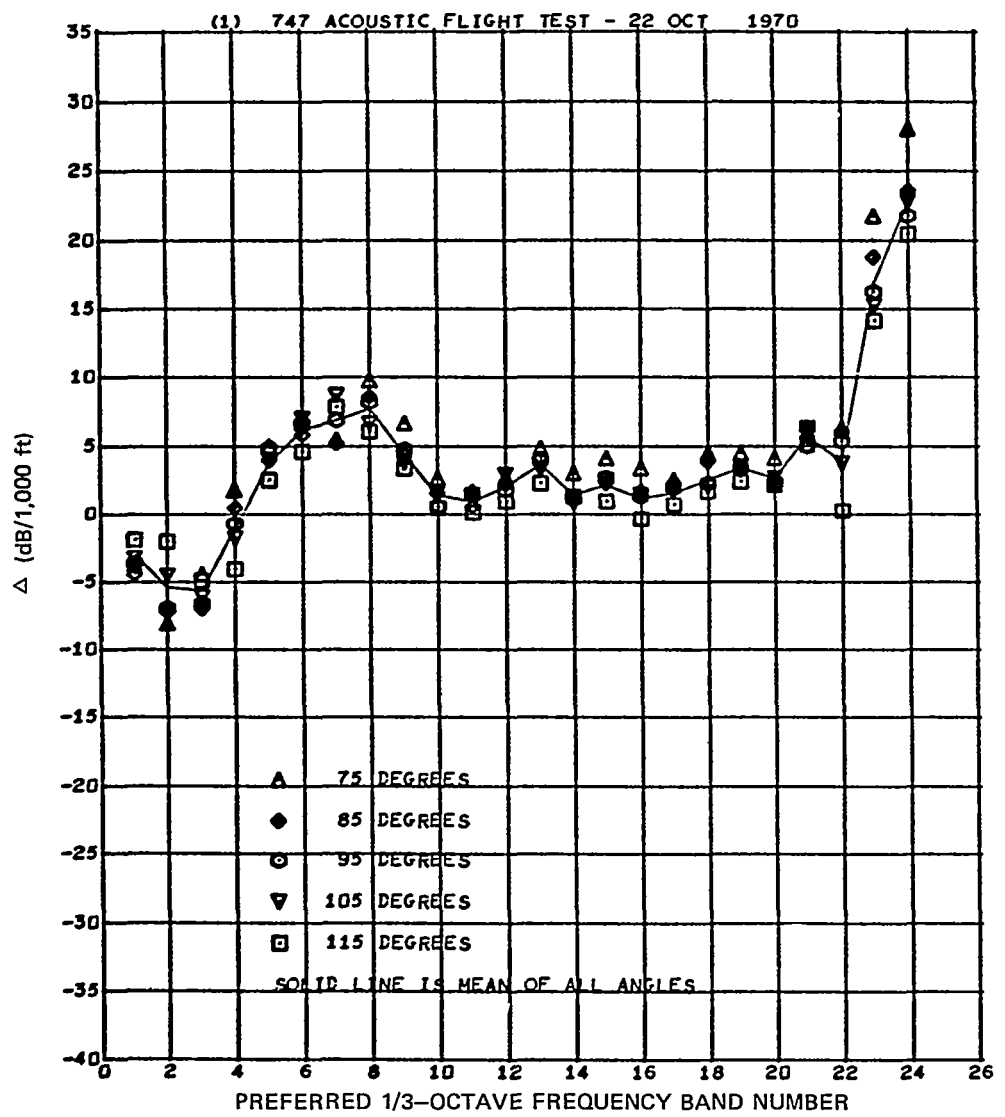


Figure A-23. Summary Plot of Differences (Δ) Between Experimental and ARP 866 Absorption Coefficients for Test Condition 004.1

Table A-24. Estimated Sample Variances and Number of Microphones for Test Condition 006

1/3-OCT FREQ BAND	DIRECTIVITY ANGLE (DEG)									
	75	90	95	90	95	100	105	110	115	120
1	2.89	2.52	1.51	1.84	4.18	6.19	1.77	1.35	1.10	5.03
	13	13	13	13	13	13	13	13	13	13
2	7.27	7.89	6.35	6.90	5.37	5.67	4.08	3.52	2.04	3.36
	13	13	13	13	13	13	13	13	13	13
3	4.18	2.51	4.99	3.71	2.47	2.74	3.44	7.13	5.60	5.72
	13	13	13	13	13	13	13	13	13	13
4	1.36	1.85	2.89	3.67	4.53	5.35	4.00	6.50	4.20	6.63
	13	13	13	13	13	13	13	13	13	13
5	.95	.94	.39	1.16	1.98	2.51	3.42	5.54	5.09	5.02
	13	13	13	13	13	13	13	13	13	13
6	2.69	2.55	1.47	1.48	2.28	2.03	2.03	2.27	3.56	4.43
	13	13	13	13	13	13	13	13	13	13
7	2.85	3.06	3.36	3.31	3.11	2.74	2.37	2.11	2.32	1.62
	13	13	13	13	13	13	13	13	13	13
8	6.20	5.02	3.67	5.86	6.50	5.93	5.25	7.37	6.05	4.20
	13	13	13	13	13	13	13	13	13	13
9	7.63	6.27	8.45	8.97	7.90	6.53	6.39	5.26	3.97	3.19
	13	13	13	13	13	13	13	13	13	13
10	4.12	4.21	5.16	4.62	3.33	3.07	4.07	4.53	4.25	5.07
	13	13	13	13	13	13	13	13	13	13
11	3.12	2.64	3.15	2.96	2.85	1.93	2.00	2.76	4.83	2.88
	13	13	13	13	13	13	13	13	13	13
12	2.95	1.76	1.56	1.45	1.57	1.37	1.74	2.33	1.53	1.65
	13	13	13	13	13	13	13	13	13	13
13	4.36	2.71	2.32	3.02	1.96	1.63	1.61	1.27	1.98	3.34
	13	13	13	13	13	13	13	13	13	13
14	4.56	2.50	3.00	2.55	1.92	1.27	1.15	.76	1.09	2.70
	13	13	13	13	13	13	13	13	13	13
15	2.12	.88	1.83	1.93	1.90	2.22	2.06	2.14	1.92	4.02
	13	13	13	13	13	13	13	13	13	13
16	2.65	1.30	2.11	1.78	.99	.66	1.22	1.42	2.59	3.09
	13	13	13	13	13	13	13	13	13	13
17	1.64	.50	.95	1.25	1.18	1.46	1.30	1.52	2.71	1.89
	13	13	13	13	13	13	13	13	13	13
18	2.46	1.64	1.33	3.17	.95	1.05	.90	.85	2.10	1.93
	13	13	13	13	13	13	13	13	13	13
19	2.69	.96	1.44	2.28	.99	.65	.46	1.29	2.55	2.75
	13	13	13	13	13	13	13	13	13	13
20	1.84	1.03	1.38	1.94	1.35	.71	.76	1.07	2.42	1.62
	13	13	13	13	13	13	13	13	13	13
21	1.19	.72	1.35	3.57	2.43	1.18	1.05	1.17	1.89	1.87
	13	13	13	13	13	13	13	13	13	13
22	1.19	.55	.48	.35	.23	.30	.45	.78	.75	1.36
	11	11	11	11	11	11	11	11	11	11
23	.28	.31	.50	.26	.28	.35	.51	.72	.67	.47
	8	8	8	8	8	8	8	8	8	8
24	.44	.47	.59	.35	.48	.65	.64	.71	.58	.30
	8	8	8	8	8	8	8	8	8	8

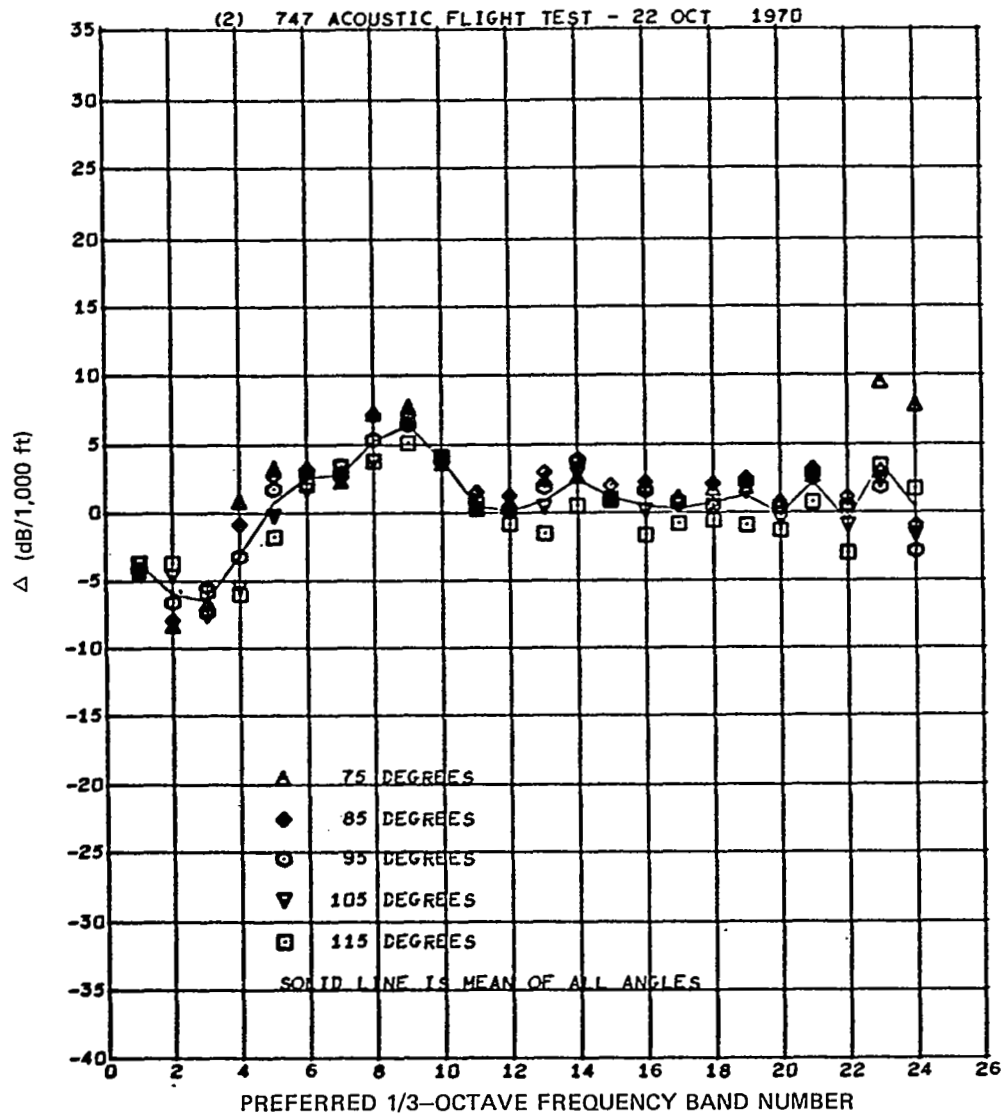


Figure A-24. Summary Plot of Differences (Δ) Between Experimental and ARP 866 Absorption Coefficients for Test Condition 006